EG&G

EGG-1183-1665
15 May 1975

AERIAL RADIOLOGICAL SURVEY OF THE SAVANNAH RIVER PLANT (AIKEN, SOUTH CAROLINA)

DATE OF SURVEY: 2 THRU 25 JUNE 1974

by Philip K. Boyns

Approved for Publication

John F. Boyle, Manager
Aerial Surveillance Department

Clyde Jupiter, Manager
Radiation and Environmental Sciences Department

This Document is
UNCLASSIFIED

E. J. Story
Classification Officer

Prepared by EG&G, Inc. for the United States Energy Research and Development Administration, Division of Operational Safety.

CONTENTS

ABSTRACT

An aerial radiological survey of the Savannah River Plant was carried out in June 1974 by EG&G, Inc. for the United States Energy Research and Development Administration, Division of Operational Safety. The survey consisted of an airborne measurement of both natural and man-made gamma radiation from the terrain surface in and around the plant site. These measurements allowed a determination of the surface terrestrial spatial distribution of isotope concentrations and equivalent gamma ray exposure rates from ^{60}Co and ^{137}Cs contaminants. Results are reported as exposure rate isopleths for the two isotopes and are superimposed on 1:48,000 scale maps of the area. Gamma ray energy spectra are also presented for the net man-made radioelements.

ACKNOWLEDGEMENTS

Appreciation is given to L. J. Deal, Assistant Director of the U S Energy Research and Development Administration's Division of Operational Safety, for his support and encouragement in this survey project.

Both Grover Smithwick and Steve Wright at the Savannah River Plant were very helpful in providing information on the plant operating characteristics and results of ground-based surveys for comparison with this work. They also provided coordination for EG&G's activities at the survey site.

Capt P. Buley and Capt J. Klem of the U S Air Force, together with their flight crew, did an excellent job of flying the helicopter under very exacting conditions.

Finally, we wish to acknowledge the contribution of the EG&G survey team: T. P. Stuart, J. Cleland, W. Ebeltoft, R. Mazerkewiz, J. T. Hess, W. Verheyden, G. Menkel, and M. Sevart. Data analysis and plotting was carried out with the assistance of T. Hendricks, C. Bluitt, S. Hatch, and J. Cates. R. Meibaum rendered photographic support.

1.0 INTRODUCTION

An aerial radiological survey was carried out during June 2 through June 25, 1974 by EG&G, Inc. over the Savannah River Plant, operated by the duPont Company for the U. S. Energy Research and Development Administration (ERDA). The survey consisted of an airborne measurement of both natural and man-made gamma radiation from the terrain surface, as well as airborne radioactive contaminants in and around the plant site. Special missions were flown to track the airborne radioactive effluent from reactors as part of a plume dispersion experiment.[1]

The Savannah River Plant,[2] was established in 1950 to produce nuclear materials for national defense. Nuclear materials are produced at this site by transmutation of elements in large nuclear reactors that are moderated and cooled by heavy water. Support facilities extract heavy water from natural water, fabricate nuclear fuel and targets, dissolve the irradiated materials, and separate nuclear products from the intensely radioactive byproducts. Chemical processing of irradiated materials produces radioactive liquid waste that requires continuous management to prevent contamination of the plant environs.

The Savannah River Plant, shown in Figure 1, is drained by six tributaries of the Savannah River. These streams provide natural drainage for the area, as well as receive discharges[3] of industrial wastes from the various plant operations, and they drain through the swamp south of the plant before entering the Savannah River. The Upper Three Runs Creek receives industrial discharges from the 300/700 areas, including research and reactor fuel and target fabrication operations. The Four Mile Creek receives discharges from the 400-D heavy water production and reclamation area. The Pen Branch stream receives effluents from the 100-K reactor area. Steel Creek receives discharges from the 100-P reactor area, while Lower Three Runs Creek receives occasional overflows from Par Pond, a 2,500-acre artificial impoundment used for cooling and recirculating cooling water to the 100-P reactor.

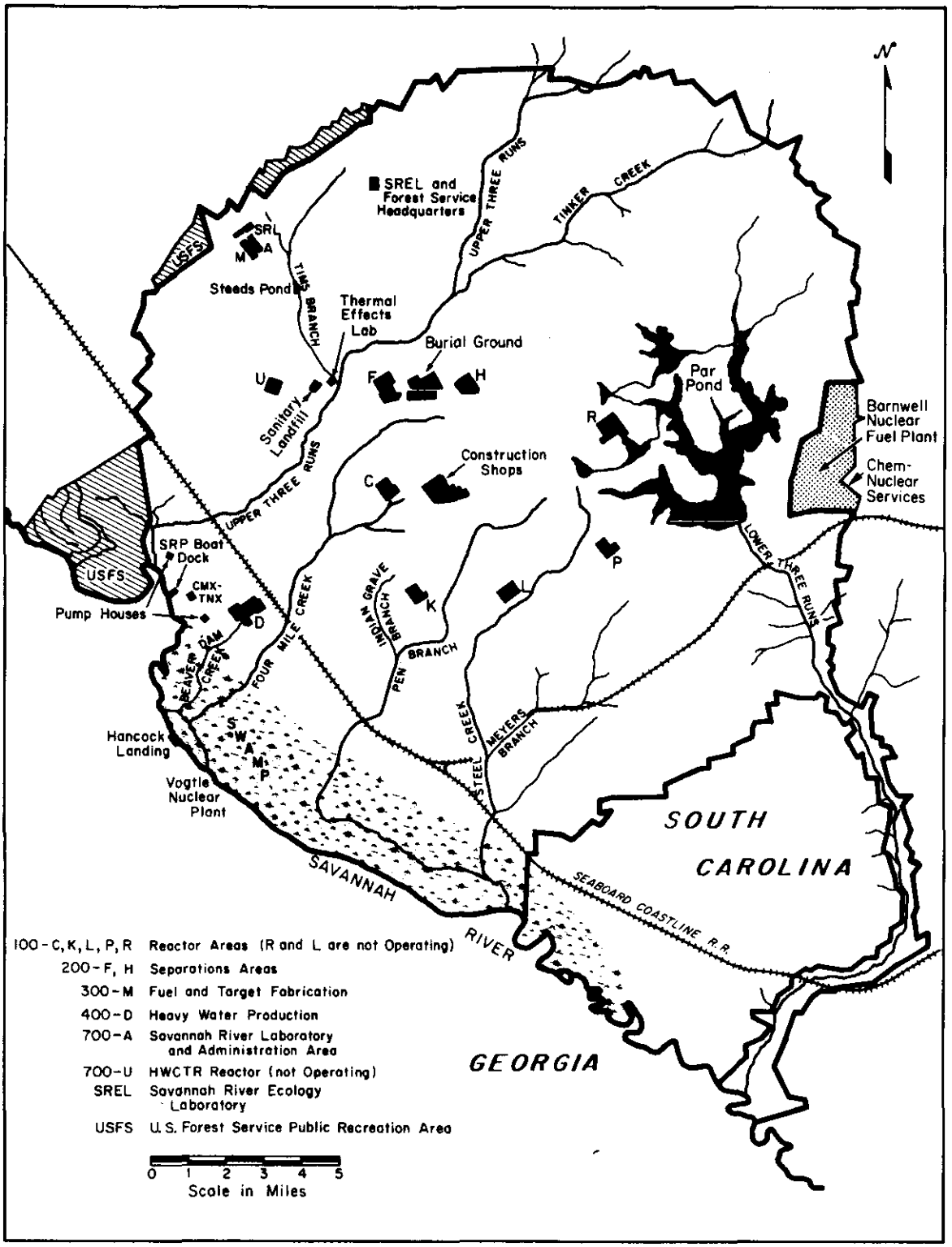

Figure 1. Site location of the Savannah River Plant near Aiken, South Carolina operated by the Du Pont Company for the U. S. Atomic Energy Commission.

The measurement system used in the survey was a 40-crystal array of large NaI(Tl) gamma-ray spectrometers, which measured terrestrial gamma intensity and energy spectra from a helicopter platform. This detection system is operated by EG&G, Inc. for the ERDA. The survey described here was carried out for the ERDA's Division of Operational Safety as part of a continuing nationwide program[4] to determine the extent of both natural and man-made radioactivity in and around ERDA or licensee plants that use, process or store nuclear material.

Results are presented as gamma exposure rate isopleths for the two principal contaminants, ^{60}Co and ^{137}Cs, as well as for the naturally occurring radioelements in the surface soil. These isopleths are plotted over 1:48,000 scale maps of the area. In addition, gamma energy spectra are presented for the measured radiation fields due to the combined natural radioelement and contaminant radioactivity.

2.0 NUCLEAR INSTRUMENTATION SYSTEMS AND PROCEDURES

2.1 Radiation Detectors

The gamma radiation detectors employed in the Savannah River Plant survey consisted of forty 12.7-cm diameter by 5-cm thick NaI(Tl) crystals, arranged in two arrays externally mounted on a Bell UH-1N helicopter. One of these arrays of 20 crystals is shown in Figure 2, with the detector pod service covers removed.

Preamplifier signals from each detector were combined in a summing amplifier in each detector pod. Outputs from the amplifiers were fed to a summing junction in the data acquisition system, referred to as Radiation and Environmental Data Acquisition and Recording (REDAR). The summing junction output is fed to an analog to digital converter (ADC) and then to a 300-channel pulse height analyzer and a set of five variable-width single-channel analyzers. This instrumentation allowed a measurement of selected gamma energies corresponding to radioactive isotopes of interest, as well as the complete gamma energy spectrum from 50 keV to 3.0 MeV, covering all pertinent natural and man-made radiations.

2.2 Position Measuring Systems

Accurate position data for the surveying aircraft were obtained from two systems, a Trisponder/202A microwave ranging system* and a model YG9000D1 radar altimeter.** These inputs were updated every second to fix the position of the helicopter during its flight over the plant site so that measured radiation data could be accurately associated with position.

The Trisponder master station, mounted in the helicopter, interrogated two remote transceivers at fixed locations outside the survey area. By measuring the round-trip propagation time between the master and the remote stations, the master station computed the distance to each. The distance displayed and recorded each second

*Manufactured by Del Norte Technology, Inc.
**Manufactured by Minneapolis Honeywell.

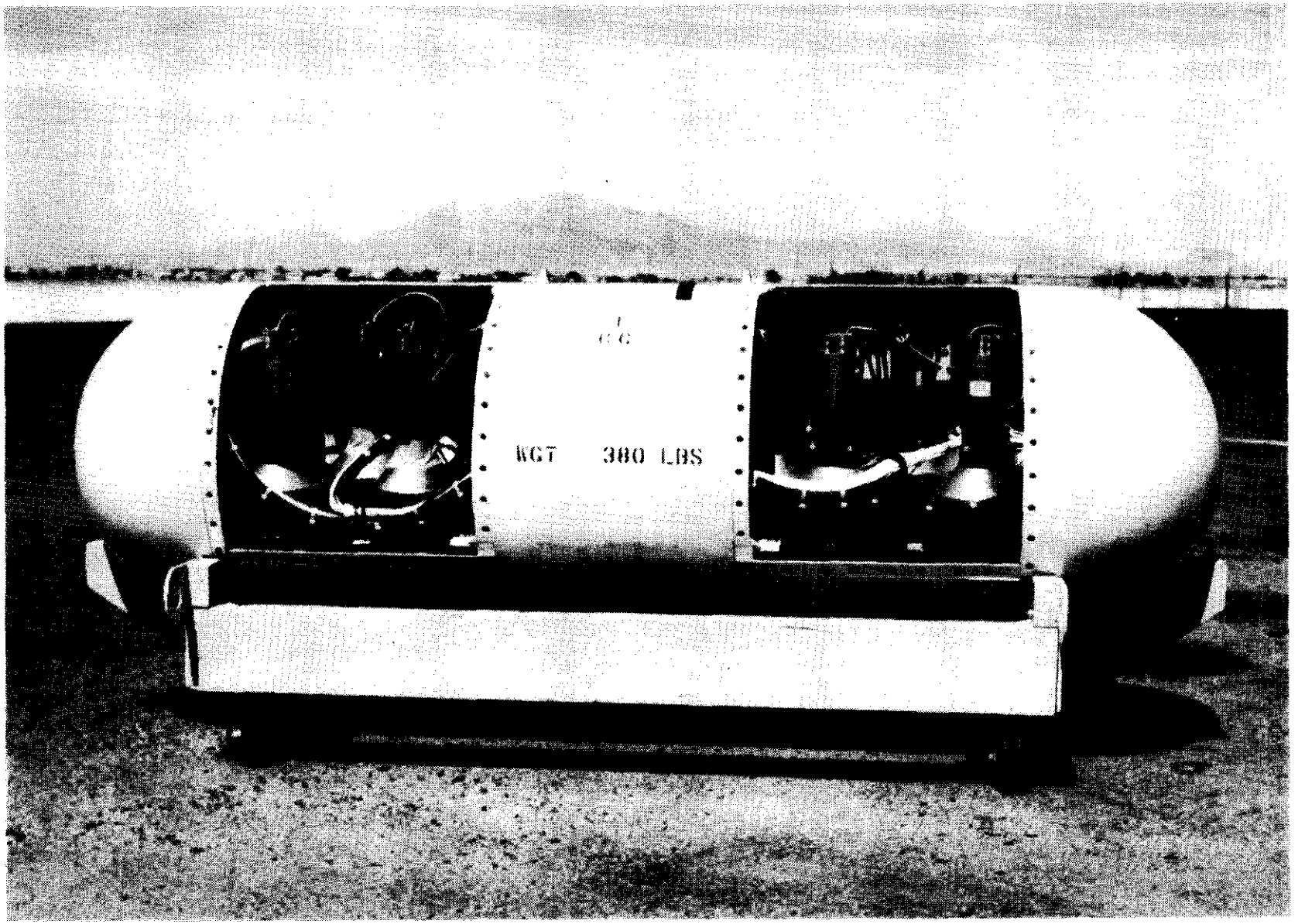

Figure 2. One of the gamma detector pods consisting of an array of twenty 12.7 cm diameter, 5 cm thick NaI(Tl) crystals and matching photomultiplier tubes.

was the average of 10 measurements, which minimized statistical errors and increased system accuracy and stability. The position uncertainty of the helicopter, at any location within the survey perimeter, was a maximum of ±54 feet. The details of this procedure are given in Appendix A.

The radar altimeter transmits a pulsed RF signal. Pulses reflected from the nearest ground object are detected by a receiving antenna on the helicopter. The elapsed time is converted to a distance measurement with an accuracy of ± 5.0 feet, plus 3 percent of actual altitude. This survey was conducted at an altitude of 500 feet; hence, the altitude uncertainty is ± 20 feet.

2.3 Data Recording System

Summed signals from the separate gamma ray detectors were fed to (1) a 300-channel pulse-height analyzer and (2) a maximum of five single-channel analyzers with adjustable upper and lower limits. These limits were set to monitor regions of the spectrum pertinent to isotopes of interest. Accumulation time for the single-channel data was 0.2 seconds; accumulation time for multichannel data was 3 seconds. Multi- and single-channel counts occurring in the above time intervals were recorded on 9-track, IBM compatible tape.* Position data were recorded at one-second intervals. Single-channel data were also displayed in real time on the REDAR system to enable the system operators to monitor the data as they were acquired. Figure 3 is a block diagram of the detectors and REDAR system. Figure 4 shows the REDAR hardware as it was mounted in the helicopter.

2.4 Data Processing System

The data processing system, referred to as Radiation and Environmental Data Analyzer and Computer (REDAC) is shown in Figure 5. The REDAC was mounted in a mobile van based at the site. It consists basically of two Cipher Data tape drives,* a NOVA 840**

*Cipher Data Products Recorder, Model 85H.
**Manufactured by Data General Corporation.

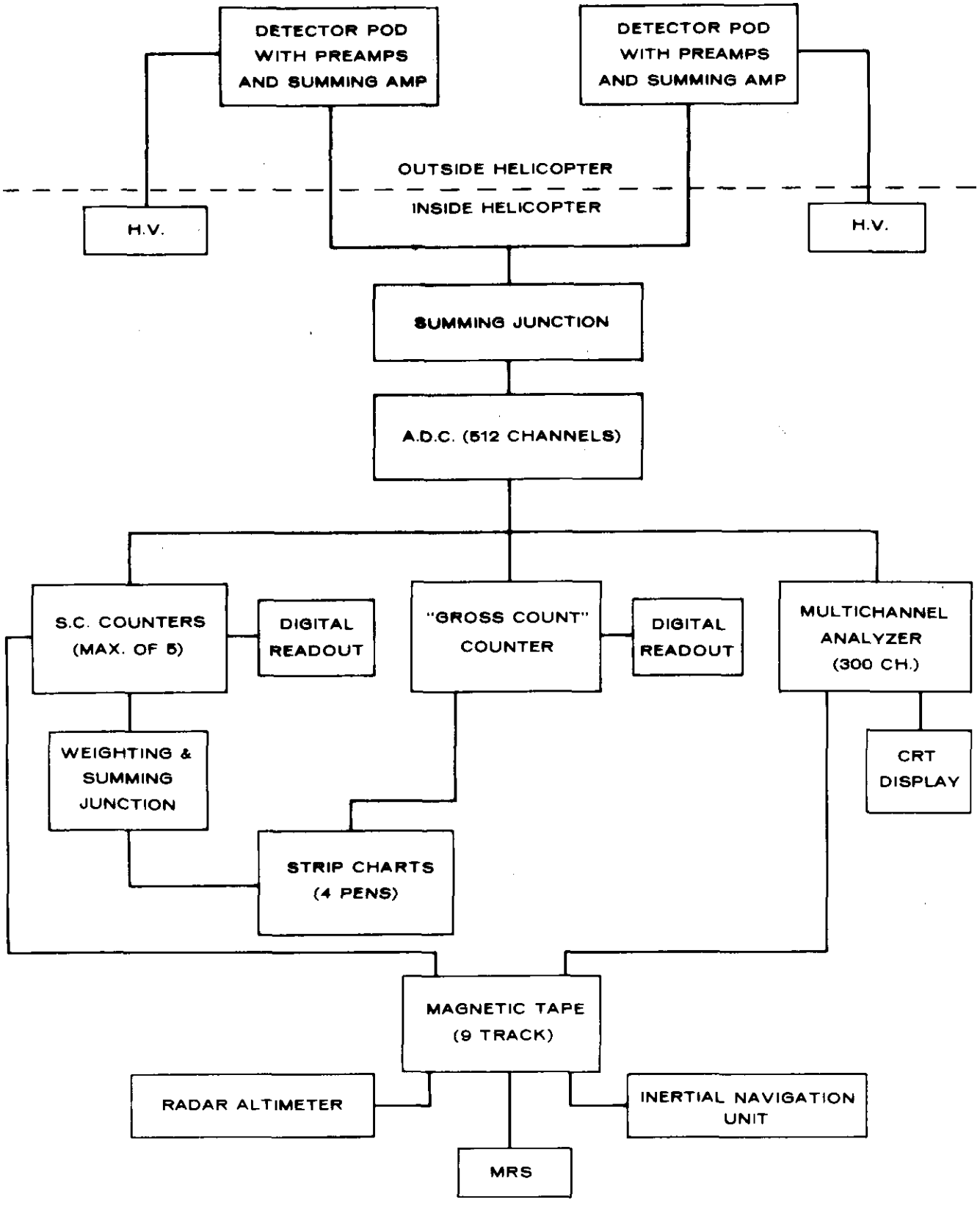

Figure 3. Block diagram of the electronic data collection and recording system.

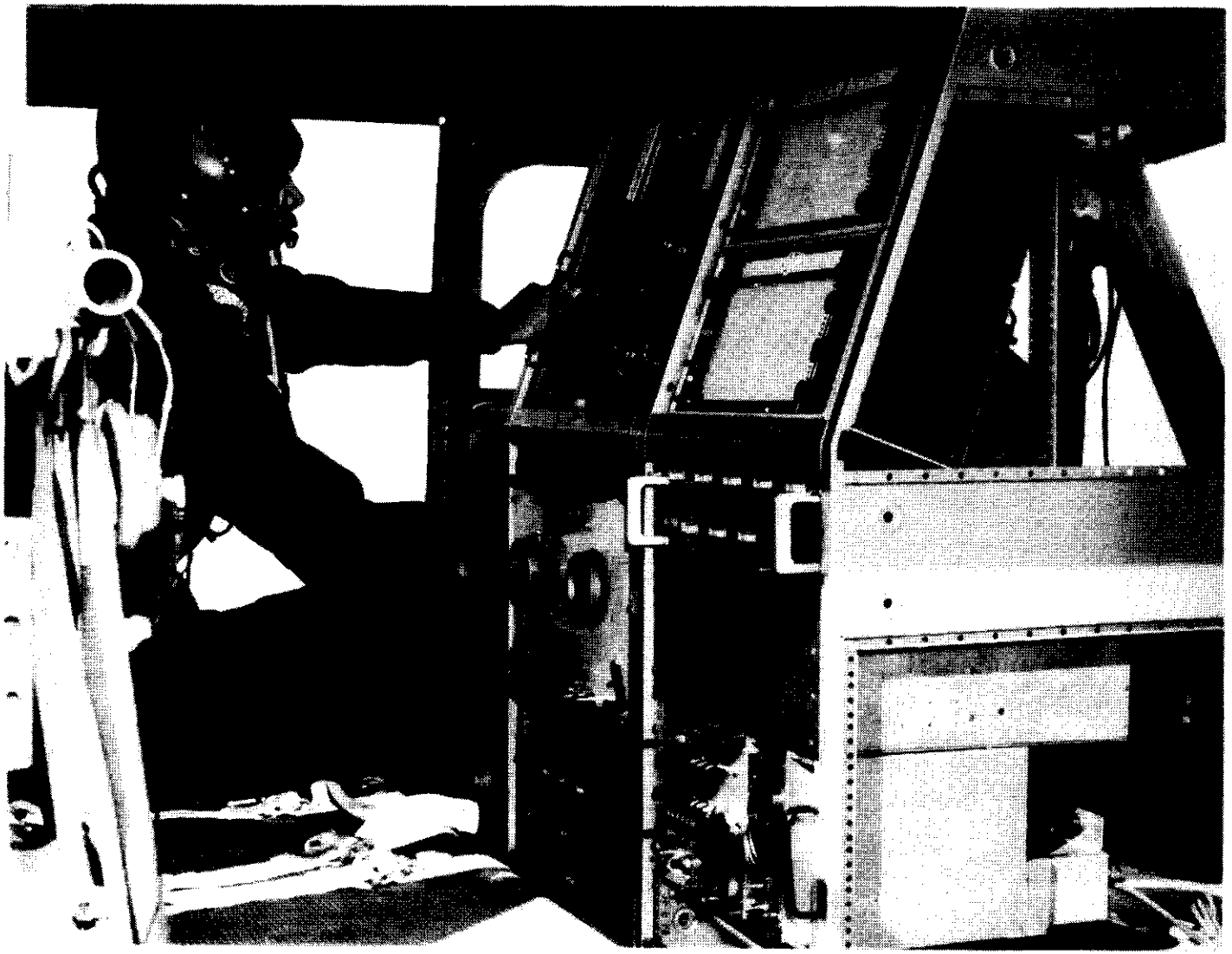

Figure 4. Photograph of the REDAR (Radiation and Environmental Data Acquisition and Recording) system, mounted in the helicopter during the Savannah River Plant survey.

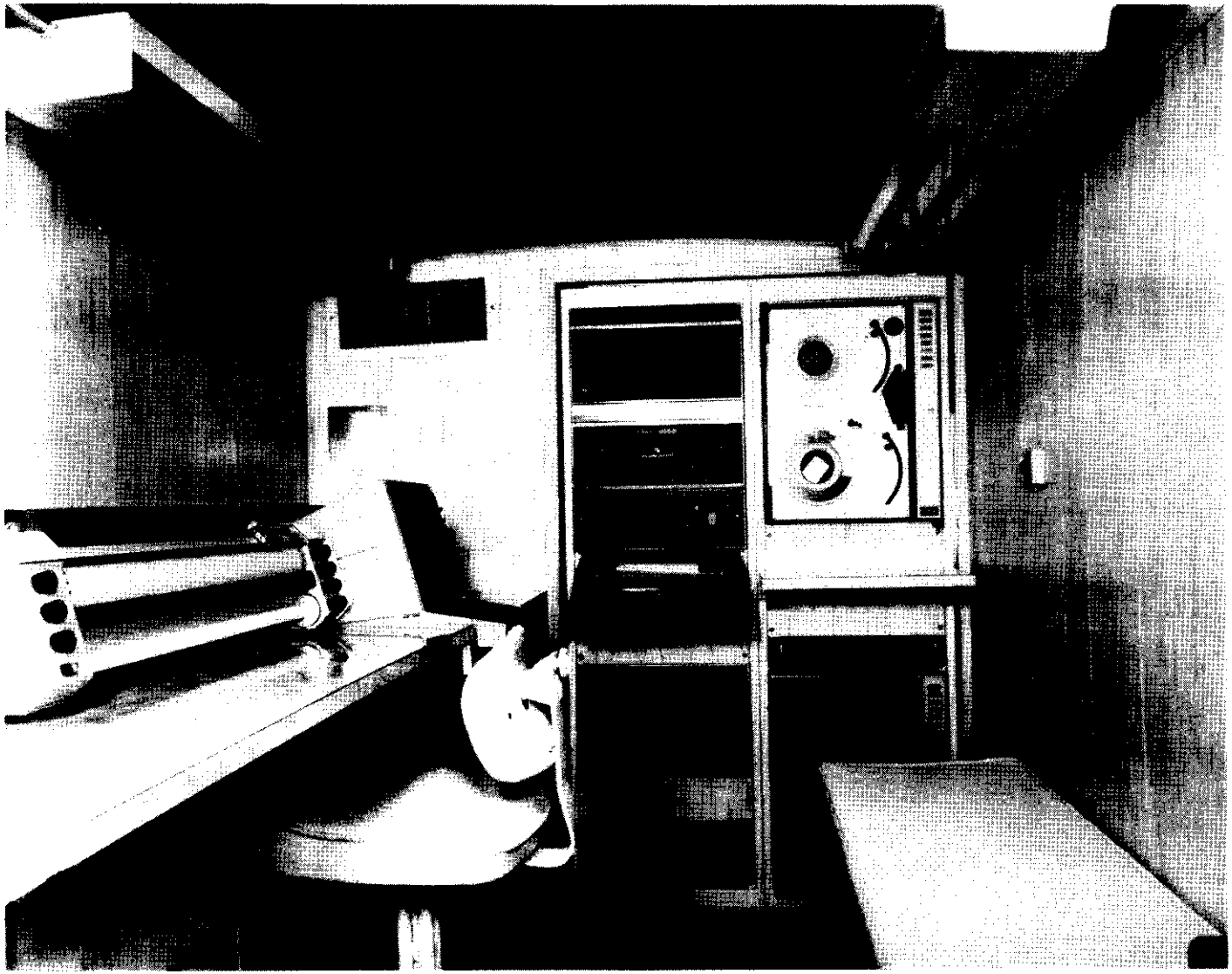

Figure 5. Photograph of the interior of the mobile van which housed the Radiation and Environmental Data Analyzer and Computer (REDAC) system, used in analysis of the Savahhan River Plant survey data.

computer, two CalComp plotters* and a CRT** display screen with a hard copier. A variety of software routines were available for analyzing the data. Pulse height windows could be selected over any portion of the gamma energy spectrum (0.050 to 3.0 MeV), in addition to the five single channel windows, and plotted as a function of time or position. Weighted combinations of windows from either the multichannel or single-channel analyzers could be summed together and the result plotted as a function of time or position. By the proper selection of windows and weighting factors, it was possible to extract the photopeak count rates for man-made isotopes deposited on the terrain in the survey area. The photopeak count rates could then be converted to isotope concentrations or exposure rates. Spectral data could be summed over any portion of the survey flight line.

*Manufactured by California Computer Products, Inc.
**Tektronix Corp.

3.0 DESCRIPTION OF THE SAVANNAH RIVER PLANT SURVEY

The survey was conducted during June 2 through June 25, 1974. The base of operation for the survey was Bush Field in Augusta, Ga. The mobile computer van was also located at the airport for immediate analysis of the computer tapes when the helicopter completed each survey flight.

The Bell UH-1N helicopter had a flight duration of 2.5 hours with approximately 1300 lbs of survey equipment (data acquisition system and the two detector pods). The flight crew consisted of a pilot, navigator and an instrument operator. The navigator visually directed the pilot along the programmed flight lines from aerial photographs of the Savannah River Plant site. Travel time to and from the survey area was a minimum of 30 minutes; therefore, actual survey time was less than 2 hours. Two or three missions were flown each day, depending on the weather. Early morning fog and late afternoon haze conditions limited the number of survey missions each day.

The survey consisted of approximately 150 flight lines that varied from 7 to 25 miles in length; it was programmed to cover the entire site area and at least one mile outside the site perimeter, with a total coverage of approximately 2800 line miles. The helicopter flight lines were plotted on a map of the survey area (Figure 6). The nominal survey altitude above terrain was 500 feet and the flight lines were programmed in an east-west direction at 1000-ft intervals. The flight line spacing was selected for complete coverage of the survey area for the response of the detectors to radiation emitted by isotopes having gamma rays of 50 keV or greater.

A special flight at 500 feet above terrain from Augusta, Georgia, to Savannah, Georgia, was flown along the approximate east and west banks of the Savannah River to detect man-made isotopes along the river. No man-made isotopes were detected outside the programmed site survey area in Figure 6.

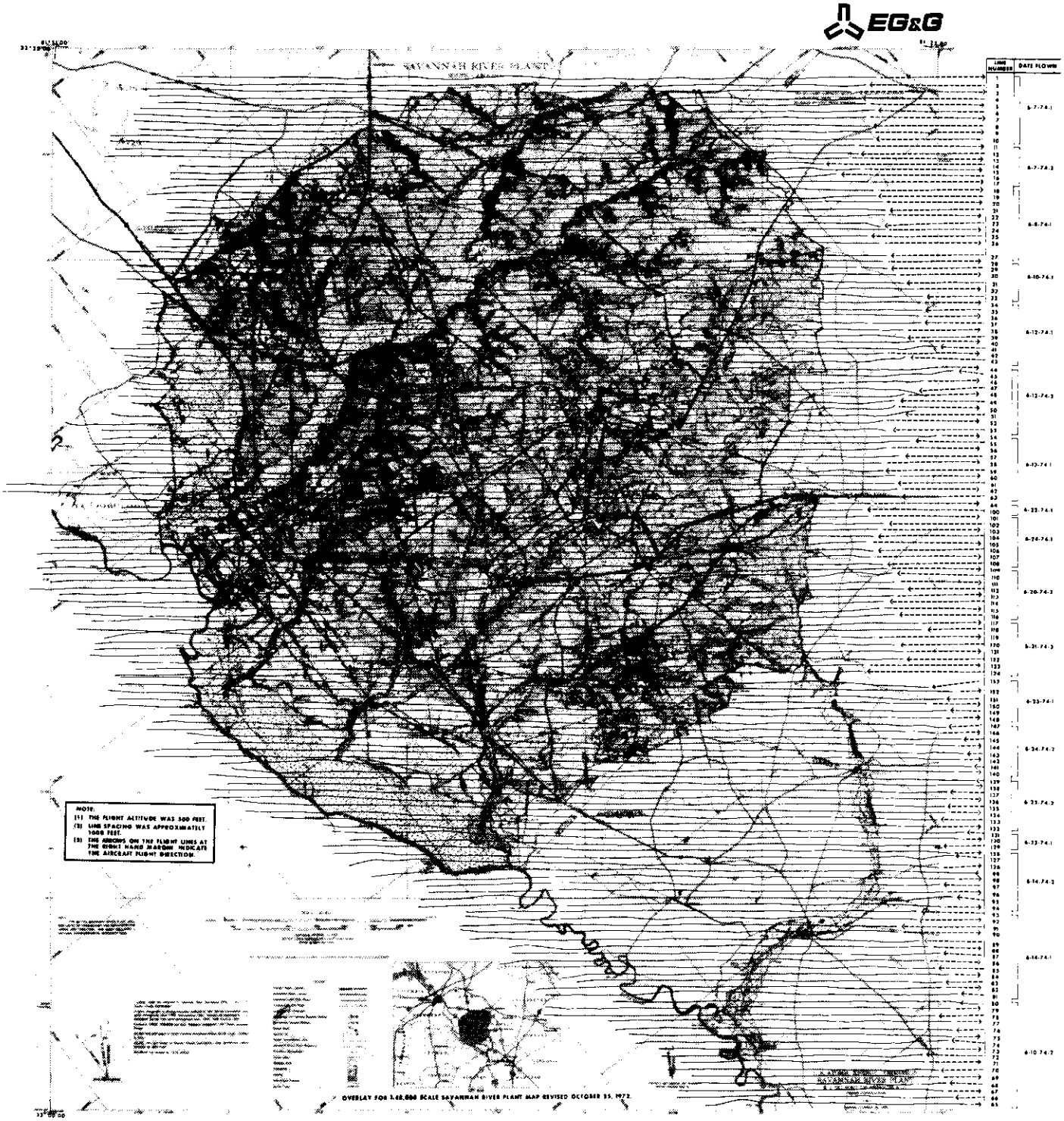

Figure 6. Map of the surveyed area at the Savannah River Plant with the helicopter flight line positions and flight directions shown.

The H facility area and the F facility area, as well as the Four Mile Creek area, were surveyed at a 150-ft altitude to detect the presence of ^{241}Am in association with plutonium contamination. Plutonium was not detected above the minimum detectable activity (MDA) of 0.6 $\mu Ci/m^2$. The MDA is dependent on the presence of other man-made isotopes; therefore, the MDA could be slightly higher, depending on the concentration of other isotopes in the survey area and the energy of their gamma rays.

4.0 DATA REDUCTION

4.1 Aircraft Position Data

The position of the aircraft was recorded once every second on magnetic tape from the MRS system (Section 2.2) and a Litton LTN-51 Inertial Navigation System.* The inertial navigation data, given in longitude and latitude coordinates, were used as a backup to the MRS data on the site survey. It was also used as the primary positioning system for the off-site survey (down the Savannah River from Augusta to Savannah, Georgia) since the MRS system was out of range for the 100-mile river flight. Some correction was necessary due to the INS system drift.

4.2 Gamma Photopeak Stripping Procedures

Analysis of the gamma energy spectra and count rate data, together with the aircraft position data, was accomplished routinely with the use of the data processing system. Computer analysis resulted in plots and data tables giving specific radionuclide concentration, exposure rate, and location of radioactivity in the surveyed area. The individual isotopic contributions to the measured gamma pulse height spectra were separated out using the spectral stripping procedure outlined in Appendix B.

From man-made gross count rate data (see Section 4.4.1) identified as being above the natural background level, the man-made isotopes of major concern at the Savannah River Plant survey were identified as ^{60}Co, ^{137}Cs, and ^{41}Ar. Stripping procedures used in separating out the representative photopeaks for these isotopes are given in Appendix B. In order to extract the contribution of each isotope when other isotopes were present, a matrix analysis technique was utilized to compute extraction coefficients.

*Manufactured by Litton Industries Aero Products.

Stripping Coefficients for removal of background under each of the photopeaks of interest were determined from a spectrum containing only natural radiation. In each case, the natural background contribution was removed by monitoring the counts above 1.4 MeV. Stripping coefficients for the removal of ^{41}Ar contributions to the ^{60}Co and ^{137}Cs photopeaks were determined by obtaining a "pure" ^{41}Ar spectral shape. This was done by subtracting a background spectrum from one obtained in a plume of ^{41}Ar (Figure 7).

Shapes for ^{60}Co and ^{137}Cs pulse height spectra and resulting stripping coefficients were obtained in a similar manner.

4.3 Altitude and Dead Time Correction

Even though the pilot attempted to keep the helicopter as close to an altitude of 500 feet as possible, small deviations occurred. All of the data, second by second, were adjusted to an equivalent 500-ft altitude by the following:

Altitude correction factor: $F = e^{-\delta (A_o - A)}$

δ = reciprocal of the mean free path of the gamma ray in air

A_o = nominal survey altitude

A = measured altitude above terrain

The same factor was used in correcting all radiometric data (gross counts, as well as photopeak area counts). The use of multiple factors for various energy values did not seem justified since the altitude deviation was only ±50 feet.

The large volume of NaI(Tl) crystals (1570 in^3) produced 5000 to 10,000 counts per second even from natural radiation in the soil. This count rate resulted in 5 to 10 percent dead time in the recording system. All data were corrected for system dead time losses.

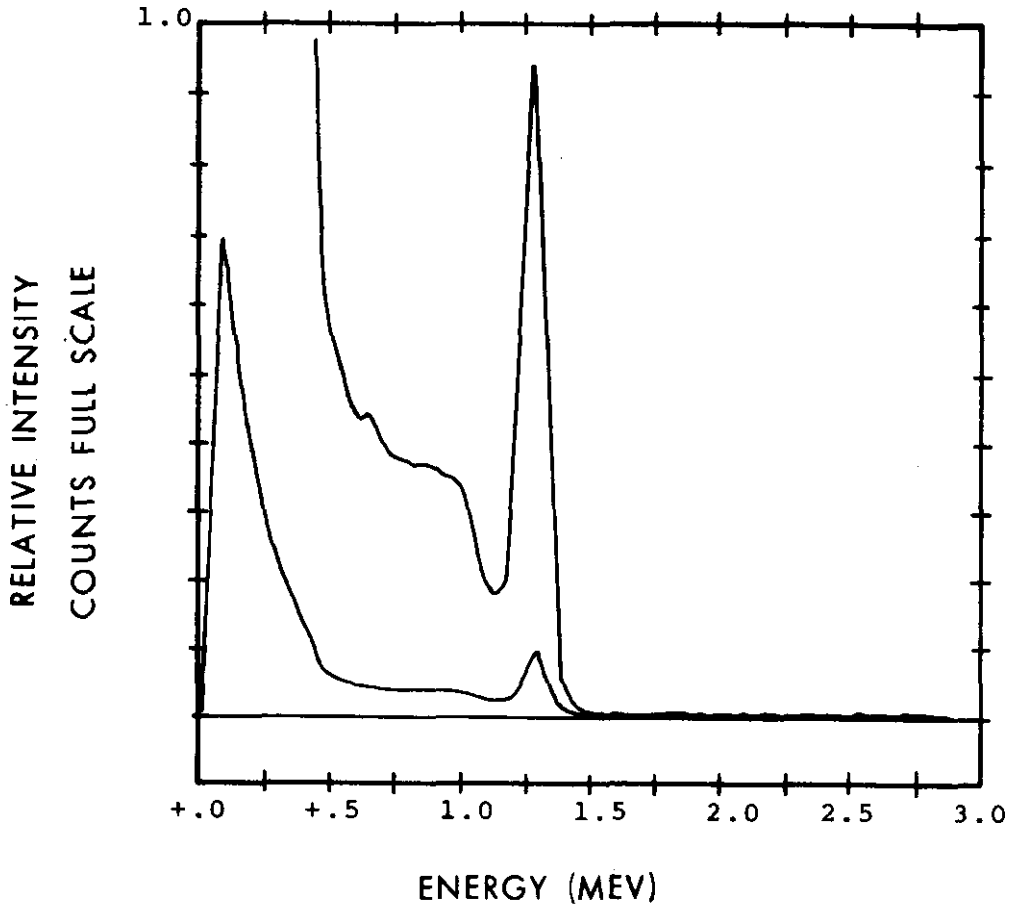

Figure 7. Gamma energy pulse height spectrum taken in an airborne plume of Argon-41 at 500 ft above terrain with the background removed.

4.4 Conversion Factors

4.4.1 Man-made Gross Count Isopleths

A sensitive method was developed for the detection of man-made anomalies in the natural background gamma ray spectrum. A full spectrum was recorded every three seconds on a multichannel analyzer. The gamma ray background spectral shape in the energy region between 0.05 and 3.00 MeV was relatively independent of variations in flight altitudes of several hundred feet, concentration of airborne radium and thorium daughters, and the natural radioelement composition in the soil.

A window was set from 1.40 to 3.00 MeV to monitor the predominant natural radioelements; namely, ^{40}K, ^{214}Bi, and ^{208}Tl (see Figure 8). Since the spectral shape is constant for natural radioelements, total counts in the 1.40 to 3.00 MeV window are indicative of the total background counts that should appear in the lower portion of the spectrum (0.05 to 1.39 MeV). A constant C was then determined for the ratio of the two windows.

The total counts in Window #1 (0.05 to 1.39 MeV) was then equal to a constant, established for the particular survey area (typically: 25 ± 25%), times the total counts in Window #2 (1.40 to 3.00 MeV).

Any perturbation in the shape of the natural isotope spectrum caused by the presence of man-made radionuclides would alter the ratio between the counts in the two windows. The "Man-Made Gross Count" (MMGC) is a measurement of the net change in the gamma counts in the lower window and is expressed as follows:

$$\text{MMGC} = \sum_{0.05\ \text{MeV}}^{1.39\ \text{MeV}} (\text{counts in Window \#1}) - C \sum_{1.40\ \text{MeV}}^{3.00\ \text{MeV}} (\text{counts in Window \#2})$$

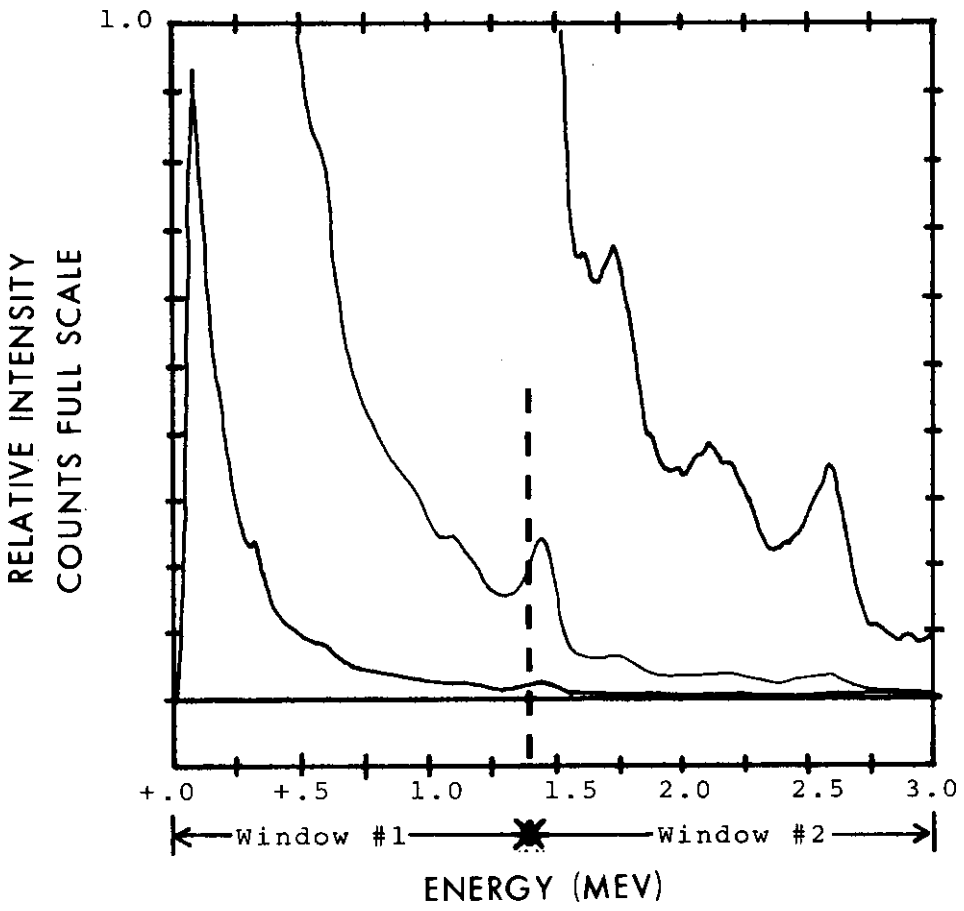

Figure 8. Window settings for the gamma pulse height spectra used to provide a normalizing factor to separate man-made radio-element contaminants from the natural background.

The MMGC stripping technique enhances the capability to detect subtle changes in the surface terrestrial radiation due to man-made isotopes over a spatially varying (in intensity) natural background radiation field. Figure 9 demonstrates the enhancement of photopeaks due to man-made isotopes using the method discussed above. (Notice the two man-made sources at the start of the flight line that were obscured by variations in the natural background.) The "Gross Count" data are the total counts in the spectrum from 0.05 to 3.00 MeV. The gross count data were typically around 4,000 counts per second and varied a factor of 2 or 3 from natural background sources, while the MMGC data are typically 0 ± 300 counts per second (at one standard deviation).

The constant C and the statistical variation in the gamma counts in the portion of the energy spectrum defined by Window #1 were determined in an area close to or in the survey area which is representative of normal background. Careful inspection of the spectral data in the background reference area was imperative to ensure that the area was not contaminated and that it was typical of the radiation from the naturally occurring radioelements in the survey area. The minimum detectable level of man-made radioelements was determined by the statistical variation of the MMGC in the background area. These data were plotted as an isopleth map shown in Figure 10. The data in the A region corresponds to normal background intensity levels, while the minimum detectable activity, which is the B level is set at ± 3 standard deviations or at the 99% confidence level for the MMGC measured the background reference area. Less than 1% of the data, therefore, would yield erroneous B levels due to the statistical variation in the count rate. All spectral data for data points of B or greater were carefully analyzed. The C level is set a factor of 2 above the B, and the D level a factor of 2 above the C, etc. The levels indicate the amount of spectral distortion in the normal background spectrum. The majority of the man-made isotopes observed in environmental surveys emit gammas with energies below 1.39 MeV, thereby producing a positive MMGC. A "@" level on the plotted isopleths is set for negative values of the MMGC.

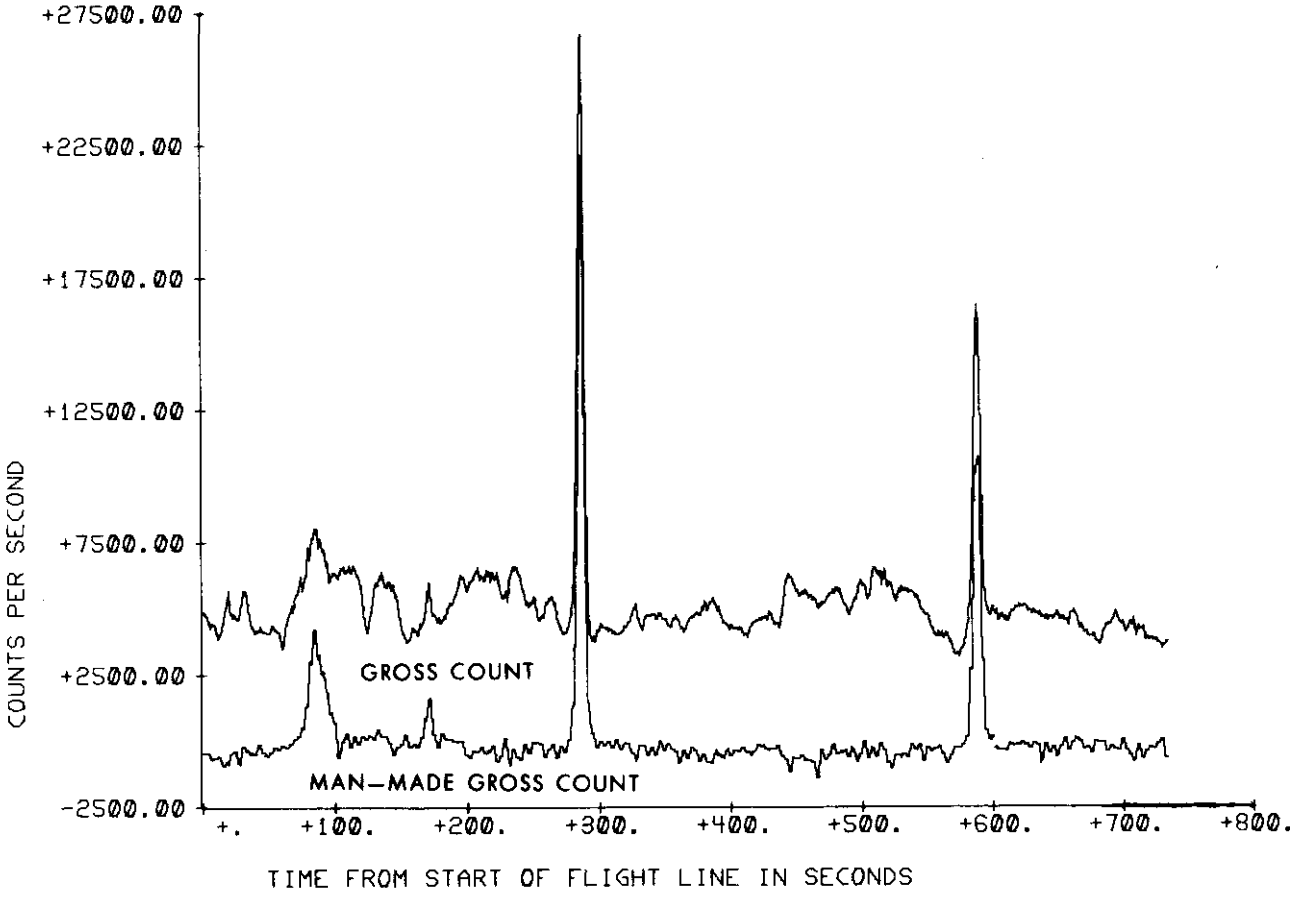

Figure 9. Example of the enhancement of the detectability of man-made contaminants over the fluctuating natural background radiation, employing the MMGC stripping technique.

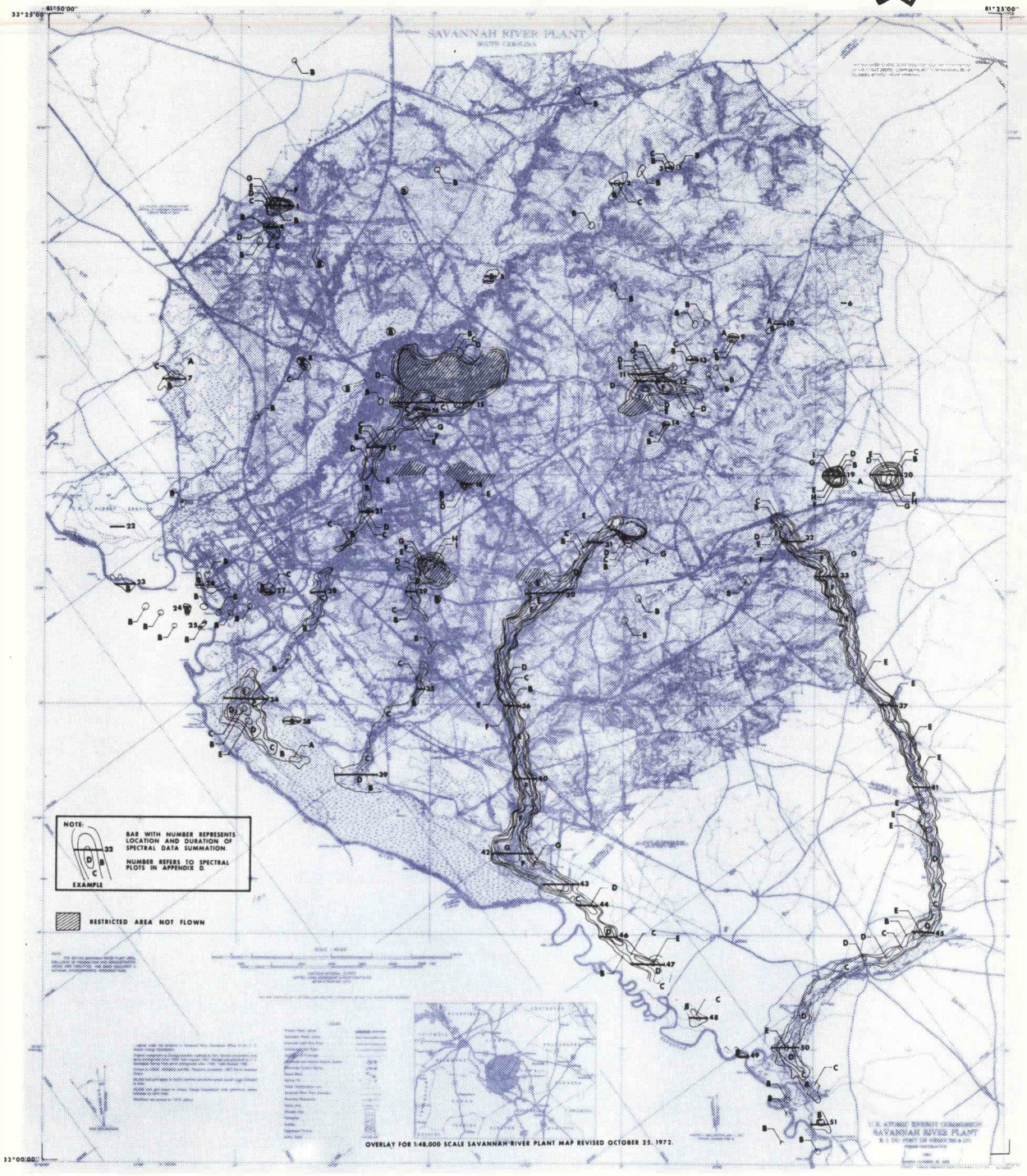

Figure 10. Map of the Man-Made Gross Count isopleths for the Savannah River Plant.

The data and procedures used in developing the MMGC values used for this survey are given in Appendix B. ^{41}Ar has been removed from the MMGC isopleth in Figure 10. This eliminates interference of airborne ^{41}Ar from the map of terrestrial man-made isotopes.

4.4.2 Isotope concentrations

It was of interest to estimate the ^{60}Co and ^{137}Cs concentrations on the terrain surface from the survey data. Isotope concentration conversion factors were derived from experimental data taken by hovering over point calibration sources of these isotopes. Isotope concentration data can be determined from the count rate data by using the conversion factors in Appendix C. The appropriate conversion factor for an infinite planar source ($\mu Ci/m^2$) or a volume source ($\mu Ci/gram$) are given for both ^{137}Cs and ^{60}Co.

4.4.3 Gamma Ray Exposure Rates

In order to calculate the gamma ray exposure rate at 3 feet above terrain from the aerial survey data, several assumptions have to be made about the distribution of the isotopes in the soil. Calculations performed here incorporate the assumption that the character of the radioactive source in the soil is a median between the two idealized cases of an infinite plane source and a uniformly distributed volumetric source.

The angular response function of the detector pod is an average between an isotropic and a cosine response function. The two responses were computed separately, then averaged. This procedure is discussed in Appendix C.

Some areas are blocked out with an (*) label. This indicates that in this region, extremely high count rates prevailed, producing spectral distortion or "pulse pileup." It was impractical to extract the individual radionuclide photopeaks from the spectra when spectral smearing due to high count rates were encountered (typically > 60,000 counts per second). The high count rates encountered here may have been due to large quantities of radioactive material on the ground or in the airborne effluent from facility operations in the survey area. In this survey, ^{41}Ar was the most prominent interfering airborne radionuclide.

5.0 RESULTS

5.1 Isopleths

Four sets of mapped isopleths have been developed from the measured spatially distributed gamma spectral data collected once every three seconds during the survey mission. They are:

Man-Made Gross Count Isopleths	Figure 10
^{137}Cs exposure rate isopleths	Figure 11
^{60}Co exposure rate isopleths	Figure 12
^{60}Co plus ^{137}Cs exposure rate isopleths	Figure 13
Natural terrestrial exposure rate isopleths	Figure 14

At the 500-ft altitude and 1000-ft flight line spacing, the ^{60}Co and ^{137}Cs isopleths represent complete coverage of the survey area. The circular area of interrogation on the terrain as viewed by the airborne detector system was approximately 1000 ft in diameter. The helicopter survey velocity was 150 ft/sec. Spectral data were collected once every 450 ft for the isopleths. Single channels were set to monitor the ^{60}Co and the ^{137}Cs windows for a 1.0-second time interval (corresponding to 150 ft spatial resolution).

The ^{60}Co and ^{137}Cs exposure rate isopleths shown in Figures 11 and 12 have the contribution from natural radioelements removed, and represent exposure rates from only these man-made isotopes. Typically, the exposure rate for natural background radiation in the Savannah River Plant area is 6 ± 2 μR/hr, depending on the surface soil geology of the particular area.

No flight lines were flown directly over reactor facilities because of safety restrictions. The areas where radiation data were not available are clearly marked on each isopleth map. Some data points were eliminated for locations where the helicopter was turning or banking to avoid reactor facilities, since the radar altimeter gives erroneous information in this flight configuration and it is impractical to determine the detector angular dependent efficiency to terrestrial radiation in a banking flight mode.

Natural terrestrial exposure rates are shown in Figure 14. These data were derived from the 1.40 to 3.00 MeV energy window, thereby eliminating the man-made isotope exposure rates. The cosmic ray and airborne radionuclide contributions have been removed from the natural terrestrial exposure rate data.

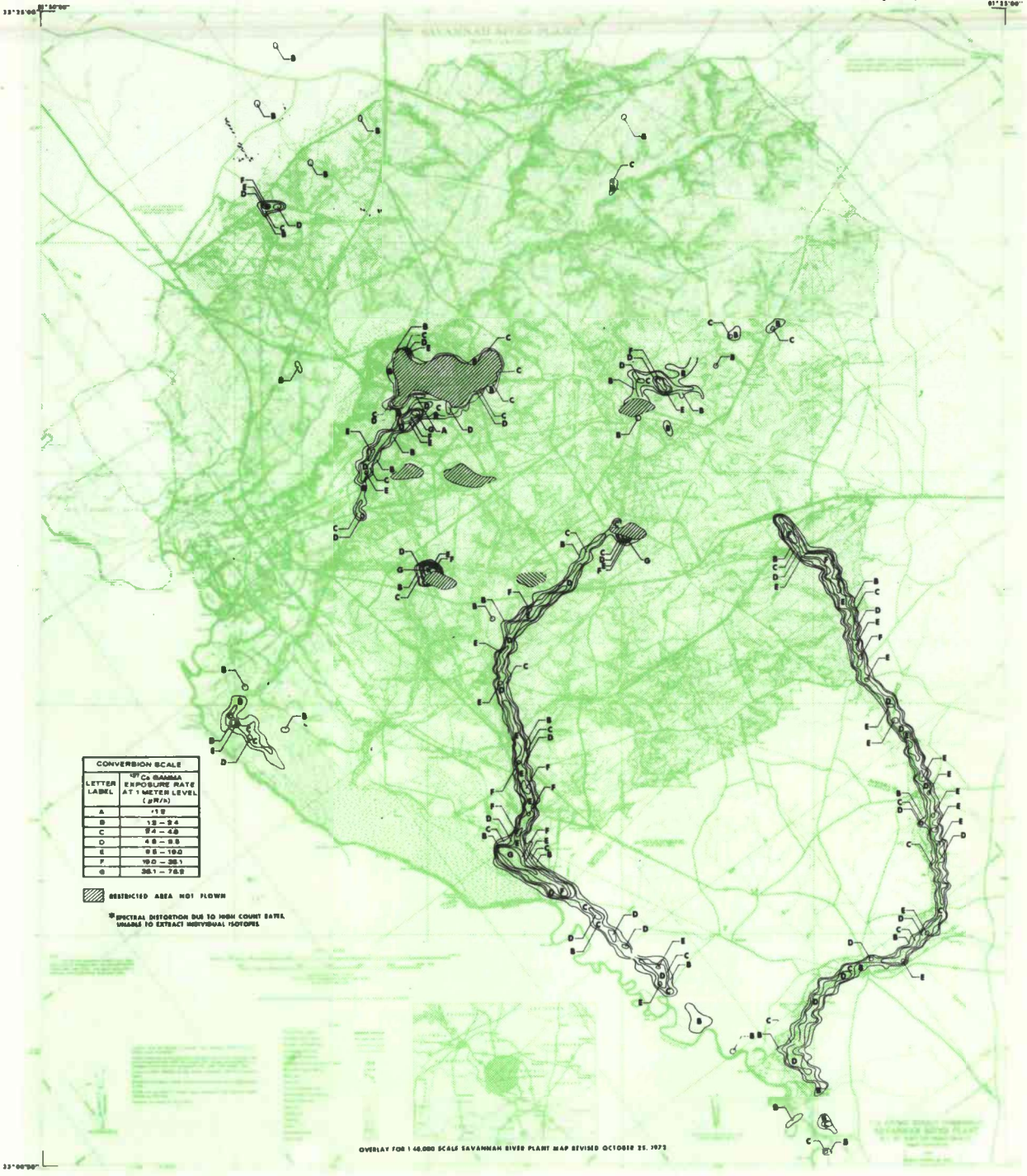

Figure 11. Map of the Cesium-137 gamma exposure rate isopleths (at the 3 ft above ground level) for the Savannah River Plant.

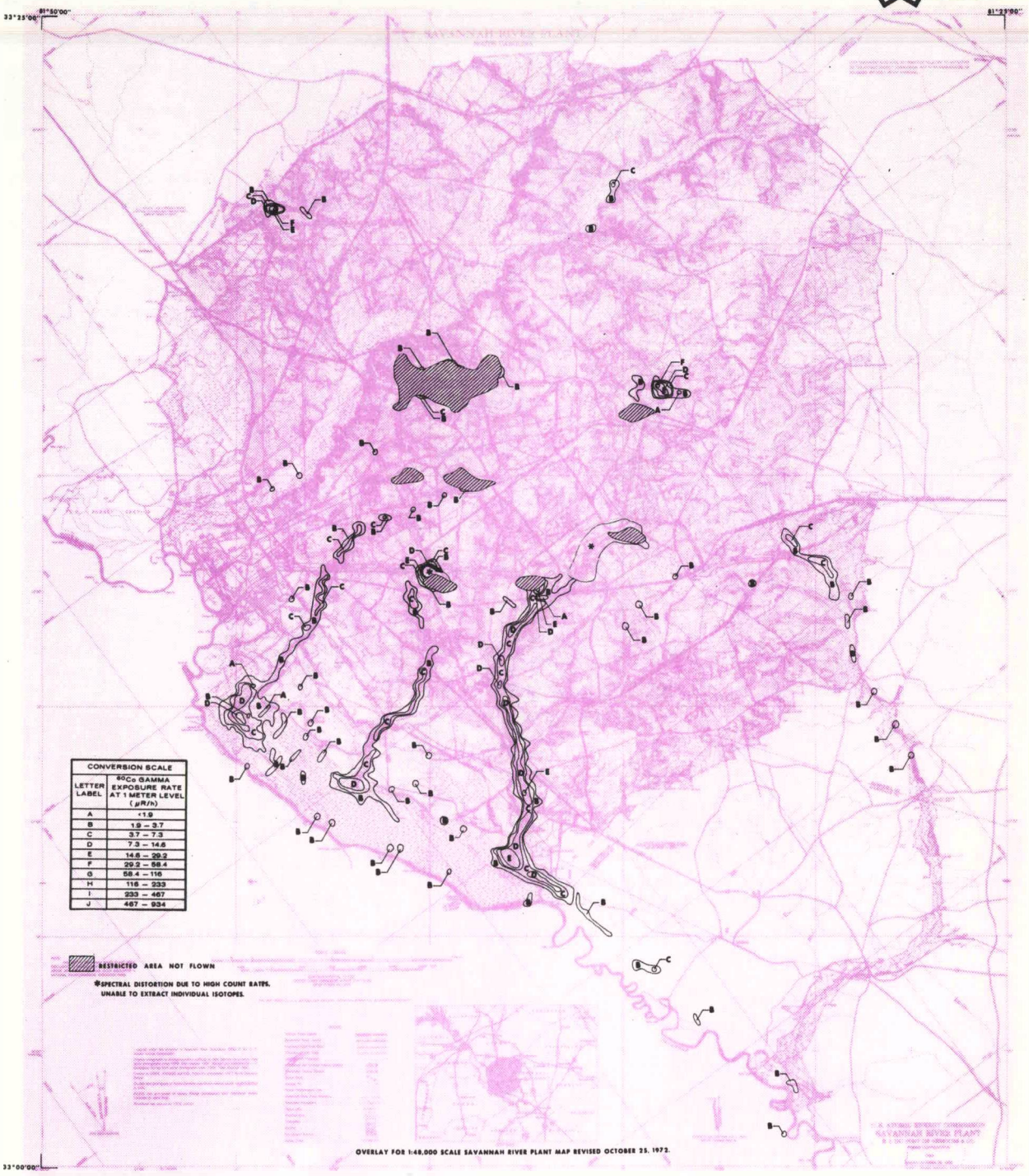

Figure 12. Map of the Cobalt-60 gamma exposure rate isopleths (at the 3 ft above ground level) for the Savannah River Plant.

Figure 13. Map of the Cobalt-60 plus Cesium-137 gamma exposure rate isopleths (at the 3 ft above ground level) for the Savannah River Plant.

Figure 14. Natural terrestrial exposure rate isopleths in μR/hr at 3 ft above ground level.

Selected spectral data are included in Appendix D. The area where the spectral data were acquired is labeled with a number and a line on the man-made gross count isopleth map. The length of the line indicates the distance over which the spectral data were summed. The spectral data in Appendix D are labeled with spectrum numbers which correspond to the numbers on the MMGC isopleth map.

5.2 Application to Surface Situations

Considerations for relating these airborne results to ground based measurements are discussed below. At 500 feet above terrain, the airborne detectors measure radiation from an area on the ground about 1000 to 1500 feet in diameter. The situation can be illustrated by visualizing that over 10^4 tons of surface soil are sampled in a single one-second airborne measurement. The airborne survey results, then, represent a pseudo-average over a large area of investigation. To obtain such an average by ground sampling requires a multitude of individual measurements. In attempting to compare aerial radiometric data with ground based measurements, one must also consider the isotope's vertical distribution in the soil, the spatial distribution contamination and terrain effects, such as ground roughness or ground cover. The airborne gamma detector cannot distinguish a point source of millicurie strength from a large area source of $\mu Ci/m^2$ strength. Lower altitude flights and closer spaced lines would be necessary for better resolution of localized "hot spots". Previous surveys have shown that an order of magnitude improvement in revealing detailed information of an area can be obtained by flying at lower altitudes (150 ft) and closer line spacing (150 ft).

A "B" level on the isopleth maps indicates the presence of man-made radiation. The threshold for the B level was set at the 3-standard deviation level of the variation in the data measured over the background reference area. From counting statistics alone, then, one would expect a B to show up about 0.1 to 1% of the time, even over the background reference area. Therefore, an isolated B on the isopleths may or may not be from man-made radiation. It is recommended that isolated B levels be discounted unless they show some

kind of trend such as congregation in a given area. In this case, the presence of the radioactive contaminant is more likely. A "C" level was set at 6-standard deviations resulting in a much stronger evidence of the presence of the radioelement contaminant.

Subsequent to the aerial survey, ground measurements were conducted by the Health Physics Environmental Monitoring Group at the Savannah River Plant.[3] The transects shown in Figure 15 were made to verify the aerial survey data. An exposure rate isopleth map derived exclusively from the ground survey data, was provided by the Savannah River Plant (Figure 16). An isoactivity map (Figure 17) was also provided by the Savannah River Plant from soil sample data.

Comparison of the aerial and ground survey data shows good correlation in the results of the two techniques and indicates the necessity for a broad view of the facility area from a survey altitude of 500 feet. However, the ground survey data suggests the need for a low altitude survey (150 feet) in areas where better resolution of the spatial distribution of the radionuclides is required.

A small area several yards wide with an exposure rate of 67 μR/hr was found during the ground survey. The aerial survey indicated this particular area had an exposure rate between 4.8 and 9.5 μR/hr. A small area source will be averaged over the entire field of view of the detector system ($\sim$1000-1500 ft) at the 500-ft survey altitude. The 150-ft altitude survey increases the accuracy of the spatial resolution and magnitude of the data by at least a factor of 3. This case exemplifies the need for a 150-ft-altitude survey over areas where distributions of man-made isotopes have been localized from the higher altitude survey.

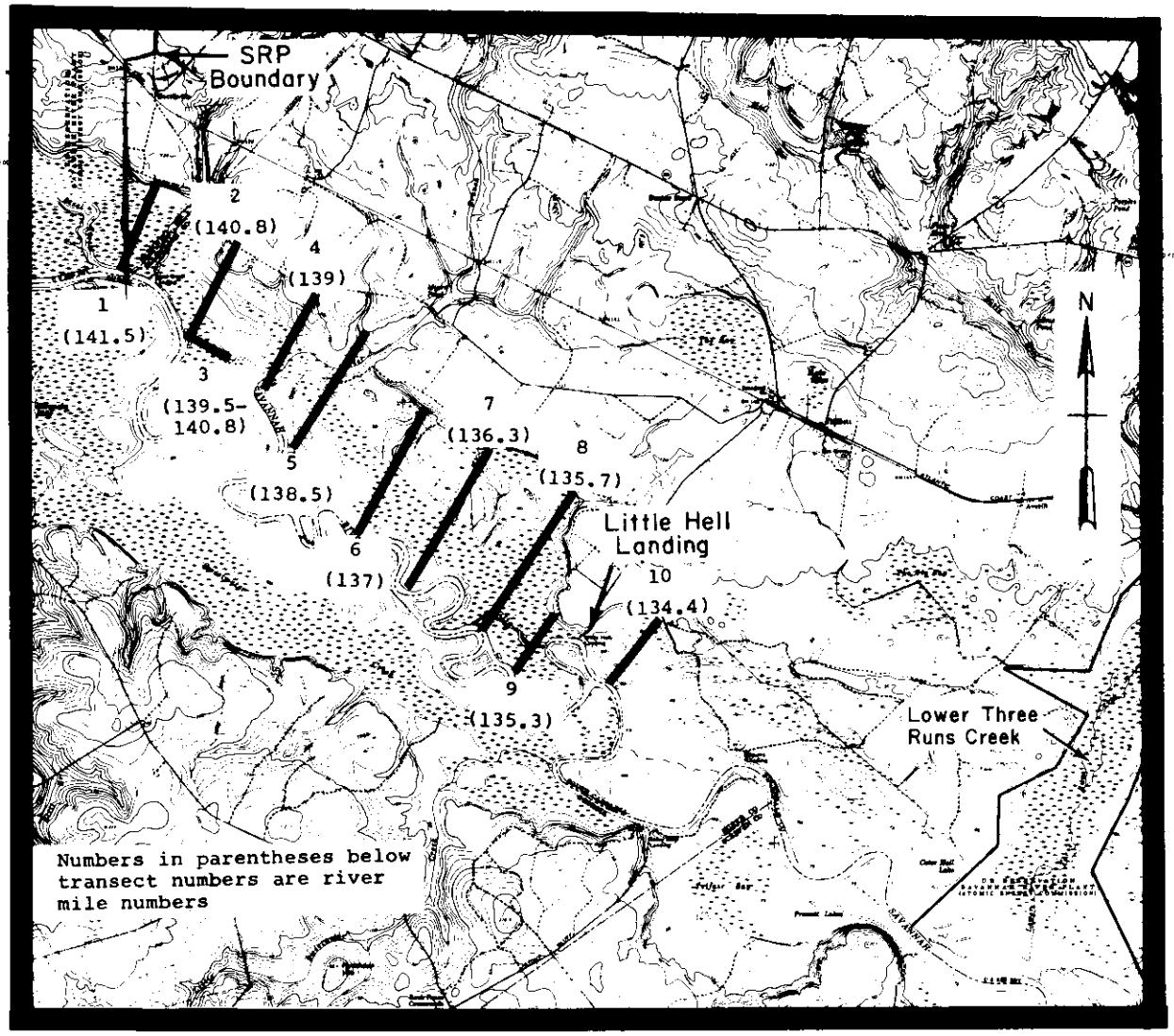

Figure 15. 1974 Ground survey transects.[3]

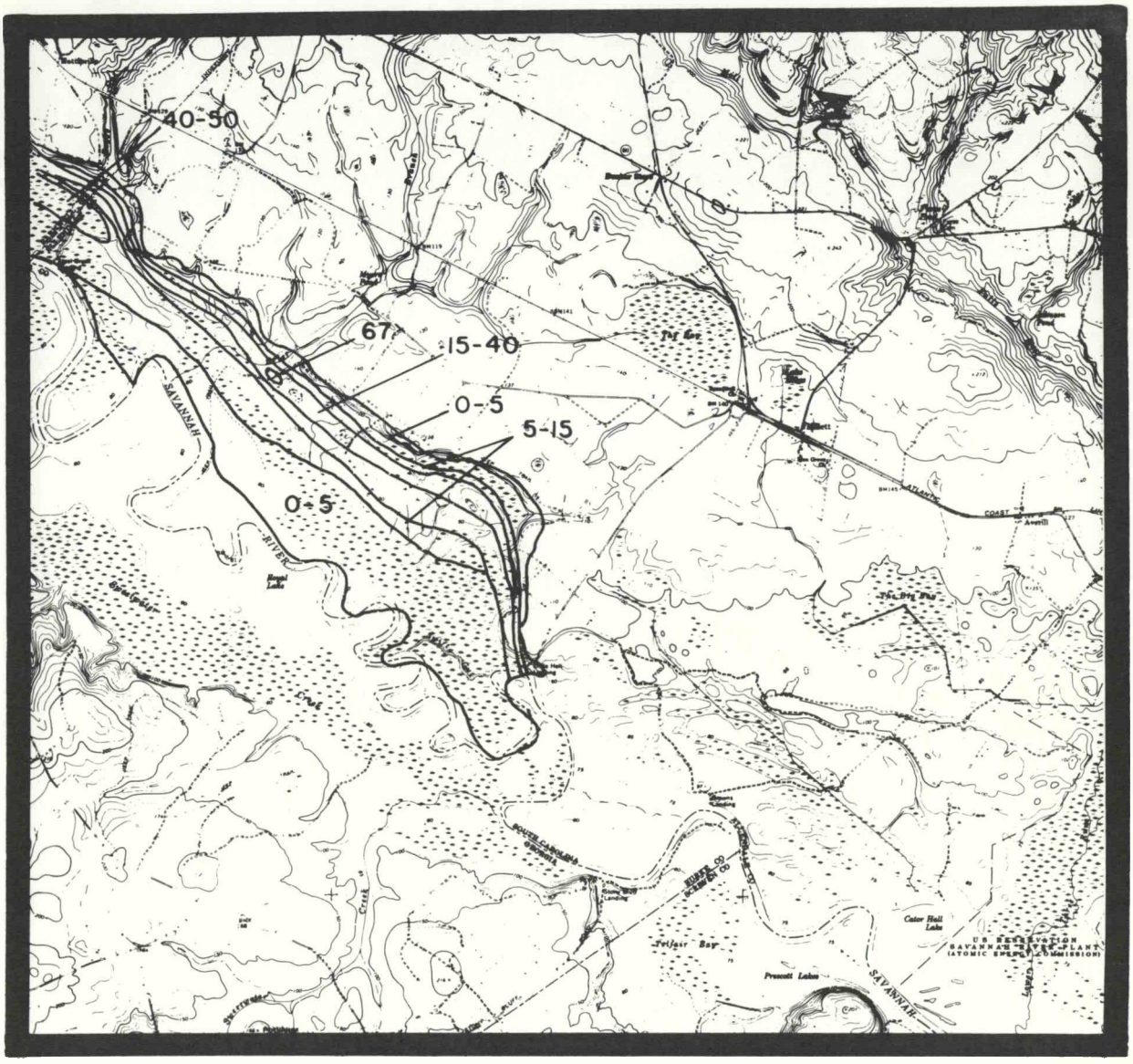

Figure 16. Exposure rate isopleths from 1974 ground survey[3] (exposure rate at 3 ft, μR/hr).

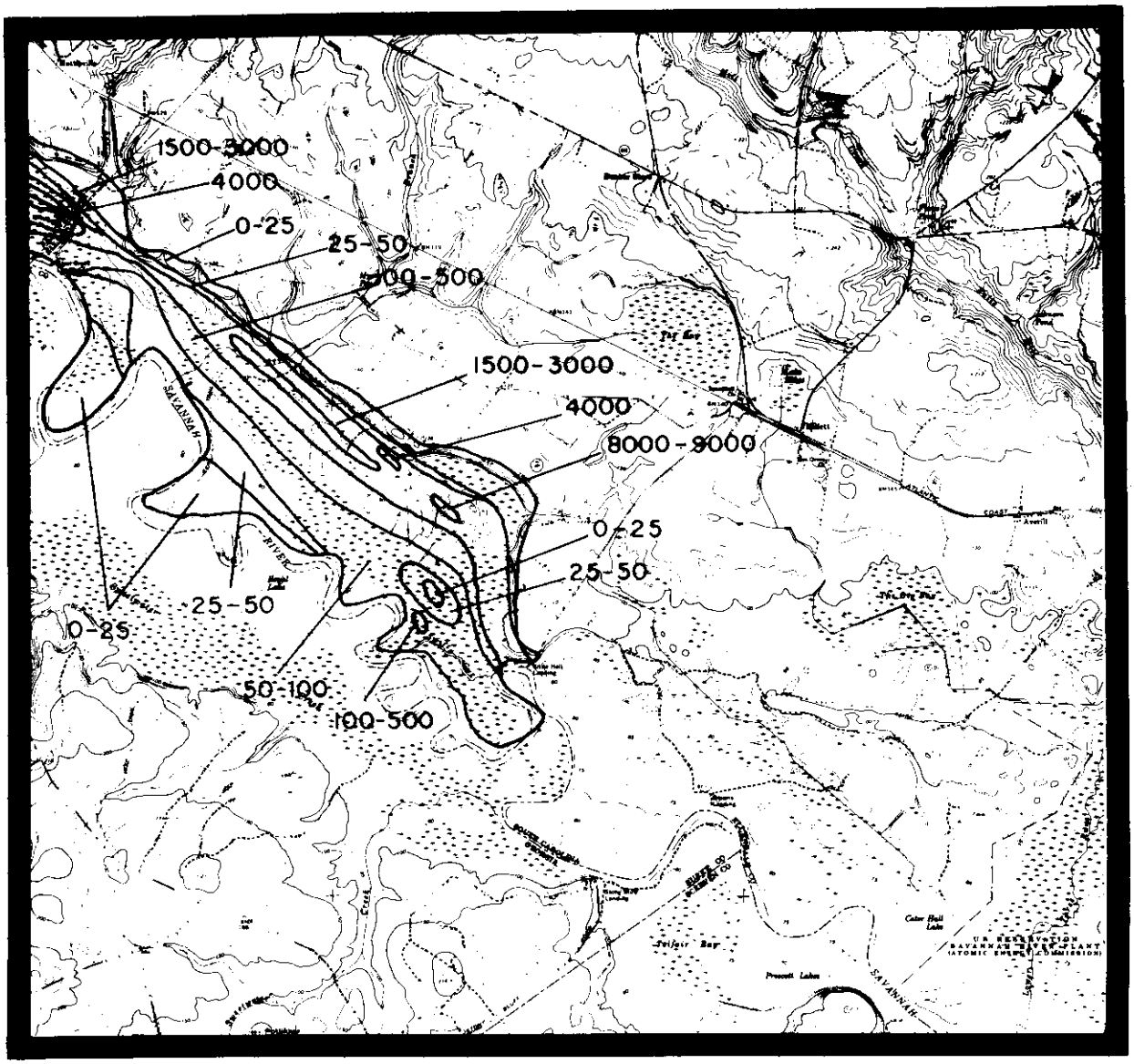

Figure 17. Radioactivity isopleths from 1974 ground survey[3] (cesium deposition, pCi/cm^2).

6.0 DISCUSSION OF ERRORS

The accuracy of the data presented here is limited by several sources of errors, which are discussed below. The primary data are presented as isopleth maps of gamma ray exposure rates, for gamma radiation from ^{60}Co, ^{137}Cs, and ^{60}Co plus ^{137}Cs. These data have the ^{214}Bi, ^{40}K, ^{208}Tl, and cosmic radiation natural background components removed.

The accuracy of the data presented as isopleths of gamma ray exposure rates is affected by several sources of error:

(a) The detector-source geometry during the measurement.

(b) Position and altitude uncertainties.

(c) Count rate losses, counting statistics and stability in the electronics system.

(d) Accuracy of conversion factors which relate photon count rates to gamma ray exposure rates at the 3-ft above ground level.

(e) Derivation of net gamma counts under a given photopeak by stripping out Compton tails from higher energy contributors.

(f) Errors in plotting the isopleths.

The survey measurements were flown at an altitude of 500 feet with a line spacing of 1000 feet. Since the detectors were unshielded, they observed the entire terrestrial plane, modified only by the increased air attenuation at large angles to the vertical direction, and the angular response of the detectors. For the gamma energy range including the 0.662 MeV, ^{137}Cs, and the 1.17 and 1.33 MeV ^{60}Co lines, the effective ground area observed by the detectors is represented by a circle approximately 1000-1500 feet in diameter (with some variation in sensitivity over that area). The flight line spacing of 1000 feet provides some overlap so that coverage of the surveyed area is essentially complete. At the 500-ft survey altitude,

a line spacing of 1000 feet was selected because the full width half maximum of the signal (as a function of aircraft position) from a point source would be greater than or equal to the line spacing. The measurements of a point or localized source will result in plotted isopleths showing a gradient of gamma exposure rate surrounding the point source. This gradient represents the gamma intensity field as viewed at an altitude of 500 feet, rather than representative of the surface terrestrial distribution of gamma source strength.

The errors associated with the position determinations of the aircraft are a function of the distance between the helicopter and the remote trisponders, and of the angle subtended by the trisponders at the helicopter. These errors are discussed in Appendix A. The distances between the helicopter and the two trisponders are recorded on magnetic tape to the nearest 10 feet.

Figure 18 shows the position of the two remote trisponders for the Savannah River Plant survey. The trisponders were calibrated for zero distance error at the center of the survey area. The maximum error of the position data in the Savannah River Plant survey was ± 54 feet.

The radar altimeter determined the altitude by measuring the time delay of a radio frequency pulse from the aircraft reflected back to the aircraft by the terrain surface. The rf pulses were radiated toward the ground by the transmitting antenna in a conical beam 35° wide. The altimeter measured the distance between the aircraft and the nearest ground object; some errors are incurred, however, over rapidly changing topography. However, the Savannah River Plant survey area is relatively flat and has only a few areas where altimeter errors are likely. The helicopter pilot was able to maintain the nominal survey altitude of 500 ± 50 feet. The radar altitude was recorded every second and all data were corrected for altitude deviations. At the 500-ft survey altitude, the accuracy of the altitude measurement was approximately 20 feet.

Since the detector system response has been established by numerous experimental techniques, the most significant error in the isopleth maps stemmed from source geometry assumptions. The

Figure 18. Position of remote trisponders.

exposure rate conversion factors can vary significantly, depending on the accepted source distribution in the soil (planar or volume sources, see Appendix C). The isopleth maps plotted in Figures 11, 12, and 13 incorporate the assumption of a uniform distribution of the radionuclides over the 1000-ft diameter circle of interrogation by the detectors at 500 feet above the terrain surface. A localized area of contamination, a few feet in diameter, would be averaged over the 1000-ft diameter circle. For this reason, a ground based survey may indicate some small areas of higher specific activity than the aerial survey (see Section 5.2).

Errors due to counting statistics were less than a few percent, using the 40 detectors. The main source of error in spectral photopeak extraction was the spectral pileup distortions caused by high count rates. Areas suspected of spectral distortions have been eliminated from the isopleths. It is very difficult to determine photopeak count rates by stripping the spectral data in high count rate areas when the spectrum is distorted.

The major radioactive contaminants at the Savannah River Plant site appear to be in stream beds and swampy areas. This makes it very difficult to compare later ground surveys because variations in the water level may alter the measured exposure rates. Small variations of the water level of a stream have a significant effect on the exposure rate measured at the 3-ft level above the terrain. Previous aerial surveys of the Savannah River Plant site have produced measured variations in exposure rates over the streams and swamps as a function of the water level at the time of the survey.

7.0 SUMMARY

Most of the man-made gamma ray emitting radionuclides in the Savannah River Plant environment, exterior to the Plant buildings, was found to be in the tributaries from the Savannah River Plant area, extending through the swamp, to the Savannah River. The gamma exposure rates measured along Lower Three Runs Creek are due principally to ^{137}Cs, with small areas of low level ^{60}Co activity near the dam on Par Pond. The highest exposure rate due to the combined ^{60}Co and ^{137}Cs contaminants was between 32 and 57 $\mu R/hr$ near the dam on Par Pond.

The gamma exposure rates along Steel Creek are due to both ^{60}Co and ^{137}Cs activity. The highest level of activity was found at the mouth of the creek as it empties into the Savannah River swamp. The total gamma exposure rates in this area were measured to be a maximum of 57 to 100 $\mu R/hr$, with levels of 38 to 76 $\mu R/hr$ attributed to ^{137}Cs and levels of 15 to 29 $\mu R/hr$ attributed to ^{60}Co.

All of the gamma activity measured along Pen Branch Creek is due to ^{60}Co. The maximum exposure rate here was determined to be in the 7 to 15 $\mu R/hr$ range.

The gamma activity along Four Mile Creek appears to be due to the combined presence of ^{60}Co and ^{137}Cs. The exposure rates between the burial grounds and road #3 are due to ^{137}Cs. From road #3 to the swamp, the gamma activity is due to ^{60}Co. At the mouth of the creek, where it enters the swamp area, both ^{60}Co and ^{137}Cs contaminants are present. The maximum exposure rate along the creek area was found to be 10 to 18 $\mu R/hr$.

No detectable man-made radionuclides were found in Upper Three Runs Creek. However, there appears to be an increase in the ^{214}Bi activity associated with the creek drainage route.

The measured man-made gamma gross count data over the Allied Gulf Processing Plant and the Chem-Nuclear waste burial facility are not attributed to the Savannah River Plant operations. Individual isotopes were not identified in these areas because of spectral distortions due to high gamma count rates.

High count rates were also observed over the burial grounds and near the reactor facilities; however, the areas are marked on the isopleths as restricted area not flown because the aircraft was turning to avoid flying directly over the facilities. It is impossible to compute the source to detector geometry when the aircraft is turning (Section 5. 0).

The survey results reported here represent the most accurate and complete aerial measurement of radioactive contaminants conducted at the Savannah River Plant. Previous aerial surveys were carried out using a less sophisticated data acquisition system, which collected only gross gamma counts and spectral data averaged over a distance of several miles.

The 500-ft survey altitude and 1000-ft flight line spacings used in the survey provided a comprehensive measurement of the radiological contaminants at the Savannah River Plant. The spatial distribution of radioelements was resolved to approximately a 1000-ft circular area of interrogation.

It should be noted that the spatial distribution of radioelement contaminants as shown by the isopleth maps in this report are based on aerial measurements at 500-ft altitude. The data are the average exposure rates over the 1000-ft diameter circle of investigation. These may be somewhat different (particularly for the case of a point source or a line source of contaminants) from isopleths developed from ground-based measurements. Any comparison of the data to that measured employing ground-based instrumentation should take into account these differences.

APPENDIX A

TRANSFORMATION RELATING THE MICROWAVE RANGING SYSTEM (MRS) COORDINATES TO THE SURVEY COORDINATES AND DISCUSSION OF POSITION ERRORS

The position of the survey aircraft is continuously measured and recorded, using a trisponder microwave ranging system. Two remote trisponders are interrogated by a master trisponder in the aircraft; the round trip time of travel for the pulsed microwave signal is measured and used to establish the aircraft's position with respect to the ground-based trisponders.

The distances r_1 and r_2 (see Figure A1) between the aircraft and the two remote trisponder units are documented on magnetic tape once every second. In order to relate r_1 and r_2 to the survey coordinate system the MRS base (b) has to be measured after the trisponders have been positioned. The geometry of the MRS to survey coordinate system transformation is shown in Fig A1, as a generalized configuration. After b has been measured, H_o, V_o and angle α can be calculated and used as inputs to the NOVA computer. All data are then plotted relative to the survey coordinate system H and V. The mathematical solution for H and V in terms of MRS coordinate system parameters is derived from simple trigonometry (see Figure A1) and is expressed as

$$H = H_o + x \cos \alpha - y \sin \alpha$$

$$V = V_o + x \sin \alpha + y \cos \alpha$$

Position errors are related to the distance parameter (between the aircraft and the remote trisponder) as well as to the angle α between the directions to the remote trisponder at the aircraft position. The variation of these distance - related and angle - related errors are shown in Figures A2, and A3, respectively. From Figure A3 it is apparent that the normal or operating value for the angle α is between 30° and 150°.

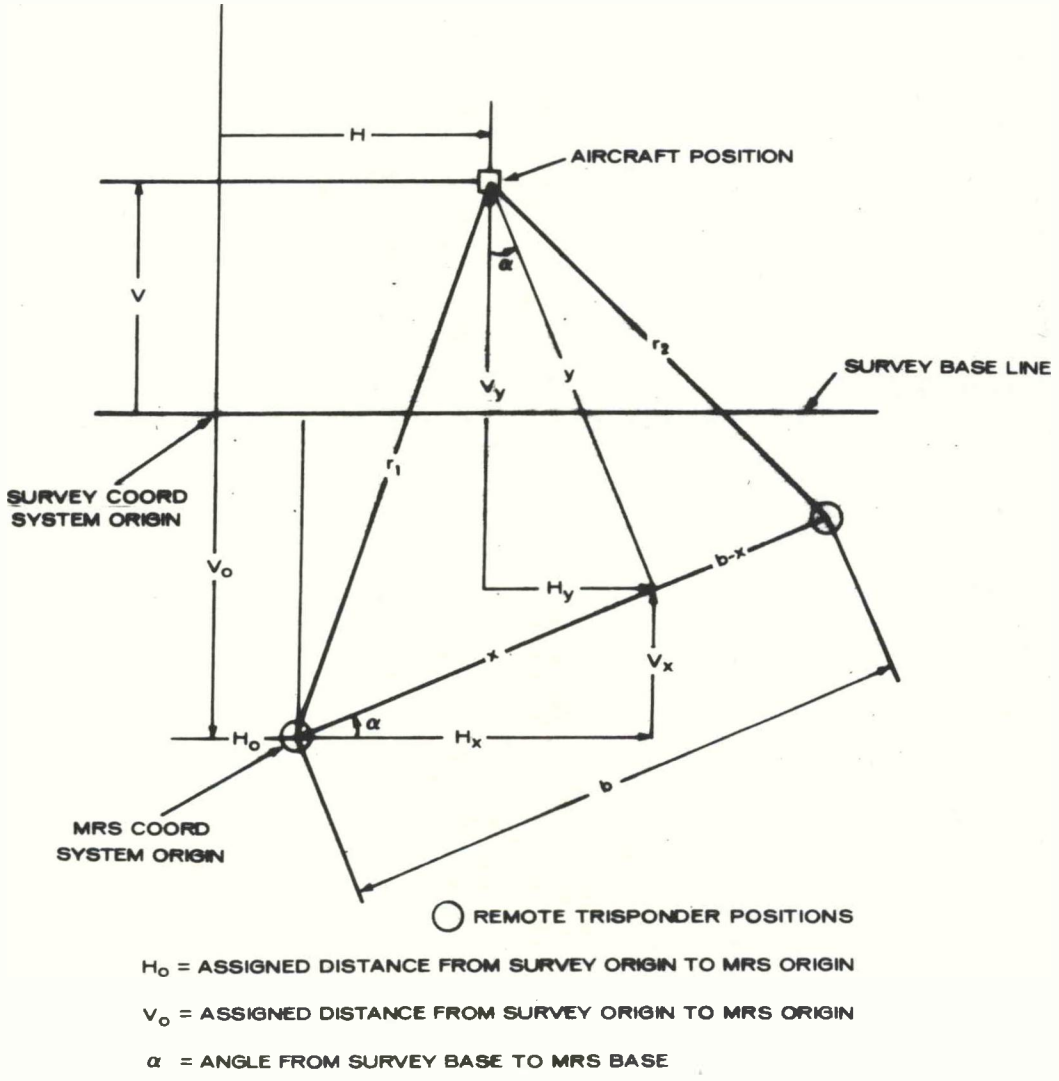

Figure A-1. Geometry relating the MRS and survey coordinate systems.

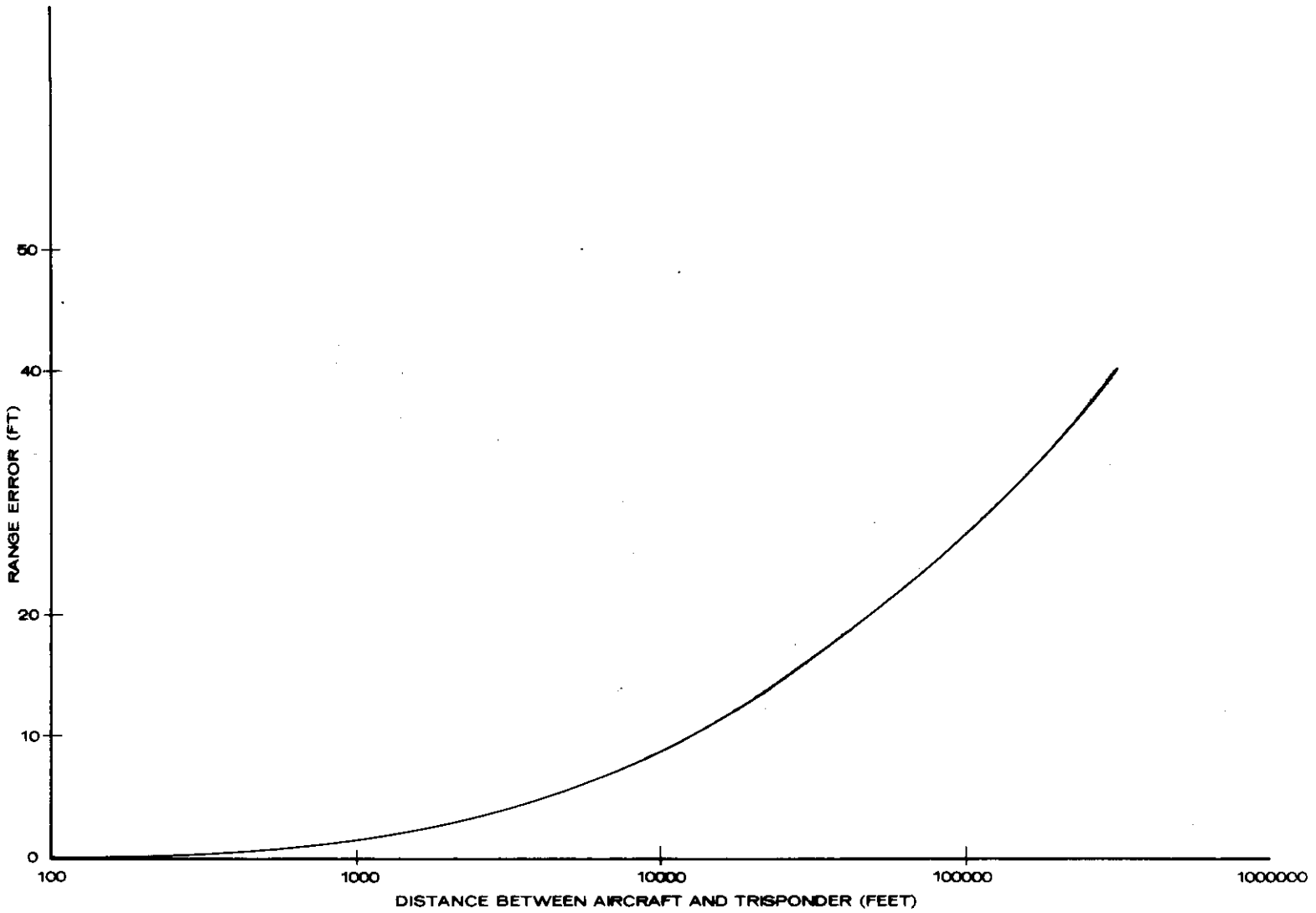

Figure A-2. Systematic range error curve for Del Norte microwave ranging system.

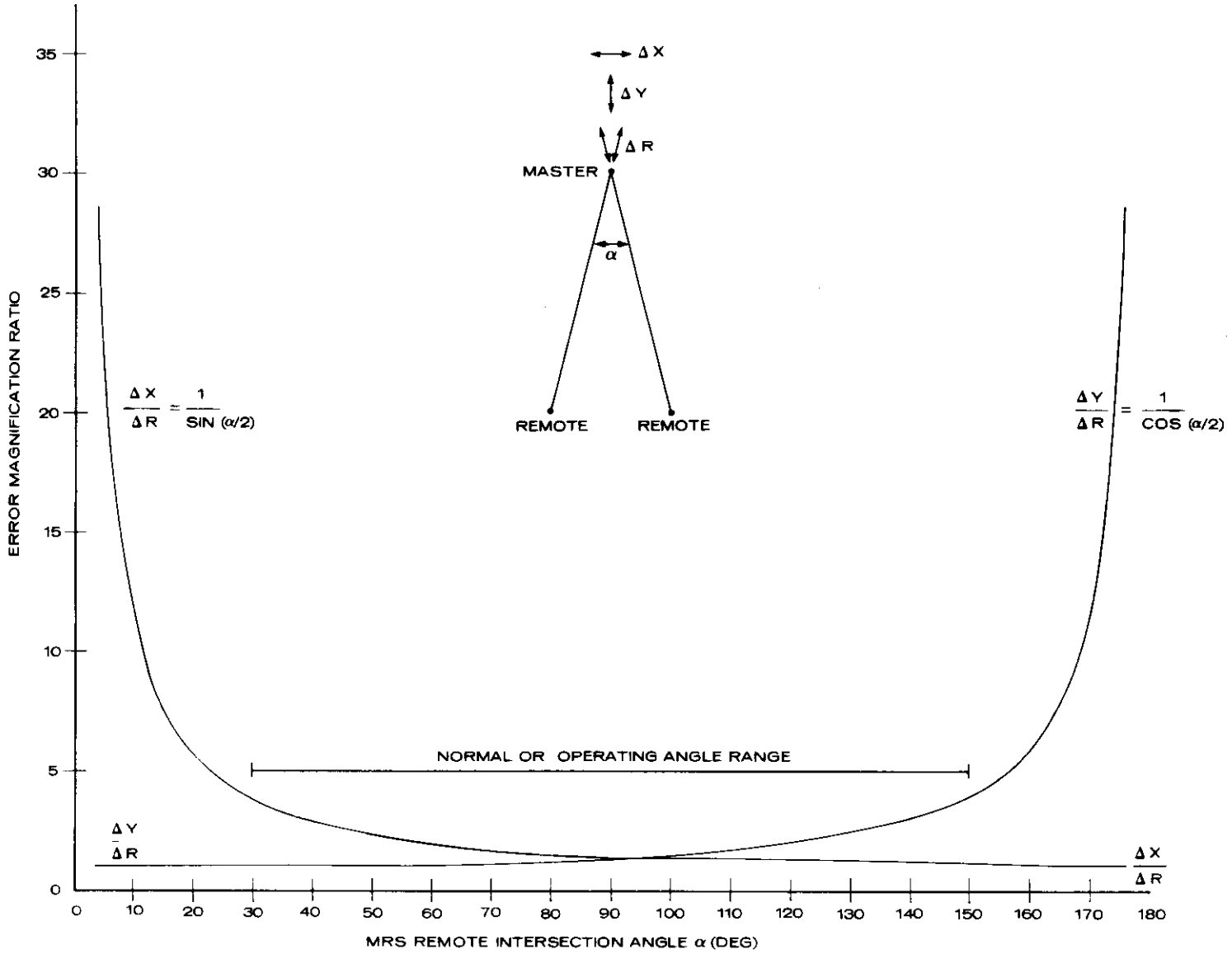

Figure A 3. The errors in the magnification rates $\Delta X/\Delta R$ as a function of the MRS remote intersection angle α.

APPENDIX B

DERIVATION OF GAMMA ENERGY SPECTRAL STRIPPING COEFFICIENTS

The gamma ray spectrum as measured during the aerial radiological survey of the Savannah River Plant consisted generally of gamma lines from two groups: gamma from natural radioelements and those from man made contaminants. The natural radioelements are represented principally by ^{40}K, ^{208}Tl from the thorium decay chain and $^{214}B_i$ from the uranium decay chain. Principal man made contaminants found at the Savannah River Plant were ^{137}Cs, ^{60}Co and ^{41}Ar.

In order to extract the contributions of the individual man made radioisotopes from the complex spectral data, a matrix analysis technique was utilized to derive extraction coefficients, and this derivation is outlined here.

The nature of the gamma pulse height distribution as measured by the NaI(Tl) detector array is illustrated in Figure B1. Gamma rays from naturally-occurring radioelements as well as from man made contaminants are shown. The gamma counts under any photopeak of interest is related to a specific radioisotope and is an indicator of the relative concentration of that particular isotope. However, the pulse height energy window encompassing each photopeak generally contains contributions from the Compton tails of higher energy gammas from other isotopes. In the analysis carried out here, the pulse height windows and related isotopes are defined in Table B1. In Figure B1, the contribution of gamma counts from ^{137}Cs, ^{60}Co, ^{41}A and natural background radioelements are indicated by the lower case letters c_s, c_ℓ and c_h, a, and b, respectively. The subscripts on these letters refer to the pulse height window number in which the particular contribution exists. For example, the gamma counts denoted as a_5 represents the Compton tail contribution from ^{41}Ar appearing in window #5, whereas a_3 represents the ^{41}Ar photofraction. The measured value of the gamma counts in the respective windows are sums of the separate contributions and are defined as B_2, A, C_L and C_S, where

$$B_2 = b_2 \quad \text{for window \#2} \qquad \text{Eq. 1}$$

$$A = a_3 + c_{h_3} + b_3 \quad \text{for window \#3} \qquad \text{Eq. 2}$$

$$C_L = c_{\ell_4} + a_4 + b_4 \quad \text{for window \#4} \qquad \text{Eq. 3}$$

$$C_S = c_{s_5} + c_{\ell_5} + a_5 + b_5 \quad \text{for window \#5} \qquad \text{Eq. 4}$$

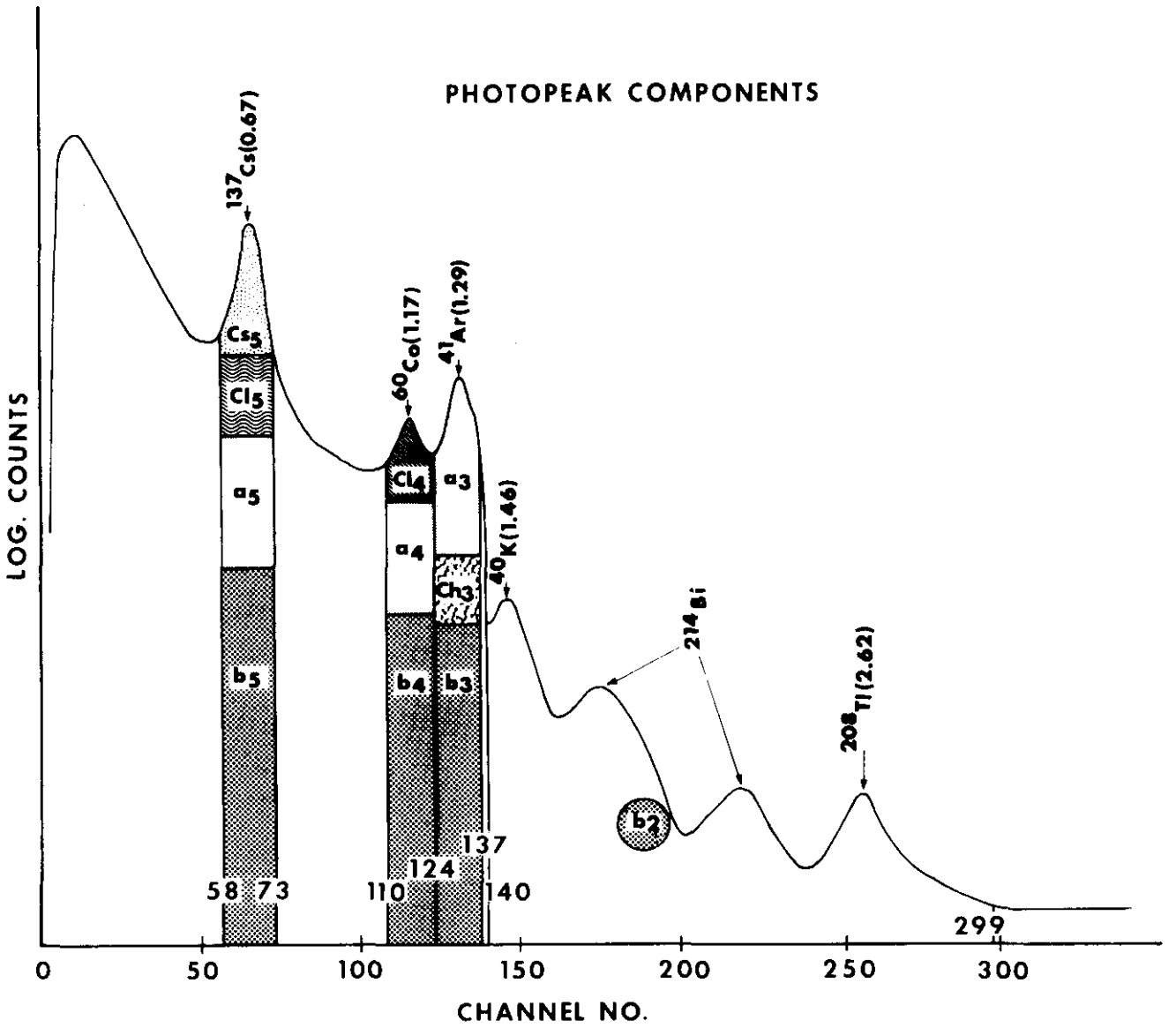

Figure B1. A gamma-ray pulse height spectrum from the NaI(Tl) crystal detectors used in the SRP survey, showing the position of the pulse height windows used in determination of spectral stripping coefficients. The letters c_s, c_l, a and b refer to spectral components related to ^{137}Cs, ^{60}Co (lower energy photopeak), ^{41}Ar, and natural background gamma radiation, respectively. The numerical subscripts indicate the window number (see Table B1) in which the spectral component resides.

Table B1. Definition of pulse height windows and related radioisotopes for derivation of spectral extraction coefficients.

Symbol	Window Number	Isotope	Channel Range of Window	Energy Range (MeV)
B_1	1	Background (Window #1)	0 → 139	0 → 1.39
B_2	2	Background (Window #2)	140 → 299	1.40 → 2.99
A	3	Argon-41	124 → 137	1.24 → 1.37
C_h	3	Cobalt-60 (high peak)	124 → 137	1.24 → 1.37
C_ℓ	4	Cobalt-60 (low peak)	110 → 123	1.10 → 1.23
C_s	5	Cesium-137	58 → 73	0.58 → 0.73

For a spectrum containing natural background contributions only, the following ratios were measured:

$$K_B = \frac{\text{counts in window \# 1}}{\text{counts in window \# 2}} = 23.44 \qquad \text{Eq. 5}$$

$$K_{BA} = \frac{A}{B_2} = 0.2329 \qquad \text{Eq. 6}$$

$$K_{BC_L} = \frac{C_L}{B_2} = 0.2955 \qquad \text{Eq. 7}$$

$$K_{BC_S} = \frac{C_s}{B_2} = 1.196 \qquad \text{Eq. 8}$$

For a spectrum of gammas from ^{41}Ar only (derived by subtracting a normalized background spectrum from one taken in an ^{41}Ar gas plume):

$$K_{AC_L} = \frac{C_L}{A} = 0.3815 \qquad \text{Eq. 9}$$

$$K_{AC_S} = \frac{C_s}{A} = 0.7413 \qquad \text{Eq. 10}$$

For a spectrum of gammas from ^{60}Co only (derived by subtracting a normalized background spectrum from one taken over an area containing no other man made radioelements except ^{60}Co).

$$K_{C_L C_H} = \frac{C_H}{C_L} = 0.7448 \qquad \text{Eq. 11}$$

$$K_{C_L C_S} = \frac{C_S}{C_L} = 2.291 \qquad \text{Eq. 12}$$

We may now write expressions for the measured values of gamma counts in the various pulse height windows as

$$B_2 = b_2 \qquad \text{Eq. 13}$$

$$A = a_3 + c_{b_3} + b_2 K_{BA} = a_3 + c_{\ell_4} K_{C_L C_H} + b_2 K_{BA} \qquad \text{Eq. 14}$$

$$C_L = c_{L_4} + a_3 K_{AC_L} + b_2 K_{BC_L} \qquad \text{Eq. 15}$$

$$C_S = c_{S_5} + c_{\ell_4} K_{C_L C_S} + a_3 K_{AC_S} + b_2 K_{BC_S} \qquad \text{Eq. 16}$$

$$B_1 - B_2\, K_B = \text{mmgc} = \text{true value of the man made gross counts} \qquad \text{Eq. 17}$$

Rearranging the terms in Equations 13 through 16, we have

$$a_3 + K_{C_L C_H} c_{\ell_4} + 0 c_{S_5} = A - K_{BA} B_2 \qquad \text{Eq. 18}$$

$$K_{AC_L} a_3 + c_{\ell_4} + 0 c_{S_5} = C_L - K_{BC_L} B_2 \qquad \text{Eq. 19}$$

$$K_{AC_S} a_3 + K_{C_L C_S} c_{\ell_4} + c_{S_5} = C_S - K_{BC_S} B_2 \qquad \text{Eq. 20}$$

Solving Equations 18, 19 and 20 for a_3 which is the ^{41}Ar gamma photofraction, we have:

$$a_3 = \frac{\begin{vmatrix} (A - K_{BA}B_2) & K_{C_L C_H} & 0 \\ (C_L - K_{BC_L}B_2) & 1 & 0 \\ (C_S - K_{BC_S}B_2) & K_{C_L C_S} & 1 \end{vmatrix}}{\begin{vmatrix} 1 & K_{C_L C_H} & 0 \\ K_{AC_L} & 1 & 0 \\ K_{AC_S} & K_{C_L C_S} & 1 \end{vmatrix}} \qquad \text{Eq. 21}$$

$$a_3 = \left[\frac{1}{1 - K_{C_L C_H} K_{AC_L}}\right] \left[A + \left(K_{C_L C_H} K_{BC_L} - K_{BA}\right) B_2 - K_{C_L C_H} C_L\right] \quad \text{Eq. 22}$$

Substituting the numerical values for the K_{ij} constants into Equation 22, we have

$$a_3 = 1.397\ A - 0.01790\ B_2 - 1.040\ C_L \quad \text{Eq. 23}$$

In like manner, we solve Eqs 18, 19 and 20 for c_{ℓ_4}, the ^{60}Co gamma photofraction of the lower (1.17 MeV) photopeak:

$$c_{\ell_4} = \frac{\begin{vmatrix} 1 & \left(A - K_{BA} B_2\right) & 0 \\ K_{AC_L} & \left(C_L - K_{BC_L} B_2\right) & 0 \\ K_{AC_S} & \left(C_S - K_{BC_S} B_2\right) & 1 \end{vmatrix}}{1 - K_{C_L C_H} K_{AC_L}} \quad \text{Eq. 24}$$

$$c_{\ell_4} = \left[\frac{1}{1 - K_{C_L C_H} K_{AC_L}}\right] \left[C_L + \left(K_{BA} K_{AC_L} - K_{BC_L}\right) B_2 - K_{AC_L} A\right] \quad \text{Eq. 25}$$

Substituting the numerical values of the K_{ij} constant into Equation 25, we have:

$$c_{\ell_4} = 1.397\ C_L - 0.2886\ B_2 - 0.5330\ A \quad \text{Eq. 26}$$

Finally, we solve Equations 18, 19, and 20 for c_{s_5}, the ^{137}Cs gamma photofraction:

$$c_{s_5} = \frac{\begin{vmatrix} 1 & K_{C_L C_H} & \left(A - K_{BA} B_2\right) \\ K_{AC_L} & 1 & \left(C_L - K_{BC_L} B_2\right) \\ K_{AC_S} & K_{C_L C_S} & \left(C_S - K_{BC_S} B_2\right) \end{vmatrix}}{1 - K_{C_L C_H} K_{AC_L}} \quad \text{Eq. 27}$$

$$C_{s_5} = \left[\frac{1}{1 - K_{C_L C_H} K_{AC_L}}\right] \Big[\Big(1 - K_{C_L C_H} K_{AC_L}\Big) C_s + \Big(K_{C_L C_H} K_{AC_s} - K_{C_L C_s}\Big) C_L$$
$$- \Big(K_{BC_s} + K_{C_L C_H} K_{AC_s} K_{BC_L} + K_{BA} K_{AC_L} K_{C_L C_s} - K_{BA} K_{AC_s}$$
$$- K_{C_L C_H} K_{AC_L} K_{BC_s} - K_{BC_L} K_{C_L C_s}\Big) B_2 + \Big(K_{AC_L} K_{C_L C_s}$$
$$- K_{AC_s}\Big) A\Big] \qquad \text{Eq. 28}$$

Substituting the numerical values for the K_{ij} constants into Equation 28, we have

$$C_{s_5} = C_s - 2.429\, C_L - 0.5214\, B_2 + 0.1854\, A \qquad \text{Eq. 29}$$

Substituting the value of K_B into Equation 17, the expression for the true value of the man made gross counts (mmgc) is:

$$(\text{mmgc}) = B_1 - 23.44\, B_2 \qquad \text{Eq. 30}$$

In order to separate out the gamma spectrum for the man made contaminants (mmgc) minus the ^{41}Ar contribution (to give only the terrestrial man made contaminants) we use the following procedure. For a sampled spectrum of only ^{41}Ar gammas, the counts in the argon photofraction (window #3) were measured to be 3038 counts. For the same spectrum, the total gamma counts, including the scattered gammas in window #1 were measured to be 43174 counts. The ratio of these two quantities is given as

$$\frac{\text{total counts in } ^{41}\text{Ar spectrum (window \#1)}}{\text{counts in } ^{41}\text{Ar photofraction (window \#3)}} = \frac{43174}{3038} = 14.21 \qquad \text{Eq. 31}$$

The total ^{41}Ar gamma counts, $\sum A$ may then be expressed as

$$\sum A = 14.21\, a_3 \qquad \text{Eq. 32}$$

Substituting the expression for a_3 given in Eq. 23 into Eq. 32, we get:

$$\sum A = 19.85\, A - 0.2544\, B_2 - 14.78\, C_L \qquad \text{Eq. 33}$$

Subtracting Equation 33 from Equation 30 to get the man made gross counts minus the ^{41}Ar contribution, we get

$$mmgc - \sum A = B_1 - 23.19\ B_2 - 19.85\ A + 14.78\ C_L \qquad \text{Eq. 34}$$

Examining Equations 23, 26 and 29, we see that the true values of the photofractions for the gamma spectra related to ^{41}Ar, ^{60}Co (lower energy photopeak) and ^{137}Cs, respectively are expressed by a set of products of constants and measurable quantities (total gamma counts in the pulse height window). These constant multipliers for the gamma counts in the defined windows are summarized in Table B2. Similarly the appropriate multipliers for the man made gross counts and the man made gross counts minus total ^{41}Ar counts are taken from Equations 30 and 34, respectively and are also given in Table B2. These are referred to here as photofraction stripping coefficients and are valid when either one or all three of the man made radioactive contaminants are present.

Table B2. Pulse height window multipliers (stripping coefficients) for specific isotopes measured during the SRP survey.

window number	channel number range	value of extraction coefficients				
		^{137}Cs	^{60}Co	^{41}Ar	mmgc	mmgc-$\sum A$
1	0→139	0	0	0	1.0	1.0
2	140→299	-0.5214	-0.2886	-0.0179	-23.44	-23.19
3	124→137	0.1854	-0.5330	1.397	0	-19.85
4	110→123	-2.429	1.397	-1.040	0	14.78
5	58→ 73	1.0	0	0	0	0

APPENDIX C

GAMMA RAY EXPOSURE RATE CONVERSION FACTORS

In order to convert the aerial measurement of the number of gamma photopeak counts to an exposure rate 1 meter above the ground it is necessary to consider two important factors:

1) the response of the NaI detectors to photons entering off-axis, i.e at $\theta > 0$ (see Fig. A-1) and

2) the distribution of radionuclides in the soil.

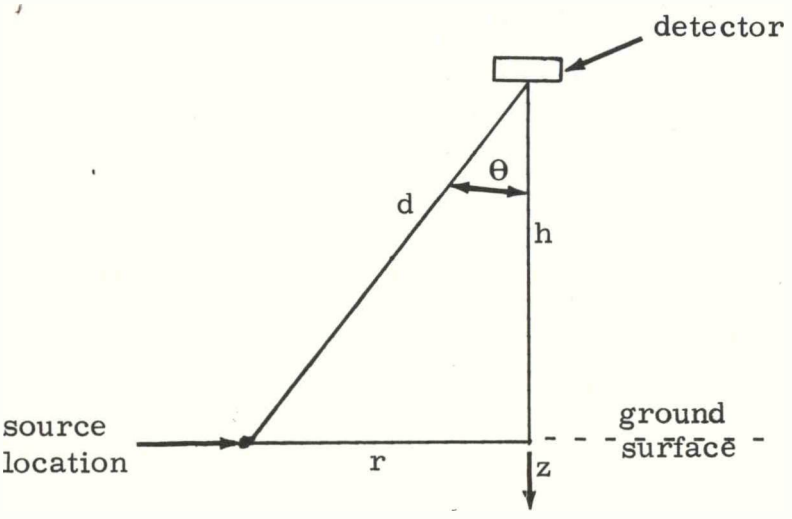

Figure A-1. Definition of geometric parameters related to the gamma detector calibration.

Two limiting cases of detector response will be considered: isotropic (uniform response for $0 \leq \theta \leq 90°$) and cosine (response decreases to zero at $\theta = 90°$ as $\cos \theta$). Similarly, two limiting cases of source distribution in the ground will be considered: uniform (isotopes are uniformly distributed both horizontally and vertically) and planar (isotopes are uniformly distributed horizontally only, with no vertical mixing in the soil). Four conversion factors are calculated with these assumptions, which are subsequently combined to yield the required exposure rate conversion factor. The counting efficiency of the helicopter-borne sodium iodide crystal detector package was determined by measuring the signal minus

background count rates while hovering over calibration sources of known strength. The photopeak window count rate, N_c, when hovering directly over a calibration source, can be written as

$$N_c = \frac{sA}{4\pi d^2} e^{-d/\lambda a} \quad (1)$$

where

- d = distance between the point source and the detector (cm),
- s = calibration source strength (photons/sec),
- λ_a = photon mean free path in air (cm),
- A = effective detector area (cm^2). This term includes an efficiency factor.

Case I. If we now assume a flux η_s (photons/sec-cm^2) at the ground surface level from an infinite planar radioactive source uniformly distributed over a ring of width dr on the ground and we assume an isotropic detector response, we can calculate N_{s1} (the total number of photons per second detected by the isotropic detector at an altitude h above the ground in the photopeak window from a planar surface aource).

$$dN_{s1} = \frac{\eta_s A e^{-\sqrt{h^2 + r^2}/\lambda a}}{4\pi(h^2 + r^2)} 2\pi r\, dr \quad (2)$$

where h = height of the detector above the ground.

Integrating for $0 \leq r \leq \infty$ we obtain:

$$N_{s1} = \frac{\eta_s A}{2} E_1 (h/\lambda a), \quad (3)$$

where $E_1 (h/\lambda_a)$ is an exponential integral of the first kind. By eliminating A between equations (1) and (3) we obtain the gamma flux η_s at the ground surface.

$$\eta_s = \left[\frac{s e^{-d/\lambda a}}{2\pi d^2 N_c E_1 (h/\lambda a)} \right] N_{s1} \quad (4)$$

The expression in brackets contains known parameters, for the conversion of counts measured by the detector to an infinite planar source (photons/cm^2-sec).

Case II. If the detector response is a function of the cosine of the angle θ between the source direction from the detector and the vertical, an additional factor of $\left|h/\sqrt{h^2 + r^2}\right|$ is included in the expression corresponding to Eq. (2). For this second case, we write the expression for N_{sc} (the total number of photons per second detected in the photopeak window).

$$dN_{sc} = \frac{\eta_s A h e^{-\sqrt{h^2 + r^2}/\lambda a}}{4\pi (h^2 + r^2)^{3/2}} 2\pi r\, dr \qquad (5)$$

Hence the count rate for a cosine-response detector is

$$N_{sc} = \frac{\eta_s A}{2} E_2 (h/\lambda a), \qquad (6)$$

where E_2 is an exponential integral of the second kind.

By eliminating A between Eqs. (1) and (6) we obtain:

$$\eta_s = \left[\frac{s e^{-d/\lambda a}}{2\pi d^2 E_2 (h/\lambda a)\, N_c}\right] N_{sc} \qquad (7)$$

Case III. Now let us consider a third case, in which the gamma flux η_U from a source which is uniformly distributed on the surface and also along the vertical z direction, i.e. from ground level to infinite depth. For this third case, we assume that the detector has isotropic response. The number of gamma rays detected in the photopeak window N_{U1} is

$$d^2N_{U1} = \frac{\rho\eta_U A e^{-\sqrt{h^2 + r^2}/\lambda a} e^{-Z\sqrt{h^2 + r^2}/\lambda_s h}}{4\pi (h^2 + r^2)} 2\pi r\, dr\, dz \qquad (8)$$

where

ρ = soil density (g/cm^3)

η_U = source strength $\left|\frac{\text{photons}}{\text{sec} \cdot \text{g}}\right|$

λ_s = mean free path of the gamma rays in soil (cm)

h = height of the detector above the ground (cm)

λa = mean free path of the gamma rays in air (cm).

Integrating over r and z we obtain:

$$N_{U1} = \frac{\rho \eta_U \lambda_s A}{2} E_2 (h/\lambda a), \tag{9}$$

where E_2 is again an exponential integral of the second kind.

We note that $\lambda_s = 1/\mu$, where μ is the linear attenuation coefficient. We eliminate the effective area A using Eqs. (1) and (9) to obtain:

$$\eta_\mu = \left[\frac{\mu}{\rho} \frac{s e^{-d/\lambda a}}{2 \pi d^2 N_c E_2 (h/\lambda a)} \right] N_{\mu i} \tag{10}$$

Case IV. Finally, if we assume that the detector response is a function of the cosine of the angle between the source and the detector, an additional factor of $(h/\sqrt{h^2 + r^2})$ is included in the expression corresponding to Eq. (8):

$$d^2 N_{\mu c} = \frac{\rho \eta_U A h e^{-\sqrt{h^2 + r^2}/\lambda a} e^{-z\sqrt{h^2 + r^2}/\lambda_s h}}{4 \pi (h^2 + r^2)^{3/2}} 2\pi r dr dz, \tag{11}$$

where η_u = gamma source strength $\left(\frac{\text{photons}}{\text{sec} \cdot \text{g}}\right)$

By integrating and eliminating A we obtain:

$$\eta_U = \left[\frac{\mu}{\rho} \frac{s e^{-d/\lambda a}}{2\pi d^2 N_c E_3 (h/\lambda a)} \right] N_{\mu 1}, \tag{12}$$

where E_3 is an exponential integral of the third kind.

Beck, et al*, have calculated the total exposure rate, (μR/hr) at one meter above the soil per unit concentration of source activity in the soil for monoenergetic sources. Their computations included the contributions from gamma rays scattered in both the soil and air and were determined from a polynominal solution to the gamma ray transport equation. The composition by weight of the soil used in the calculations is shown in Table C-1 below.

Table C-1. Composition by weight of soil used in Beck, et al's calculations

Al_2O_3	13.5%
Fe_2O_3	4.5%
$Si\ O_2$	67.5%
$C\ O_2$	4.5%
H_2O	10.0%

We use Beck et al's values of the calculated conversion factors J, relating the gamma flux to the gamma exposure rate at one meter above the ground surface for both surface and volume distribution of radioactive isotopes in the soil. These J values are tabulated below in Table C-2, together with the values of the mean free path λ_a in air and the mass attenuation coefficient μ/ρ for the soil composition described in Table C-1. These parameters are listed for the two difference source distribution cases described earlier for the ^{137}Cs and ^{60}Co isotopes.

The appropriate factor J from Table C-2 can be applied to the surface and volume sources to convert the source term to an exposure rate at one meter above ground in μR/hr.

The cosine and isotropic exposure rate conversion factors are averaged to approximate the actual conversion factor for the response of the detector system.

---

*Beck, H. L., DeCampo, J., and Gogolak, C., "In Situ Ge(Li) and NaI(Tl) Gamma Ray Spectrometry," Report No. HASL-258, Health and Safety Laboratory, U S Atomic Energy Commission, New York, New York, September 1972.

Table C-2. Constants used for exposure rate conversions for the Savannah River Plant survey, June 1974.

Isotope	Source Distribution	J	λa (cm)	μ/ρ for soil* (cm²/gr)
^{137}Cs	surface	3.4(μR/hr)/(photons/cm²-sec)	13,000	---
	Volume	19.6(μR/hr)/(photons/gm-sec)	13,000	0.078
^{60}Co	surface	5.8(μR/hr)/photons/cm²-sec)	17,000	---
	volume	38.4(μR/hr)/(photons/gm-sec)	17,000	0.057

The final exposure rate conversion factor used for the Savannah River Plant Survey is an average for the surface and volume sources. The exposure rate conversion factor is arrived at using the assumption that the distribution of the source is midway between an infinite planar source distribution and a volume source uniformly distributed in the soil. These conversion factors are given for ^{60}Co and ^{137}Cs in Tables C-3 and C-4, respectively.

Table C-3. ^{60}Co Conversion Factors

Source Distribution	Conversion Factor μR/hr per counts/sec: Isotropic Response	Cosine Response	Average detector response	Average detector response and source distributions
surface	0.0746	0.1141	0.0944	0.073
volume	0.0433	0.0595	0.0514	

*An average mass attenuation coefficient, $\mu/\rho = 0.057$ cm²/g, was obtained for photons of energy $E_{\gamma 1} = 1.333$ MeV and $E_{\gamma 2} = 1.172$ from Storm, E. and Israel, H. I., "Photon Cross Sections from 0.001 to 100 MeV for Elements 1 through 100," Report No. LA-3753, Los Alamos Scientific Laboratory, Los Alamos, New Mexico, 15 November 1967.

Table C-4: ^{137}Cs Conversion Factors

Source Distribution	Isotropic Response	Cosine Response	Average detector response	Conversion Factor μR/hr per counts/sec: Average detector response and source distributions
surface	0.0170	0.0245	0.02075	0.017
volume	0.0111	0.0146	0.01285	

With the spectral stripping procedure developed in Appendix B, the number of counts per second in the cobalt and cesium photopeaks was extracted from the spectral data.

From data obtained over an uncontaminated or background region, statistical fluctuations in the photopeak windows were obtained. Count rates within three standard deviations, σ, of the average are assigned the code level A (background). Rates greater than 3σ, but less than 6σ, are assigned the code level B. Each successive level limit is twice that of the previous limit. For the Savannah River Plant survey, the 3σ limit for ^{60}Co was 25 counts/sec and for ^{137}Cs was 70 counts/sec.

The code levels, together with the associated gamma count rates and exposure rates are given in Tables C-5 and C-6 for ^{60}Co and ^{137}Cs, respectively.

Table C-5: Gamma Exposure Rates for ^{60}Co at one meter above the ground

LEVEL	PHOTOPEAK COUNT RATE (counts/sec)	EXPOSURE RATE μR/hr
A	≤25	≤1.83
B	26 - 50	1.9 - 3.65
C	51 - 100	3.72- 7.30
D	101 - 200	7.37- 14.60
E	201 - 400	14.67- 29.20
F	401 - 800	29.27- 58.4
G	801 - 1600	58.47- 116.8
H	1601-3200	116.87- 233.6
I	3201-6400	233.67- 467.2
J	6401-12800	467.3 - 934.4

Table C-6: Gamma Exposure Rates for ^{137}Cs at one meter above the ground

LEVEL	PHOTOPEAK COUNT RATE (counts/sec)	EXPOSURE RATE μR/hr
A	≤70	≤1.19
B	71 - 140	1.21 - 2.38
C	141 - 280	2.4 - 4.76
D	281 - 560	4.78 - 9.52
E	561 - 1120	9.54 - 19.04
F	1121 - 2240	19.06 - 38.08
G	2241 - 4480	38.10 - 76.16
H	4481 - 8960	76.18 - 152.3
I	8961 - 17920	152.34 - 304.64
J	17921 - 35840	304.66 - 609.28

APPENDIX D

SELECTED GAMMA RAY SPECTRAL DATA

Spectral Interpretation

Spectral data have been plotted for selected areas of the SRP survey to examine the isotopic content. The spectral data were selected to verify extraction coefficients, identify isotopes other than ^{137}Cs, ^{60}Co, and ^{41}Ar, and eliminate false indications of isotopes when pulse pile-up occurs in high count rate areas. The selected ares where the spectral data were accumulated are numbered on the Man-Made Gross Count (MMGC) isopleth. The numbers correspond to the spectra in this appendix. The lines by each number indicate the position and length of the summation of the spectral data.

All selected spectral in this appendix have been background subtracted. The background data were selected in an "A" level of the MMGC, as close as possible to the area of selected spectra summation. The appropriate multiplication factors were used to equalize the total counts in the 1.39 to 3.00 MeV energy windows of both spectra, before subtraction. This normalization technique was used to eliminate the nominal background for the area from the selected data.

Some areas with a "B" level or greater on the MMGC isopleth are the results of a significant change in the geology (e.g. ^{40}K) of the area. However, all spectral data are examined for identification of isotopes responsible for any "B" level or greater in the MMGC. Table D-1 contains some examples of positive indications in the MMGC as the result of geologic variations.

Table D-1 lists the spectra number and probable isotopes present.

TABLE D-1

SPECTRUM NUMBER	PROBABLE ISOTOPES PRESENT
1	137-Cs, 60-Co
2	TRACE 60-Co
3	NATURAL
4	234M-Pa
5	NATURAL
6	ELECTRONIC NOISE
7	NATURAL
8	NATURAL
9	137-Cs
10	137-Cs
11	137-Cs, TRACE 60-Co
12	137-Cs, 60-Co, POSSIBLE TRACE 234M-Pa
13	137-Cs
14	137-Cs
15	137-Cs
16	137-Cs
17	137-Cs
18	234M-Pa
19	SPECTRAL DISTORTION (UNABLE TO IDENTIFY ISOTOPES)
20	SPECTRAL DISTORTION (UNABLE TO IDENTIFY ISOTOPES)
21	137-Cs, TRACE 60-Co
22	NATURAL
23	NATURAL
24	NATURAL
25	NATURAL
26	NATURAL
27	NATURAL
28	TRACE 60-Co
29	TRACE 60-Co
30	137-Cs, 60-Co
31	137-Cs, 41-Ar
32	137-Cs, TRACE 60-Co
33	137-Cs, 41-Ar, POSSIBLE TRACE 60-Co
34	137-Cs, 60-Co
35	60-Co
36	137-Cs, 60-Co
37	137-Cs
38	137-Cs,TRACE 60-Co
39	60-Co, TRACE 137-Cs
40	137-Cs, 60-Co
41	137-Cs
42	137-Cs, 60-Co
43	137-Cs, TRACE 60-Co
44	137-Cs, 60-Co
45	137-Cs, TRACE 60-Co
46	137-Cs
47	137-Cs
48	137-Cs
49	137-Cs
50	137-Cs
51	137-Cs

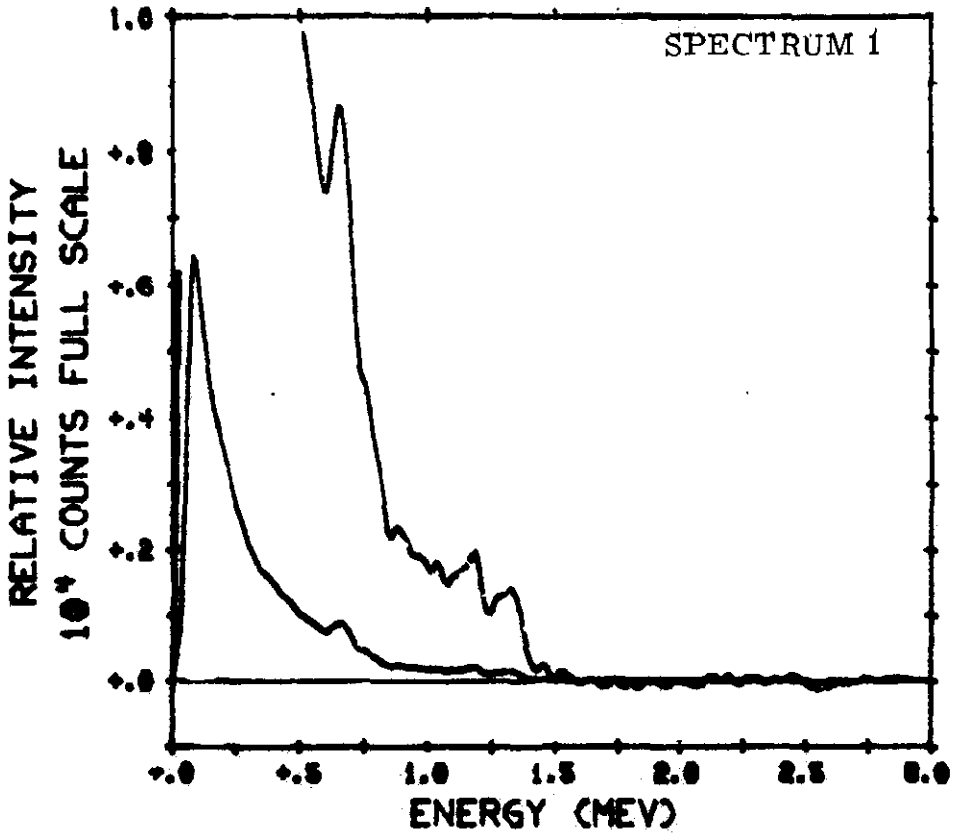
SPECTRUM 1
RELATIVE INTENSITY
10⁴ COUNTS FULL SCALE
1.0
.8
.6
.4
.2
.0
.0
.5
1.0
1.5
2.0
2.5
3.0
ENERGY (MEV)

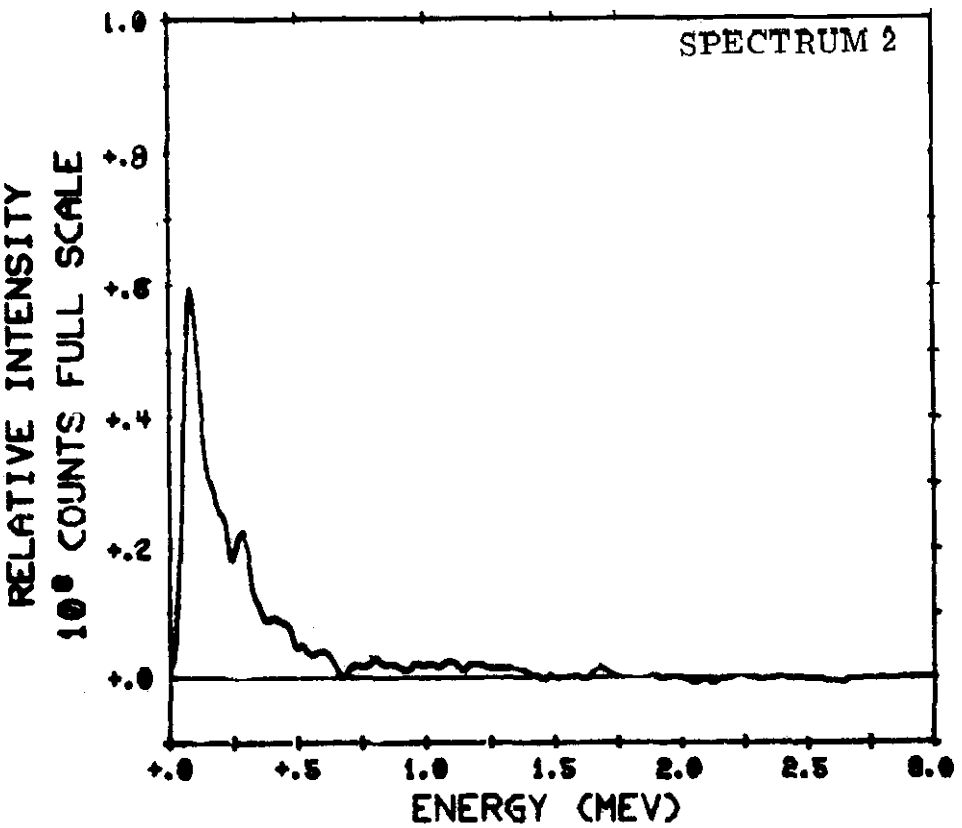
SPECTRUM 2
RELATIVE INTENSITY
10⁴ COUNTS FULL SCALE
1.0
.8
.6
.4
.2
.0
.0
.5
1.0
1.5
2.0
2.5
3.0
ENERGY (MEV)

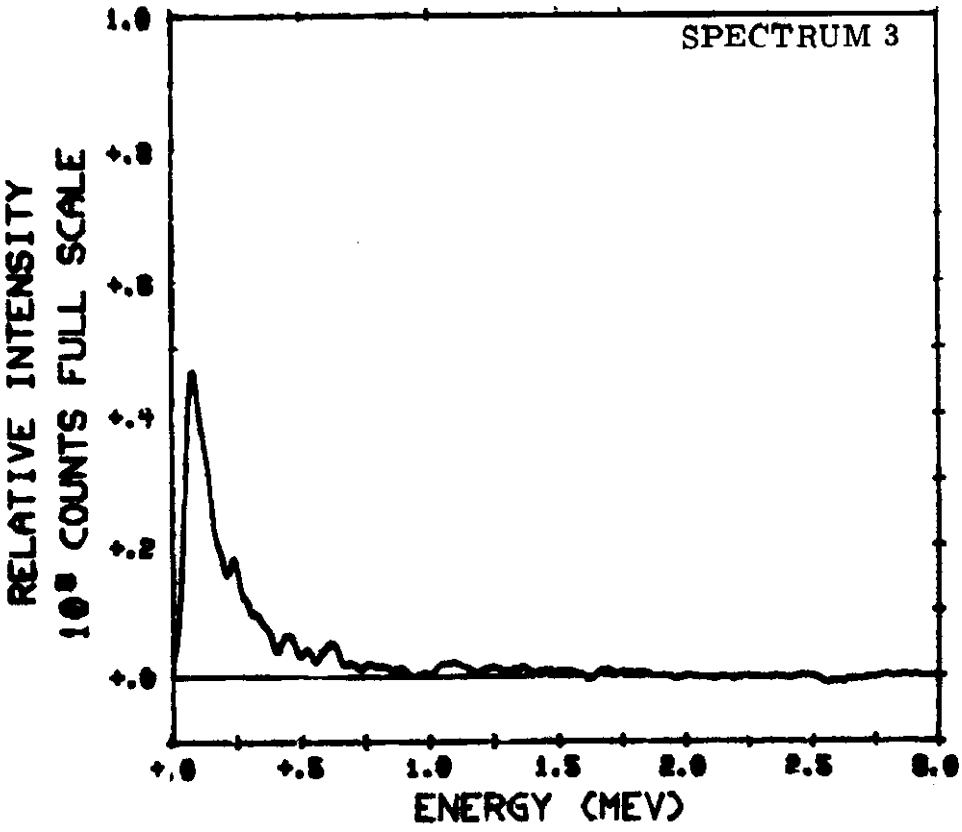
SPECTRUM 3
RELATIVE INTENSITY
10⁸ COUNTS FULL SCALE
1.0
.8
.6
.4
.2
.0
.0
.5
1.0
1.5
2.0
2.5
3.0
ENERGY (MEV)

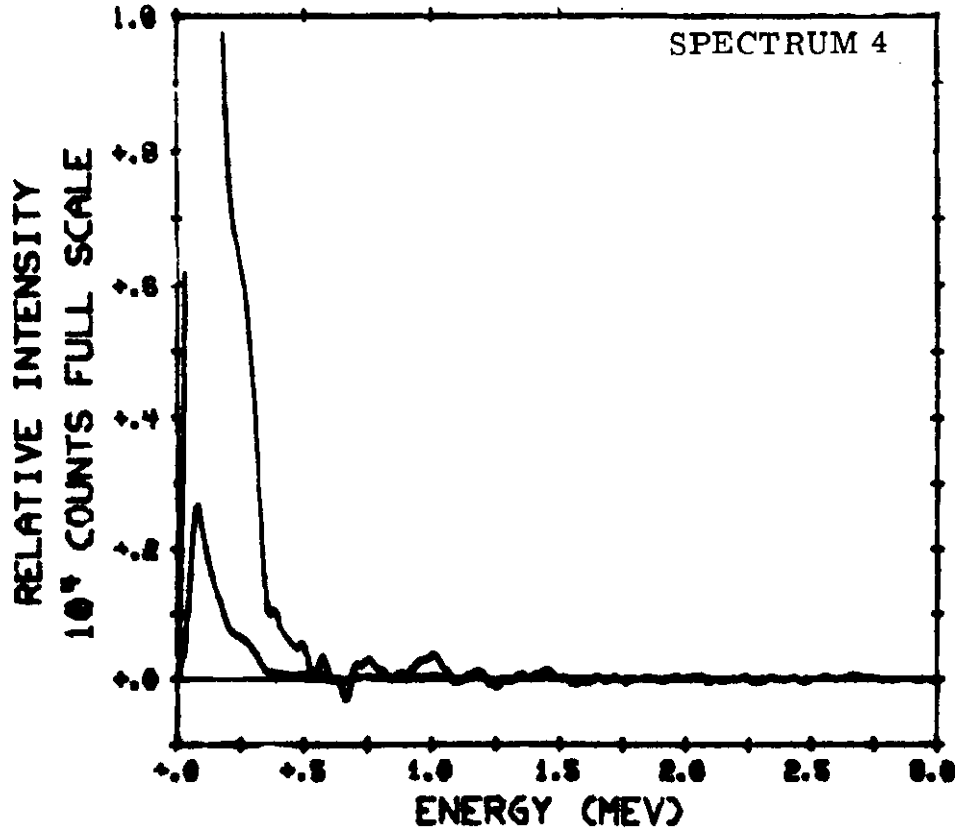
SPECTRUM 4
RELATIVE INTENSITY
10⁸ COUNTS FULL SCALE
1.0
.8
.6
.4
.2
.0
.0
.5
1.0
1.5
2.0
2.5
3.0
ENERGY (MEV)

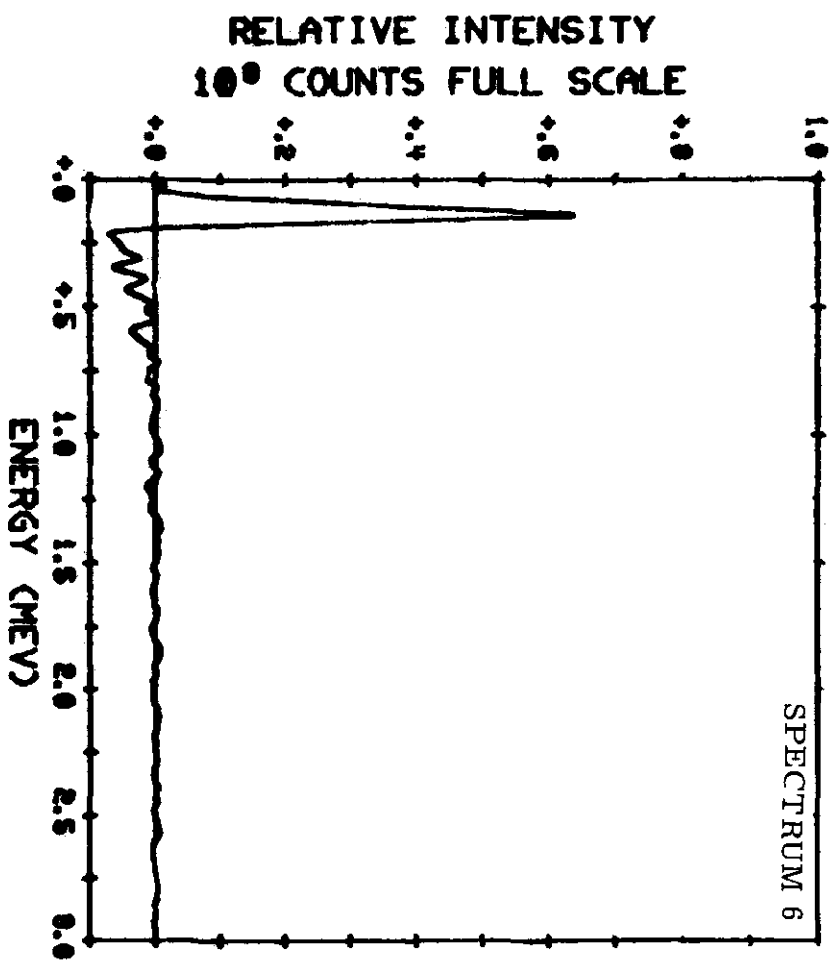
RELATIVE INTENSITY
10⁸ COUNTS FULL SCALE
+.0
+.2
+.4
+.6
+.8
1.0
+.0
+.5
1.0
1.5
2.0
2.5
3.0
ENERGY (MEV)
SPECTRUM 6

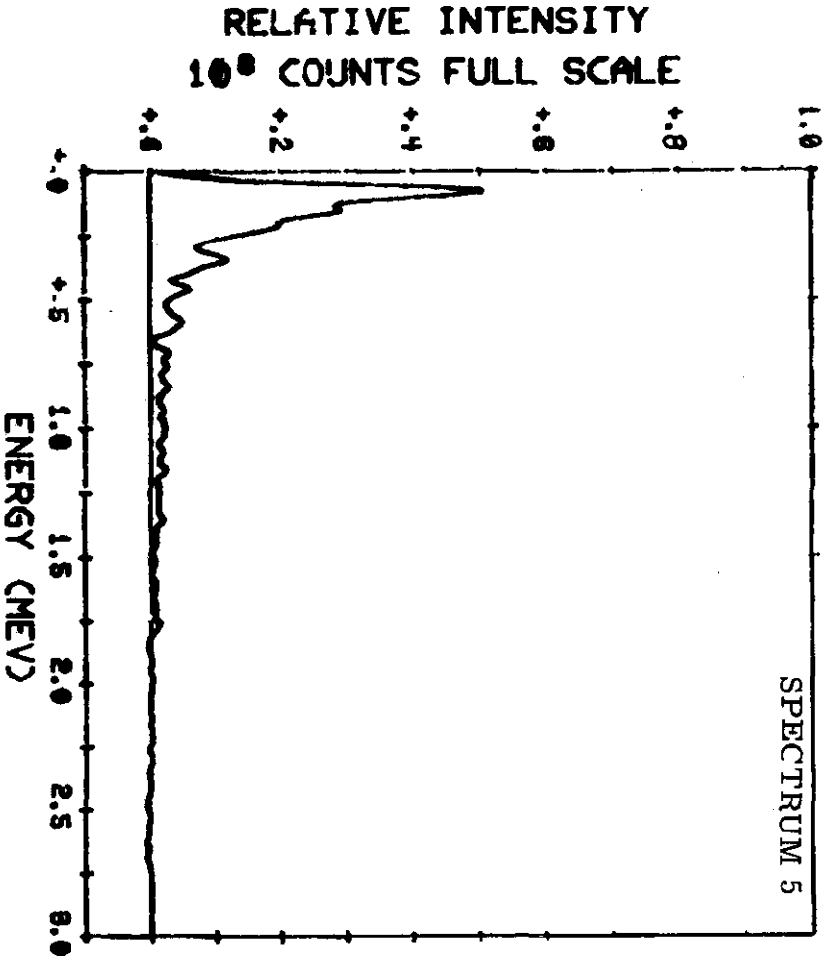
RELATIVE INTENSITY
10⁸ COUNTS FULL SCALE
+.0
+.2
+.4
+.6
+.8
1.0
+.0
+.5
1.0
1.5
2.0
2.5
3.0
ENERGY (MEV)
SPECTRUM 5

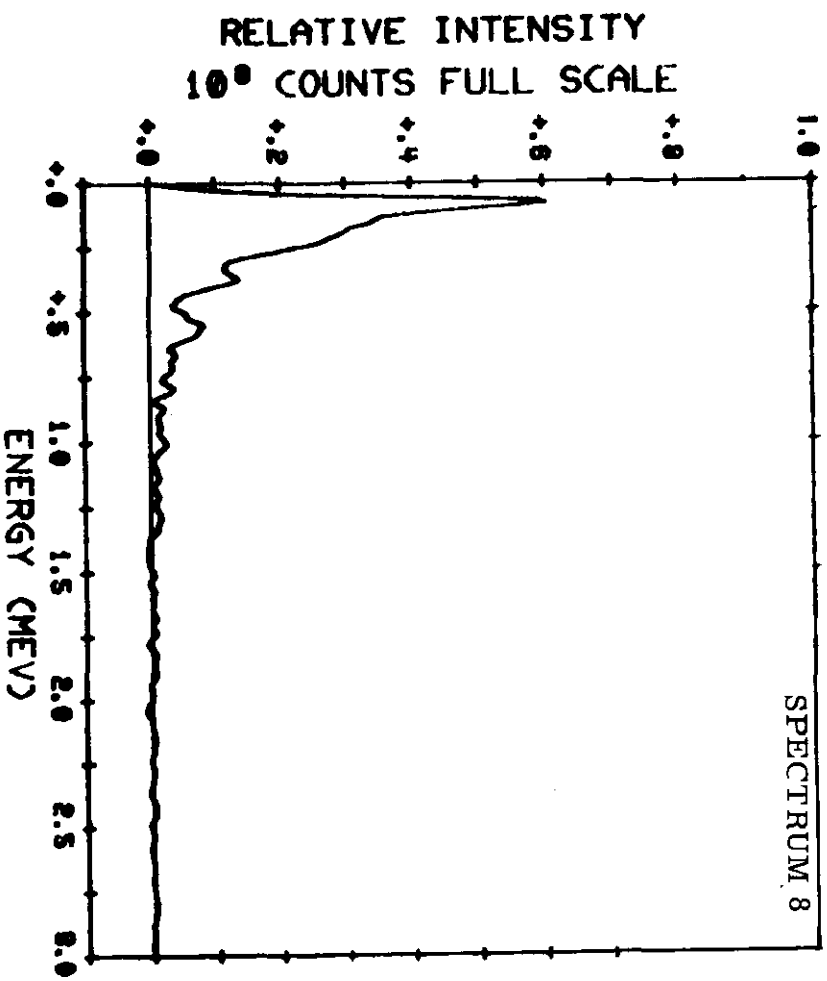
RELATIVE INTENSITY
10⁸ COUNTS FULL SCALE
.0
.2
.4
.6
.8
1.0
.0
.5
1.0
1.5
2.0
2.5
3.0
ENERGY (MEV)
SPECTRUM 8

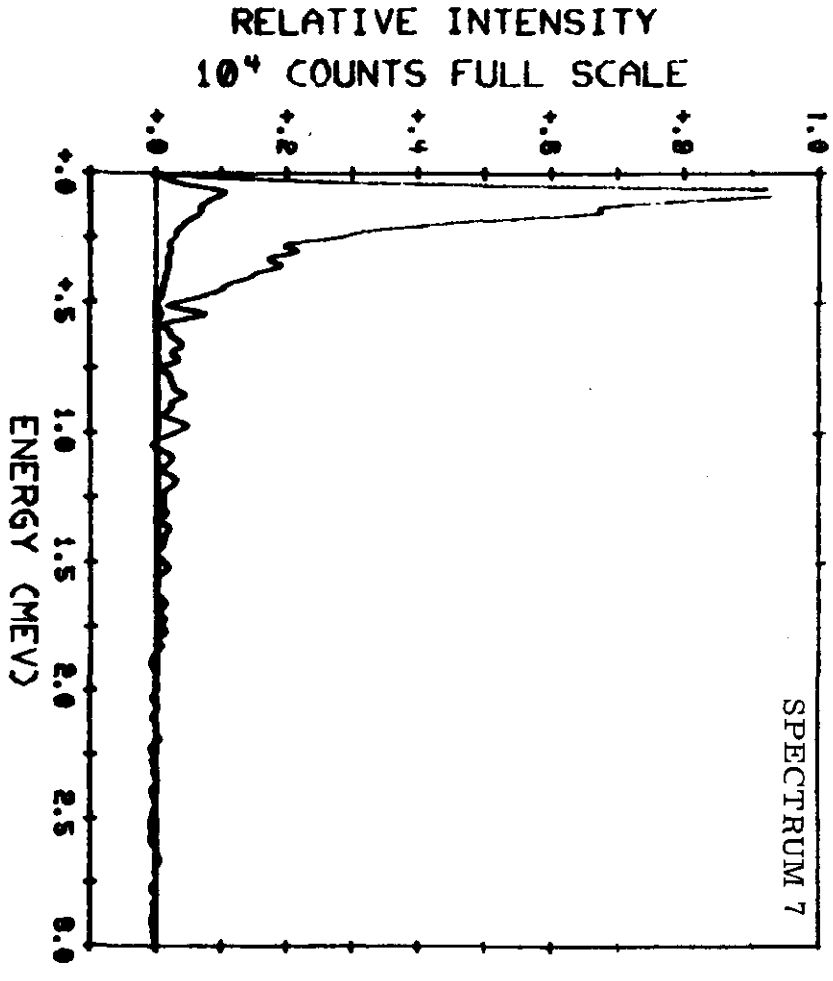
RELATIVE INTENSITY
10⁴ COUNTS FULL SCALE
.0
.2
.4
.6
.8
1.0
.0
.5
1.0
1.5
2.0
2.5
3.0
ENERGY (MEV)
SPECTRUM 7

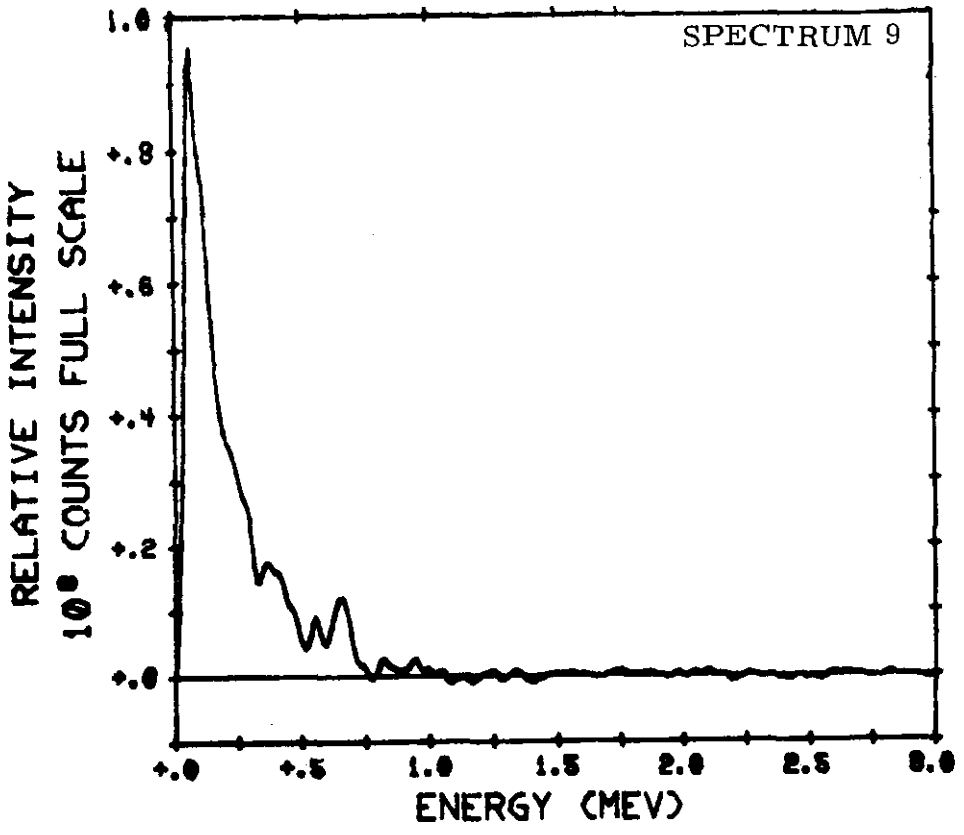
SPECTRUM 9
RELATIVE INTENSITY
10⁶ COUNTS FULL SCALE
1.0
.8
.6
.4
.2
.0
.0
.5
1.0
1.5
2.0
2.5
3.0
ENERGY (MEV)

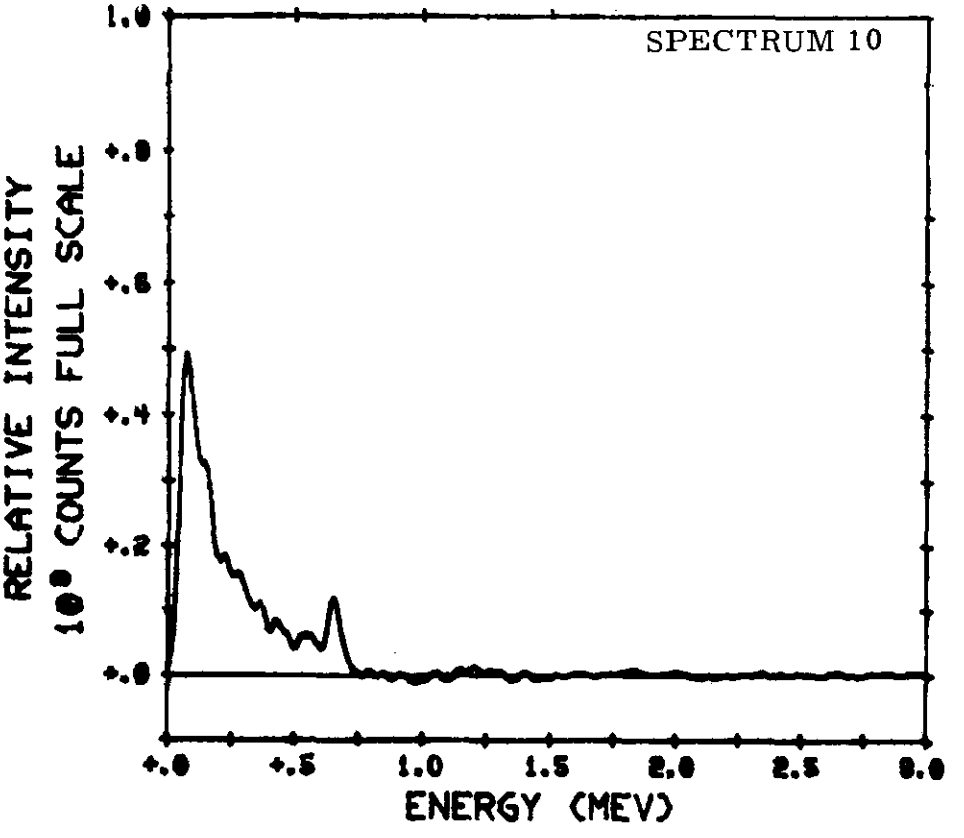
SPECTRUM 10
RELATIVE INTENSITY
10⁶ COUNTS FULL SCALE
1.0
.8
.6
.4
.2
.0
.0
.5
1.0
1.5
2.0
2.5
3.0
ENERGY (MEV)

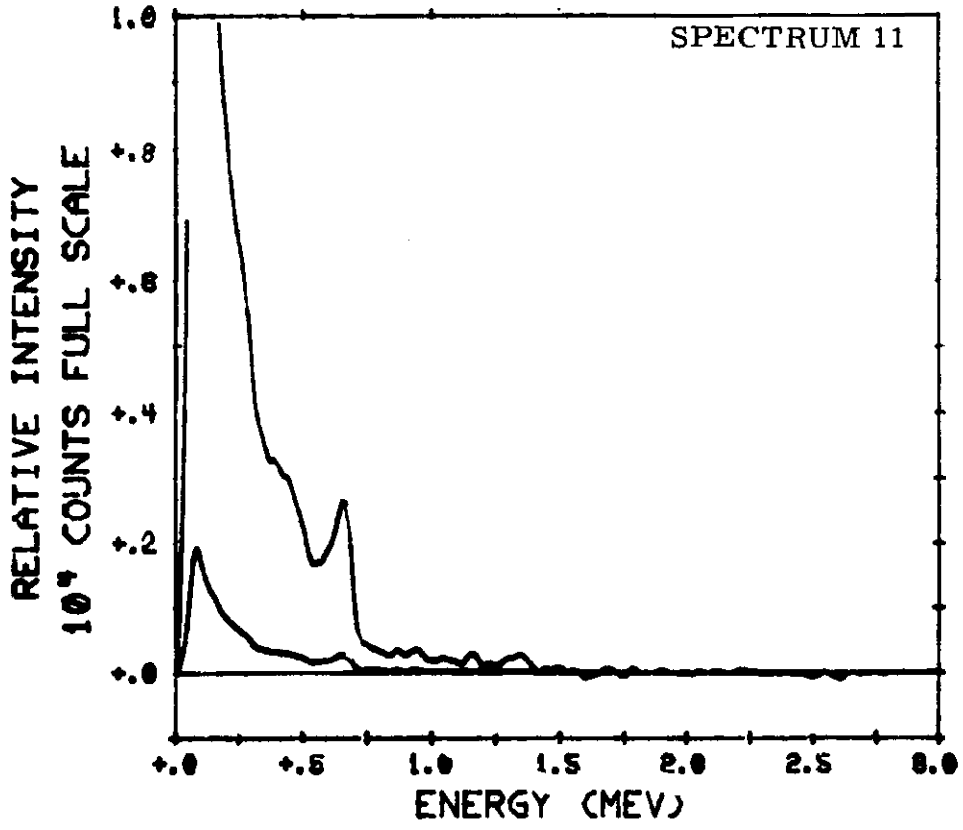
SPECTRUM 11
RELATIVE INTENSITY
10⁴ COUNTS FULL SCALE
1.0
+.8
+.6
+.4
+.2
+.0
+.0
+.5
1.0
1.5
2.0
2.5
3.0
ENERGY (MEV)

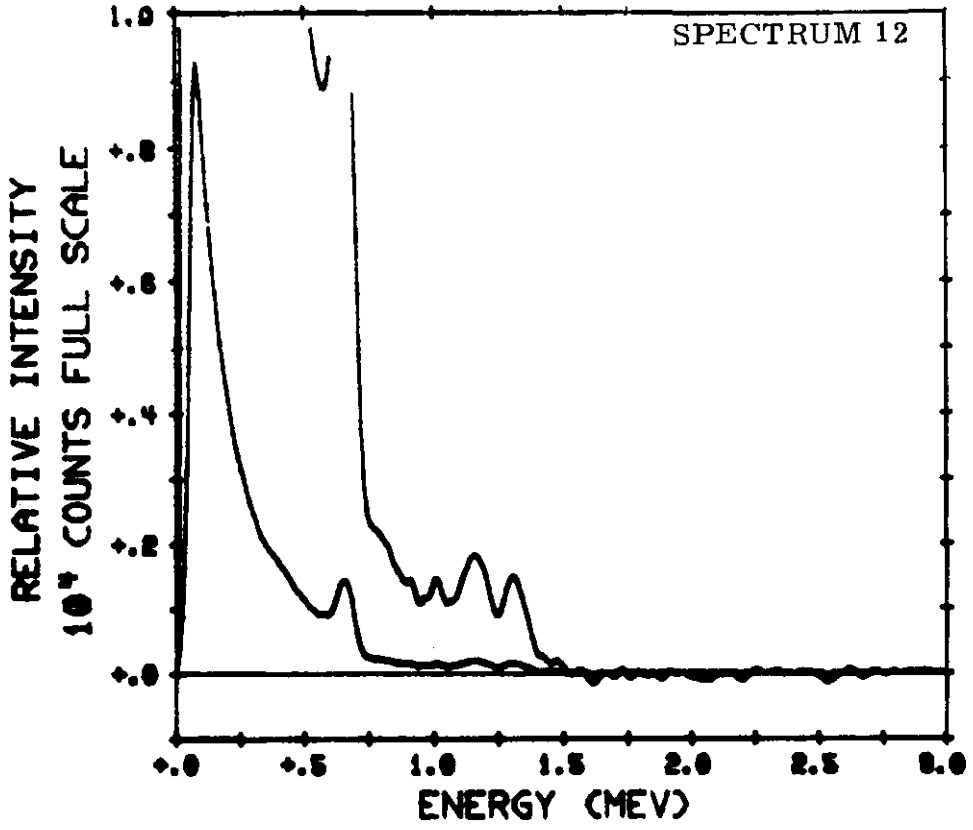
SPECTRUM 12
RELATIVE INTENSITY
10⁴ COUNTS FULL SCALE
1.0
+.8
+.6
+.4
+.2
+.0
+.0
+.5
1.0
1.5
2.0
2.5
3.0
ENERGY (MEV)

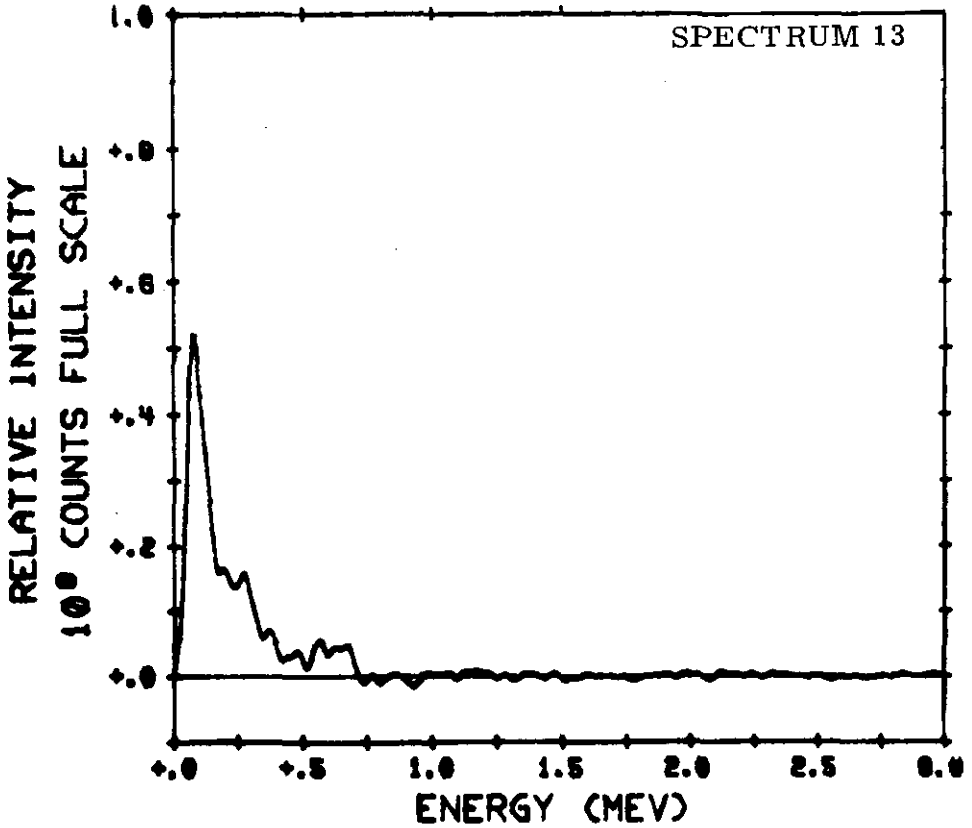
SPECTRUM 13
RELATIVE INTENSITY
10⁸ COUNTS FULL SCALE
1.0
.8
.6
.4
.2
.0
.0
.5
1.0
1.5
2.0
2.5
3.0
ENERGY (MEV)

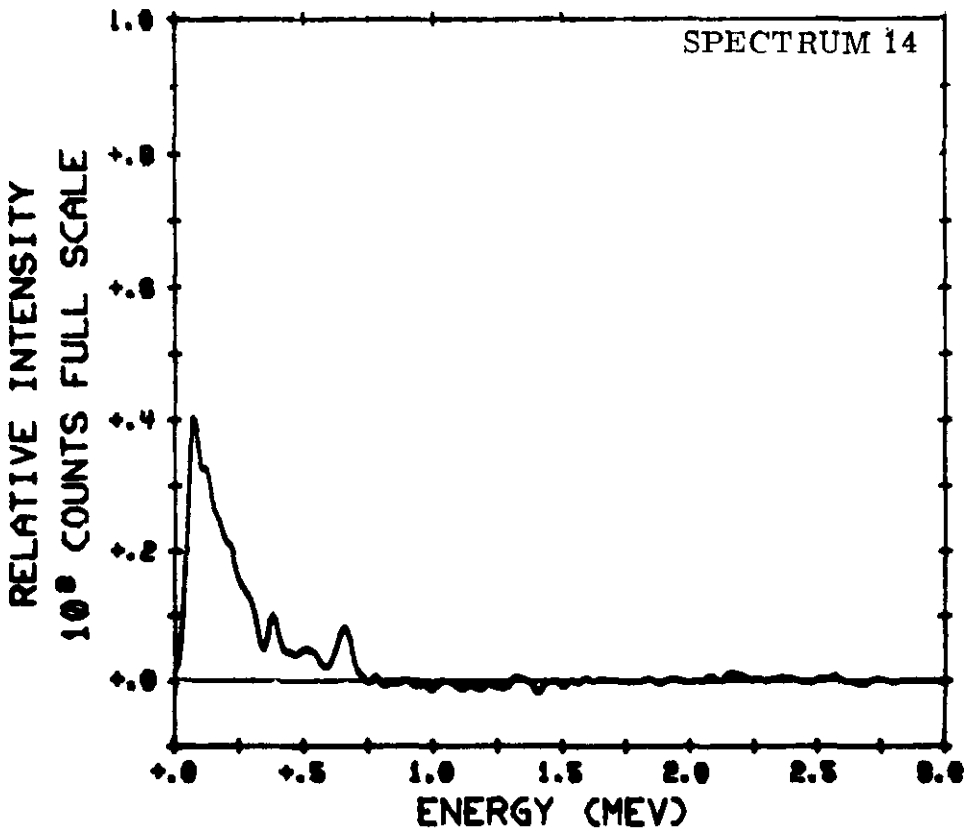
SPECTRUM 14
RELATIVE INTENSITY
10⁸ COUNTS FULL SCALE
1.0
.8
.6
.4
.2
.0
.0
.5
1.0
1.5
2.0
2.5
3.0
ENERGY (MEV)

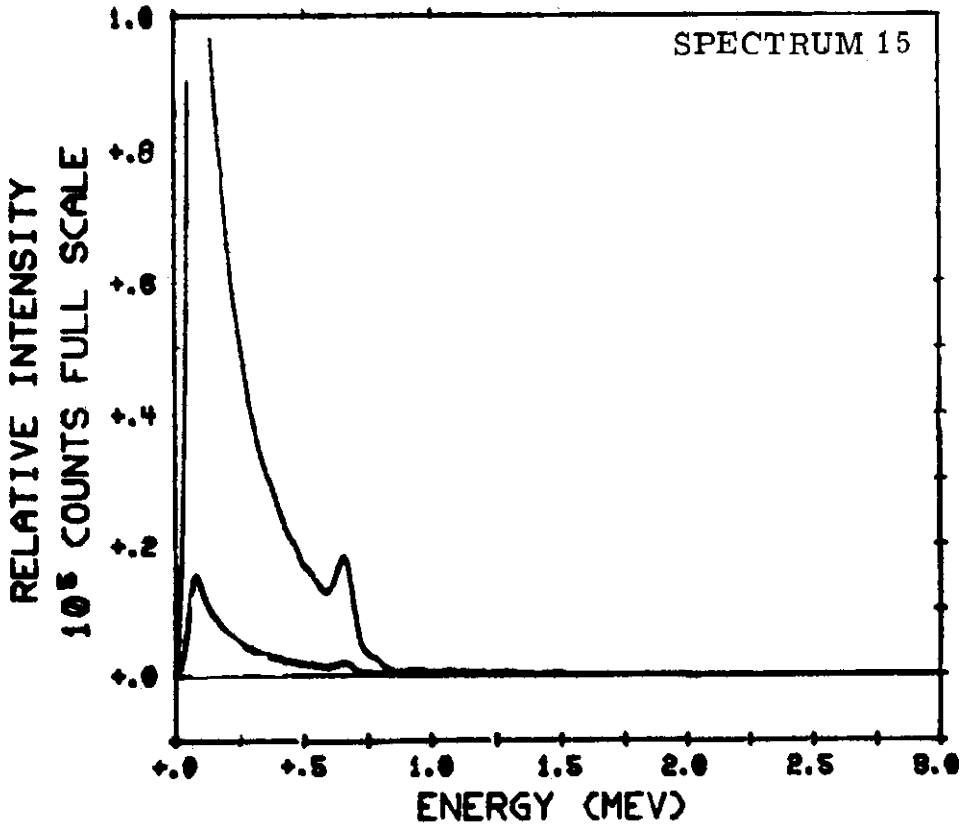
SPECTRUM 15
RELATIVE INTENSITY
10⁵ COUNTS FULL SCALE
1.0
.8
.6
.4
.2
.0
.0
.5
1.0
1.5
2.0
2.5
3.0
ENERGY (MEV)

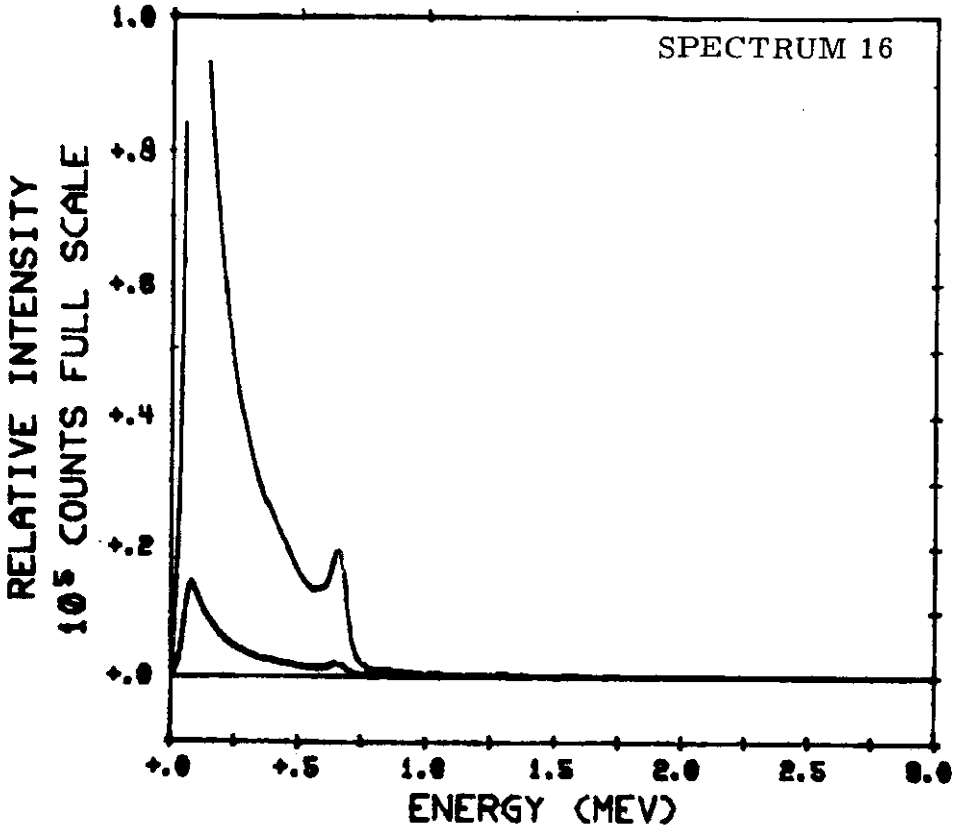
SPECTRUM 16
RELATIVE INTENSITY
10⁵ COUNTS FULL SCALE
1.0
.8
.6
.4
.2
.0
.0
.5
1.0
1.5
2.0
2.5
3.0
ENERGY (MEV)

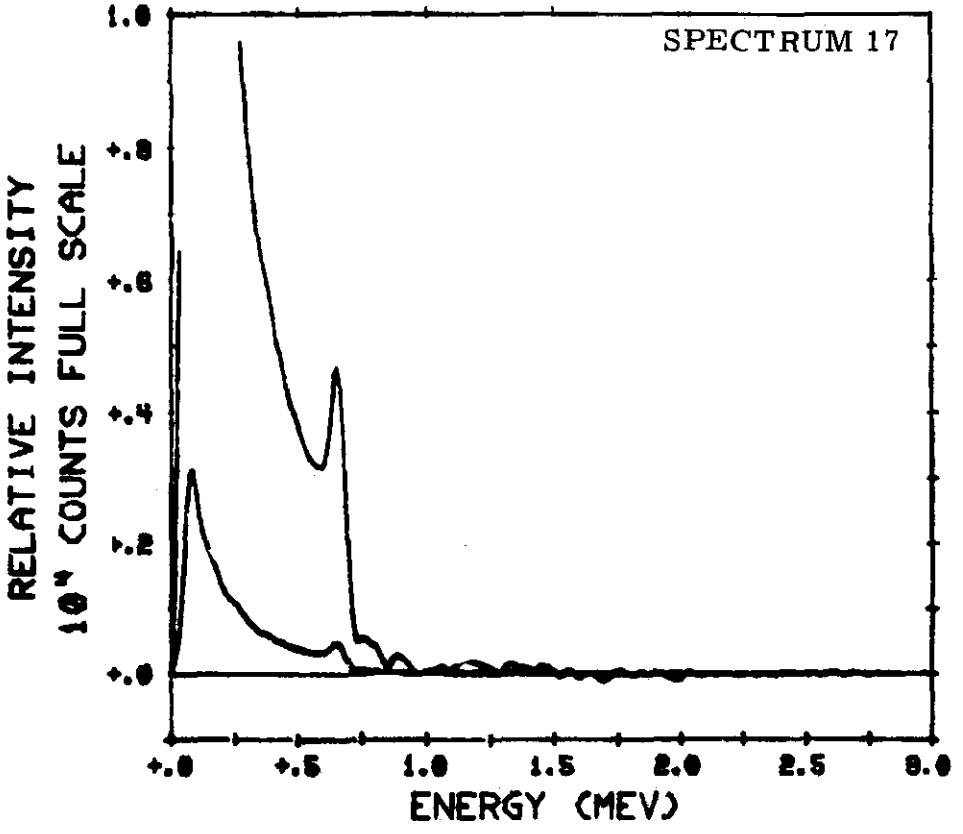
SPECTRUM 17
RELATIVE INTENSITY
10⁴ COUNTS FULL SCALE
1.0
.8
.6
.4
.2
.0
.0
.5
1.0
1.5
2.0
2.5
3.0
ENERGY (MEV)

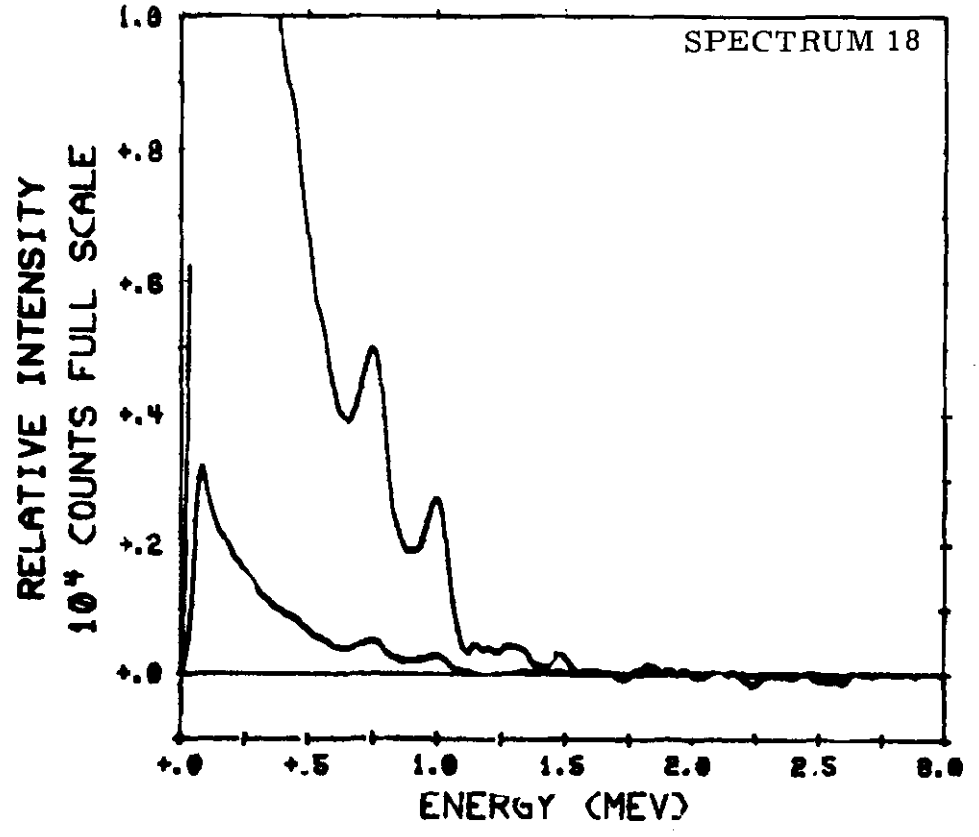
SPECTRUM 18
RELATIVE INTENSITY
10⁴ COUNTS FULL SCALE
1.0
.8
.6
.4
.2
.0
.0
.5
1.0
1.5
2.0
2.5
3.0
ENERGY (MEV)

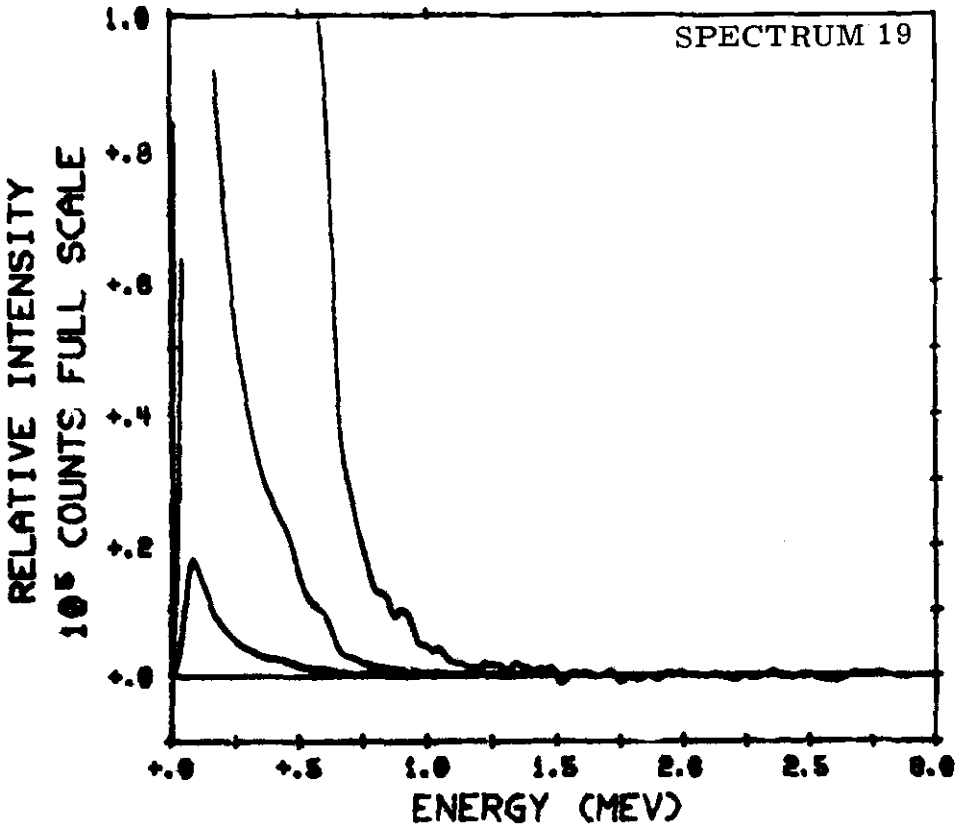
SPECTRUM 19
RELATIVE INTENSITY
10⁵ COUNTS FULL SCALE
1.0
.8
.6
.4
.2
.0
.0
.5
1.0
1.5
2.0
2.5
3.0
ENERGY (MEV)

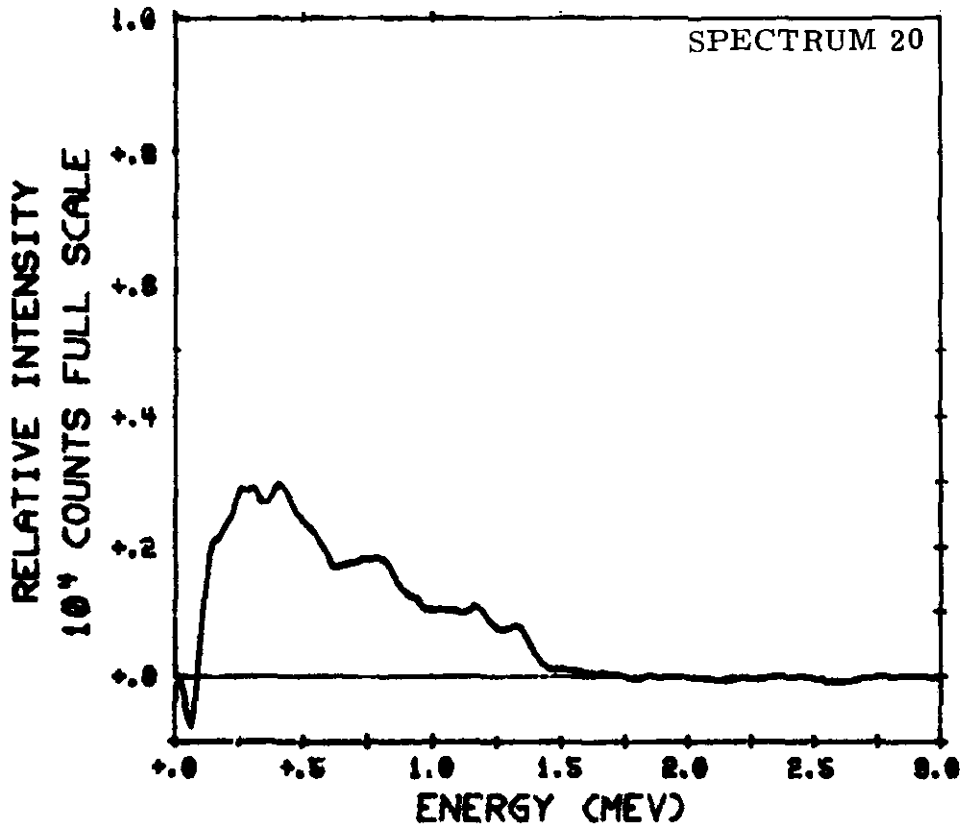
SPECTRUM 20
RELATIVE INTENSITY
10⁴ COUNTS FULL SCALE
1.0
.8
.6
.4
.2
.0
.0
.5
1.0
1.5
2.0
2.5
3.0
ENERGY (MEV)

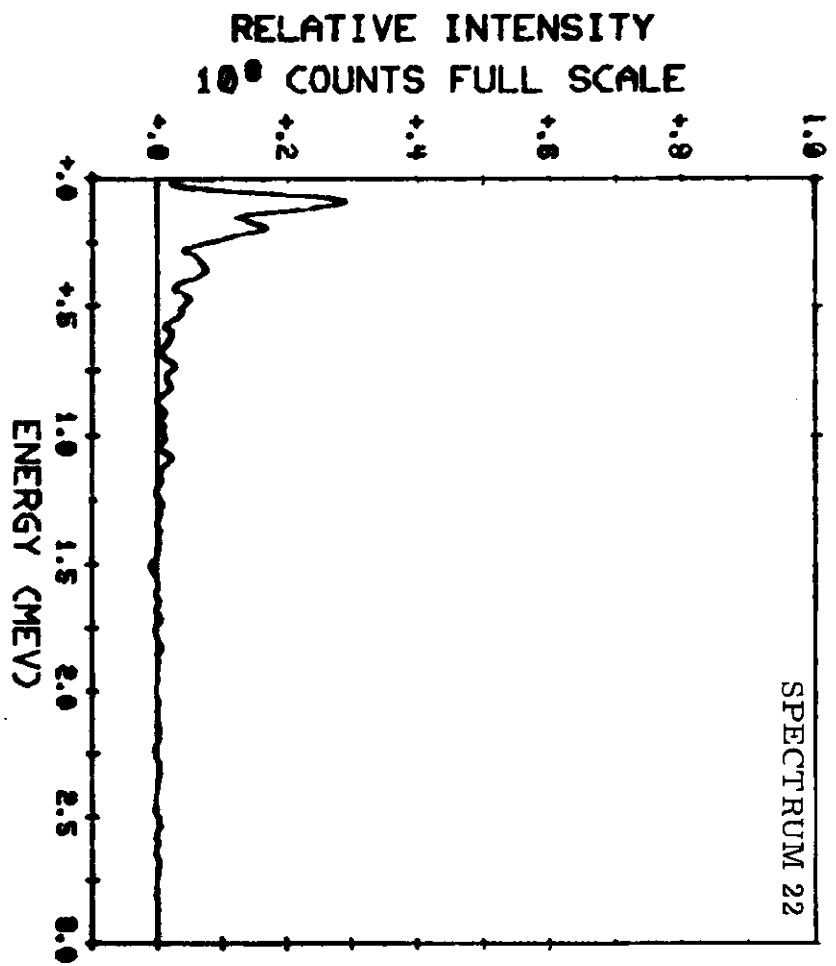
RELATIVE INTENSITY
10⁸ COUNTS FULL SCALE
+.0
+.2
+.4
+.6
+.8
1.0
+.0
+.5
1.0
1.5
2.0
2.5
3.0
ENERGY (MEV)
SPECTRUM 22

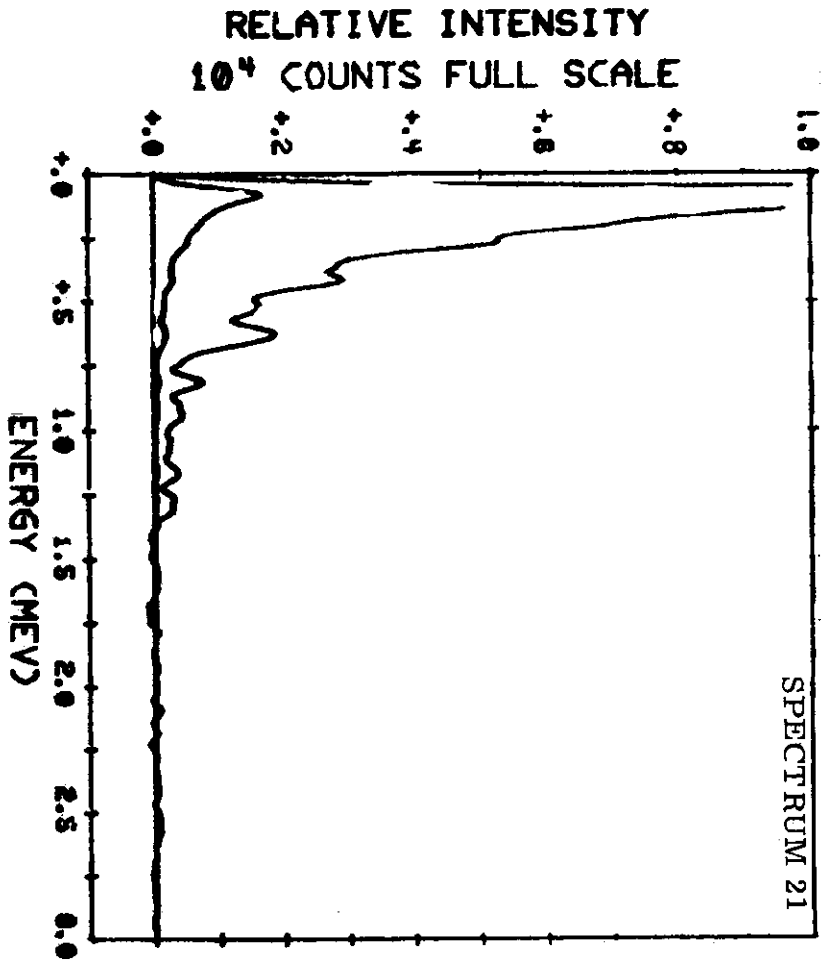
RELATIVE INTENSITY
10⁴ COUNTS FULL SCALE
+.0
+.2
+.4
+.6
+.8
1.0
+.0
+.5
1.0
1.5
2.0
2.5
3.0
ENERGY (MEV)
SPECTRUM 21

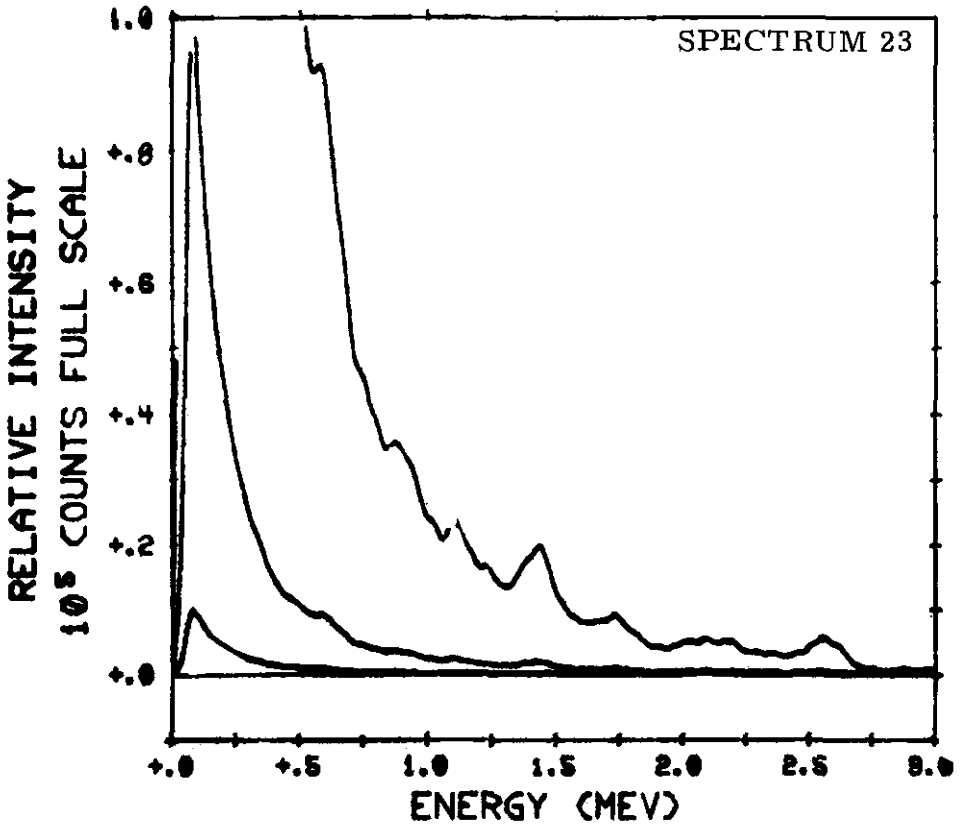
SPECTRUM 23
RELATIVE INTENSITY
10^5 COUNTS FULL SCALE
1.0
.8
.6
.4
.2
.0
.0
.5
1.0
1.5
2.0
2.5
3.0
ENERGY (MEV)

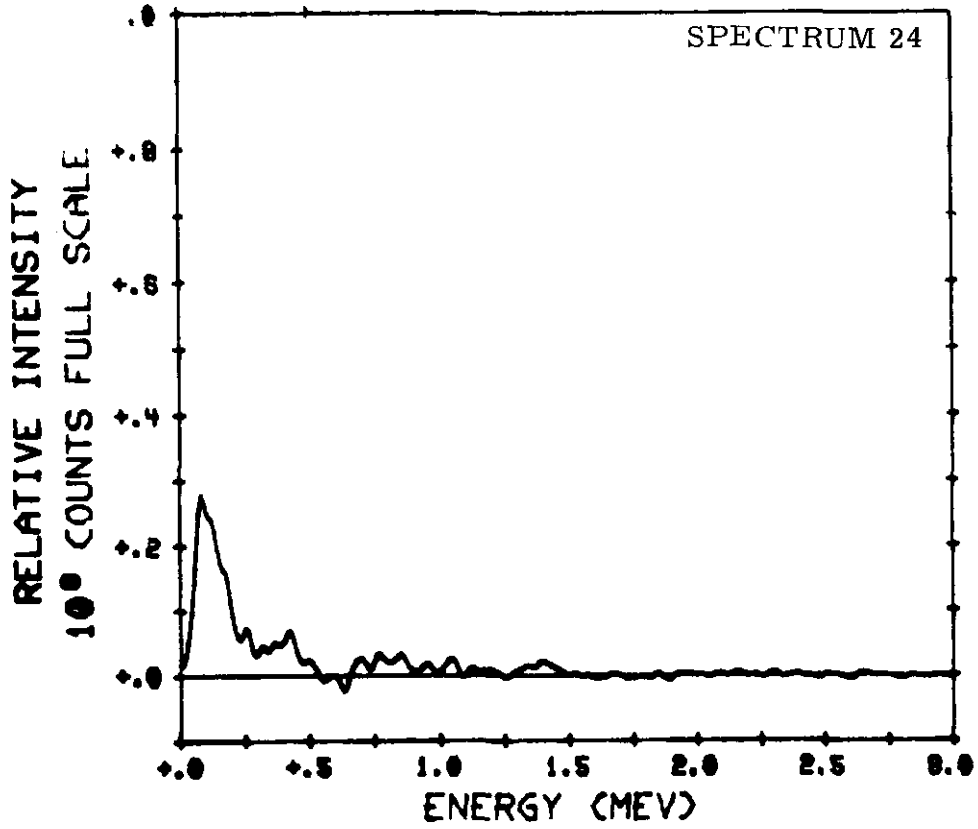
SPECTRUM 24
RELATIVE INTENSITY
10^4 COUNTS FULL SCALE
.0
.8
.6
.4
.2
.0
.0
.5
1.0
1.5
2.0
2.5
3.0
ENERGY (MEV)

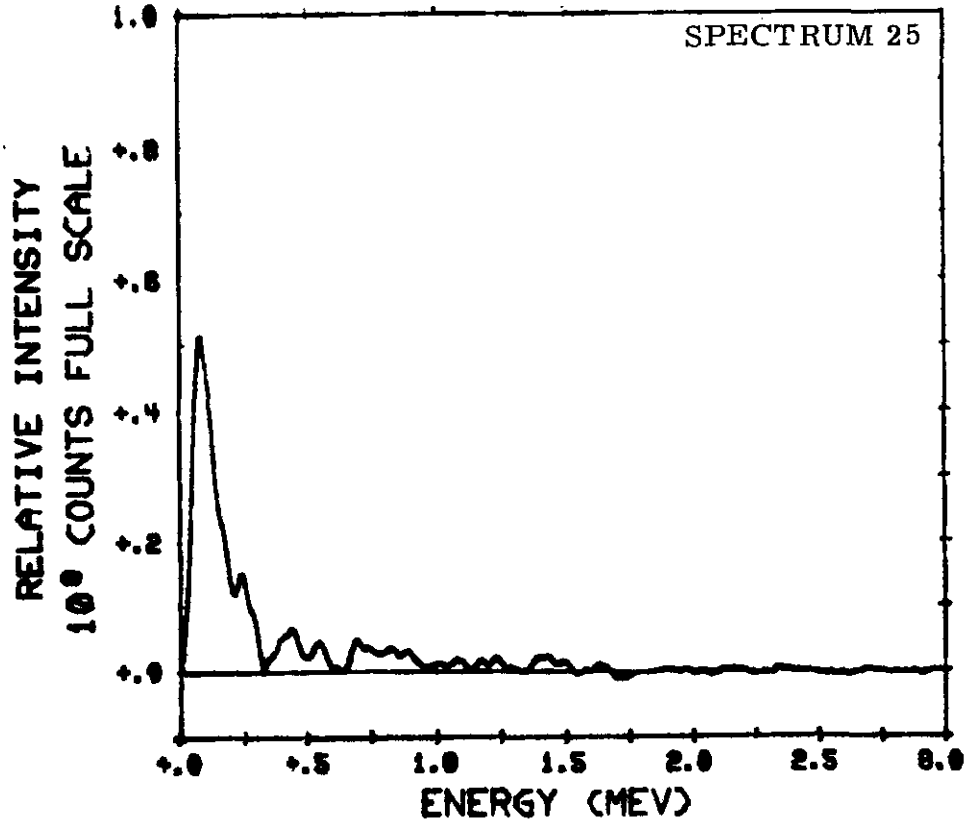
SPECTRUM 25
RELATIVE INTENSITY
10⁰ COUNTS FULL SCALE
1.0
+.8
+.6
+.4
+.2
+.0
+.0
+.5
1.0
1.5
2.0
2.5
3.0
ENERGY (MEV)

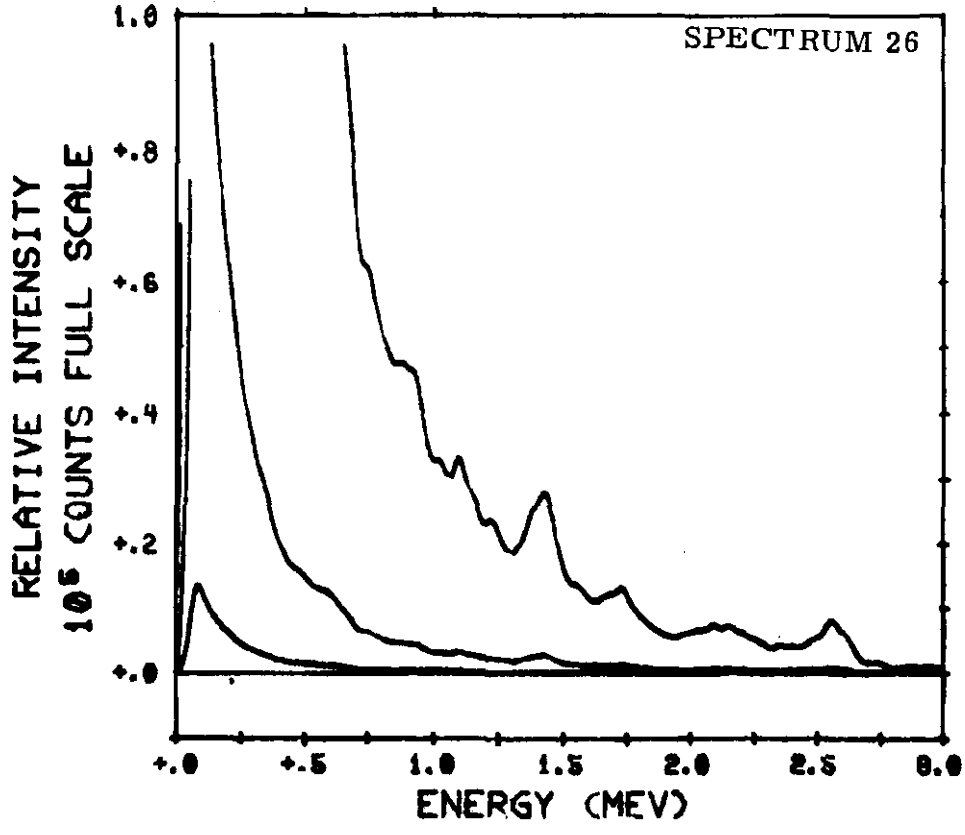
SPECTRUM 26
RELATIVE INTENSITY
10⁵ COUNTS FULL SCALE
1.0
+.8
+.6
+.4
+.2
+.0
+.0
+.5
1.0
1.5
2.0
2.5
3.0
ENERGY (MEV)

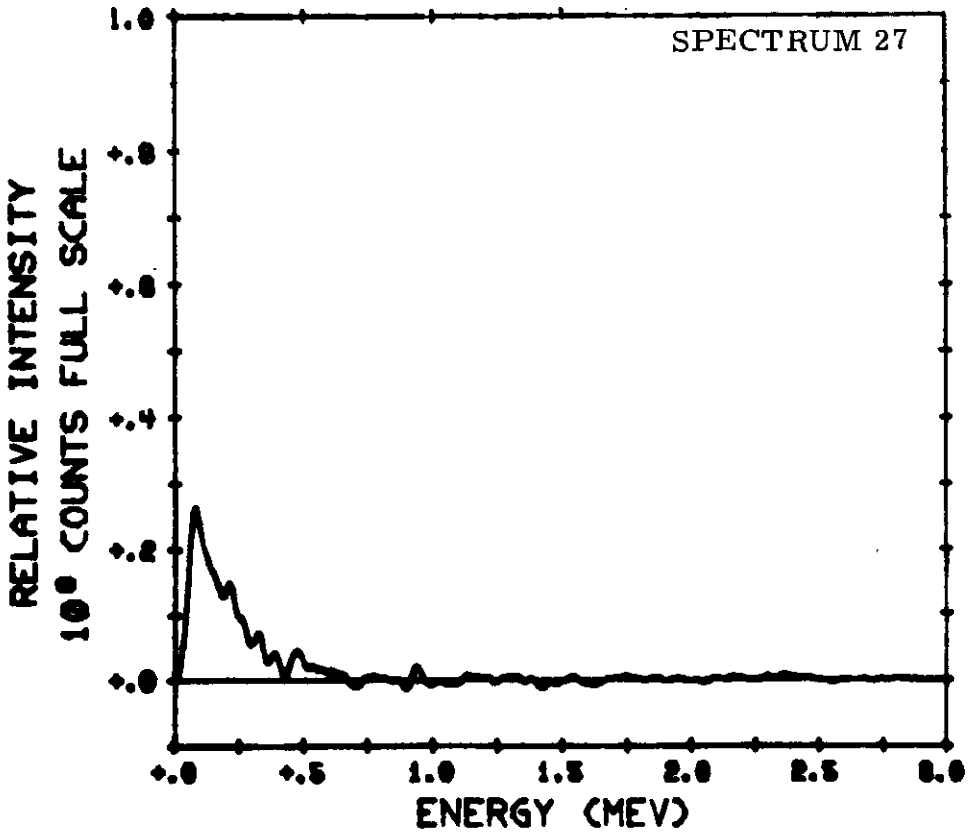
SPECTRUM 27
RELATIVE INTENSITY
10⁰ COUNTS FULL SCALE
1.0
.8
.6
.4
.2
.0
.0
.5
1.0
1.5
2.0
2.5
3.0
ENERGY (MEV)

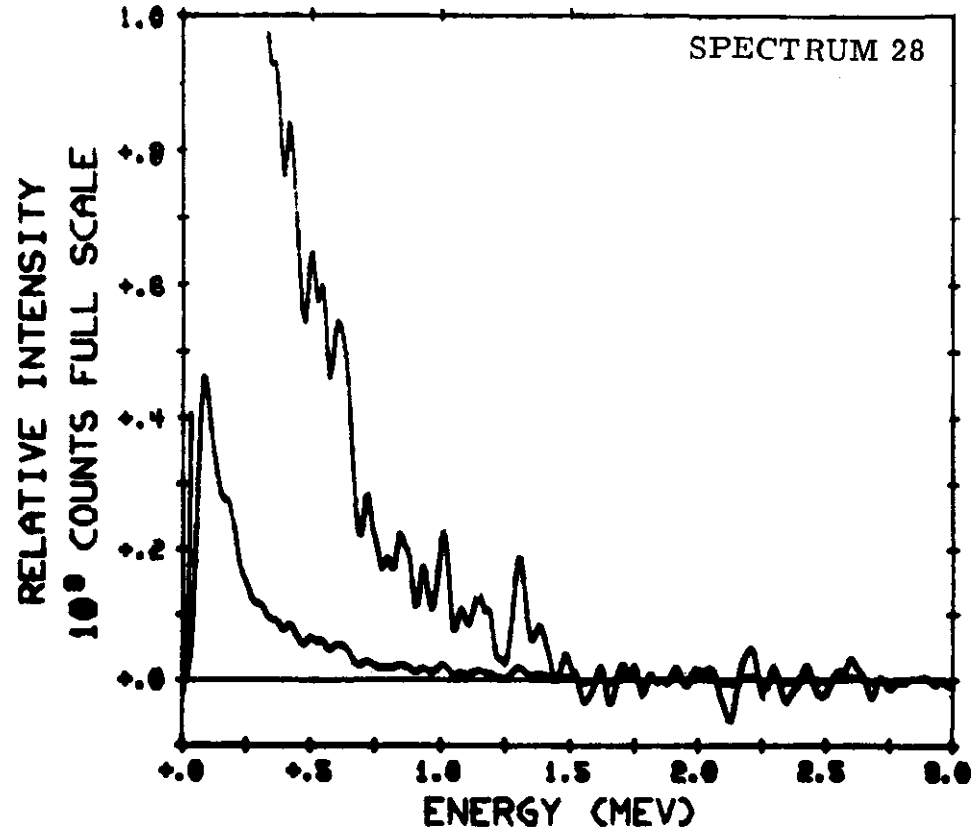
SPECTRUM 28
RELATIVE INTENSITY
10⁰ COUNTS FULL SCALE
1.0
.8
.6
.4
.2
.0
.0
.5
1.0
1.5
2.0
2.5
3.0
ENERGY (MEV)

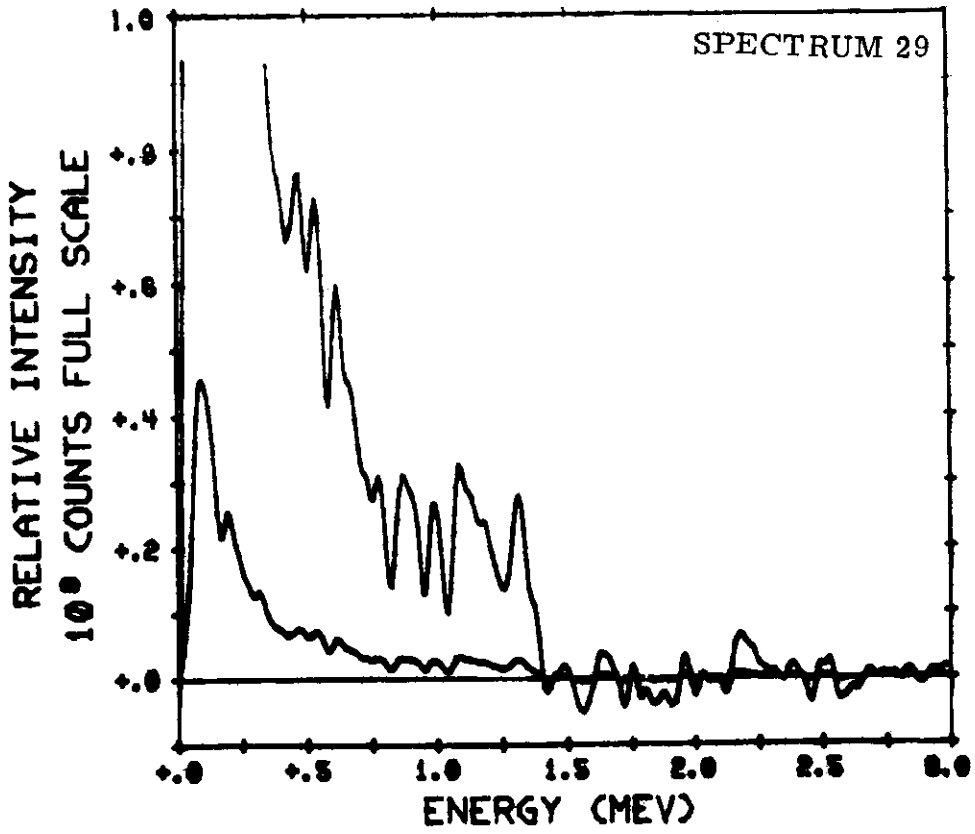
SPECTRUM 29
RELATIVE INTENSITY
10⁶ COUNTS FULL SCALE
1.0
.8
.6
.4
.2
.0
.0
.5
1.0
1.5
2.0
2.5
3.0
ENERGY (MEV)

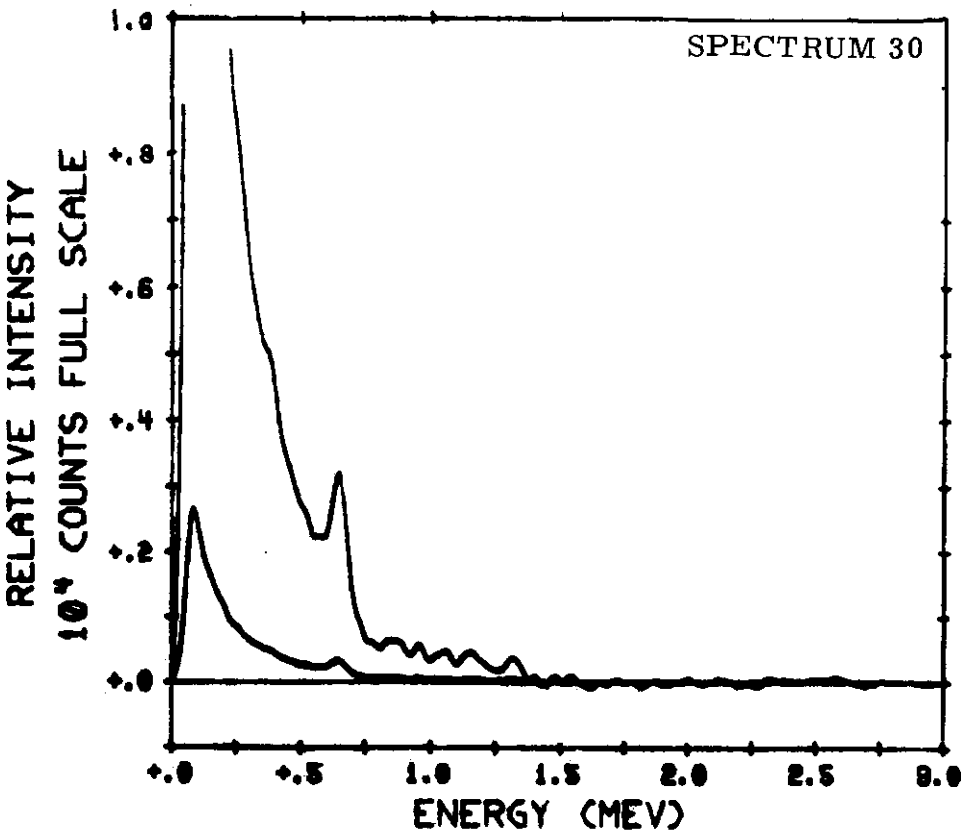
SPECTRUM 30
RELATIVE INTENSITY
10⁶ COUNTS FULL SCALE
1.0
.8
.6
.4
.2
.0
.0
.5
1.0
1.5
2.0
2.5
3.0
ENERGY (MEV)

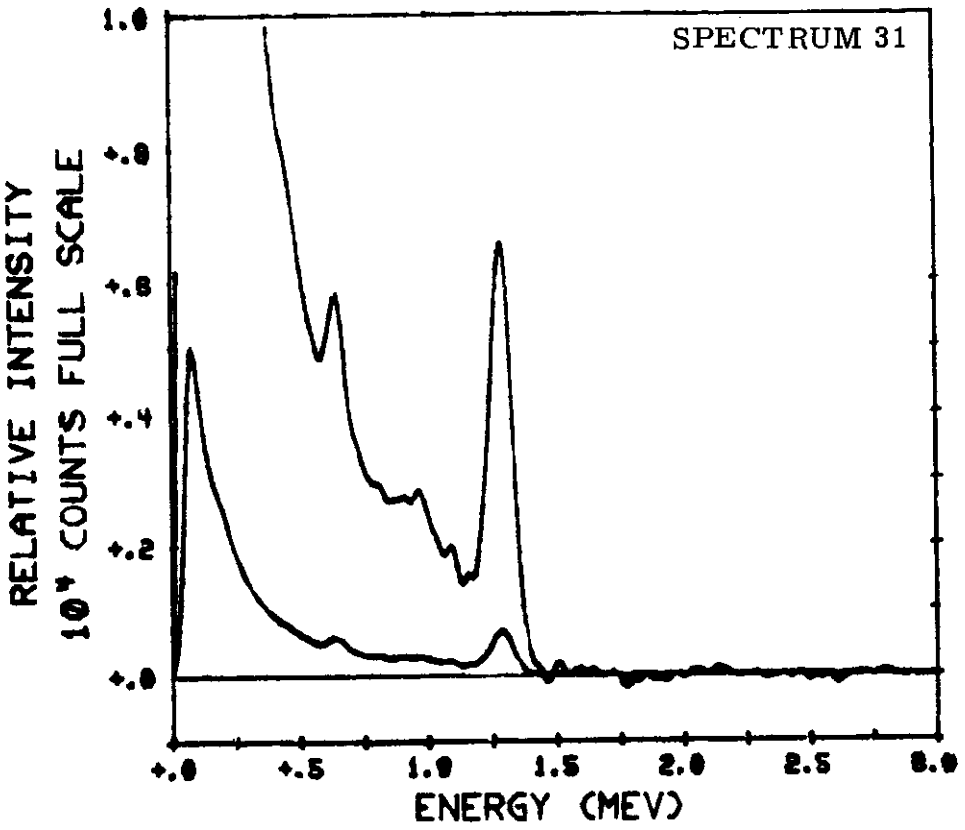
SPECTRUM 31
RELATIVE INTENSITY
10⁴ COUNTS FULL SCALE
1.0
.8
.6
.4
.2
.0
.0
.5
1.0
1.5
2.0
2.5
3.0
ENERGY (MEV)

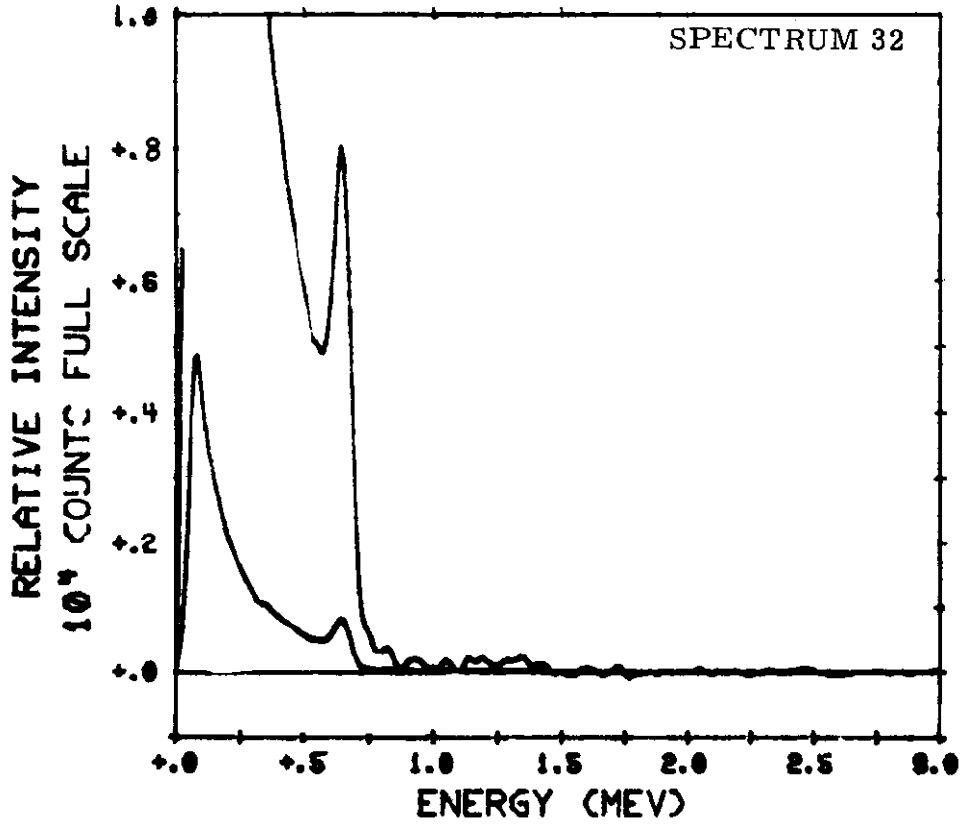
SPECTRUM 32
RELATIVE INTENSITY
10⁴ COUNTS FULL SCALE
1.0
.8
.6
.4
.2
.0
.0
.5
1.0
1.5
2.0
2.5
3.0
ENERGY (MEV)

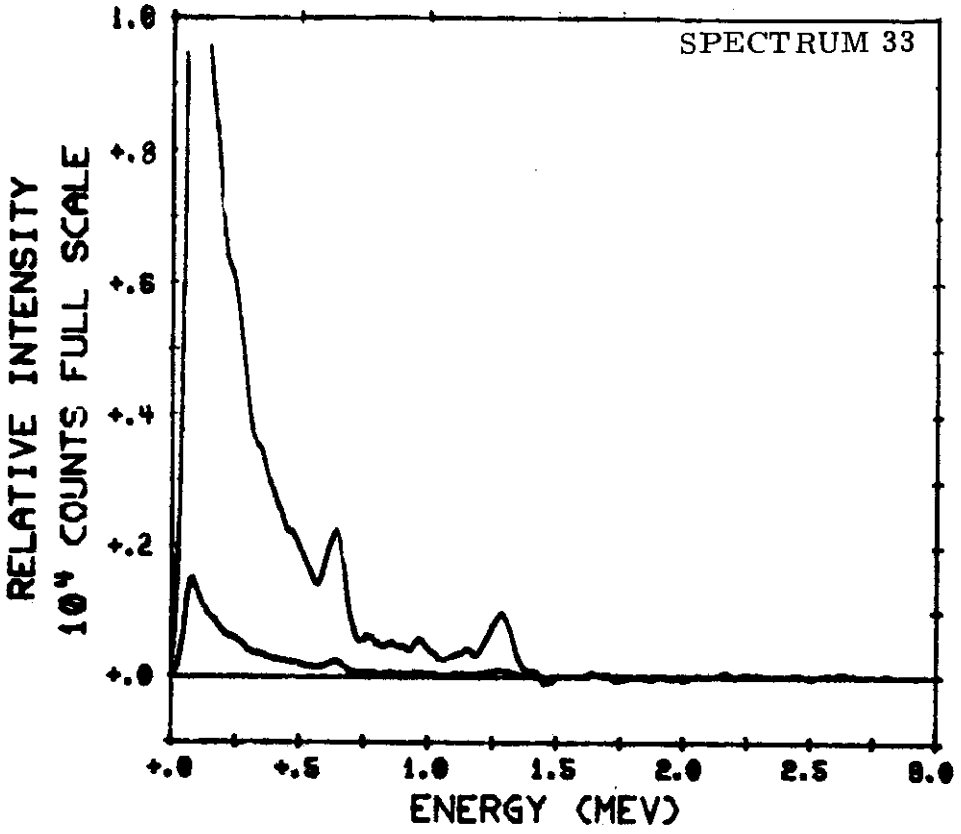
SPECTRUM 33
RELATIVE INTENSITY
10⁴ COUNTS FULL SCALE
1.0
.8
.6
.4
.2
.0
.0
.5
1.0
1.5
2.0
2.5
3.0
ENERGY (MEV)

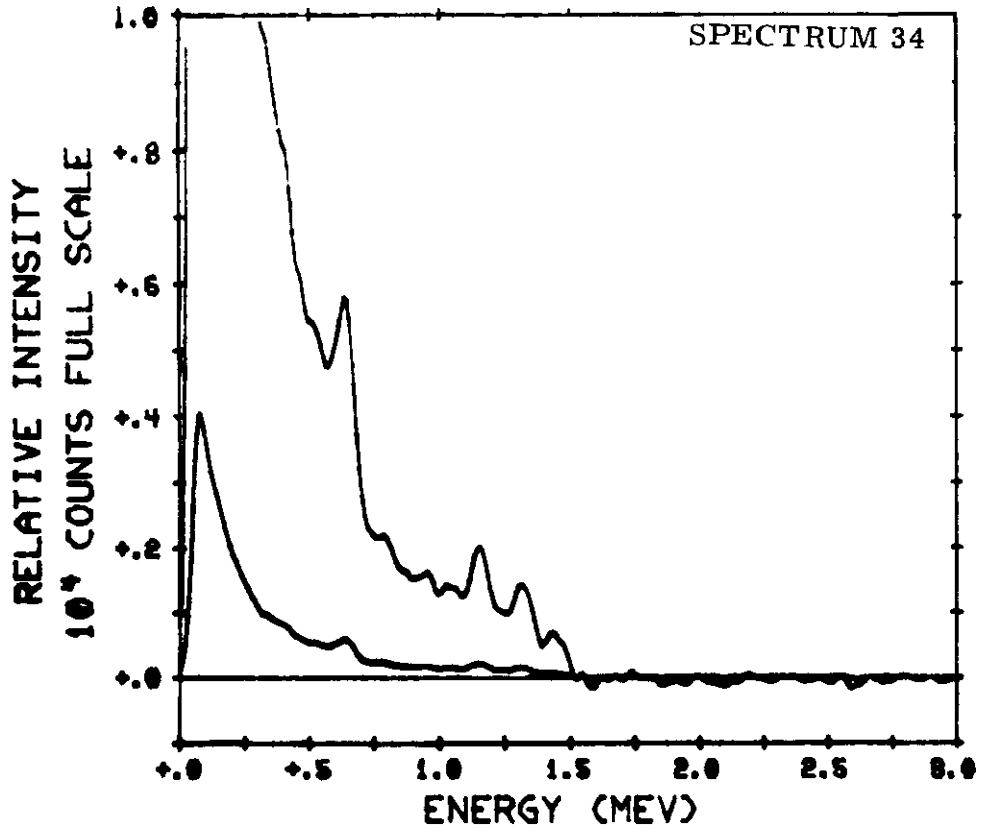
SPECTRUM 34
RELATIVE INTENSITY
10⁴ COUNTS FULL SCALE
1.0
.8
.6
.4
.2
.0
.0
.5
1.0
1.5
2.0
2.5
3.0
ENERGY (MEV)

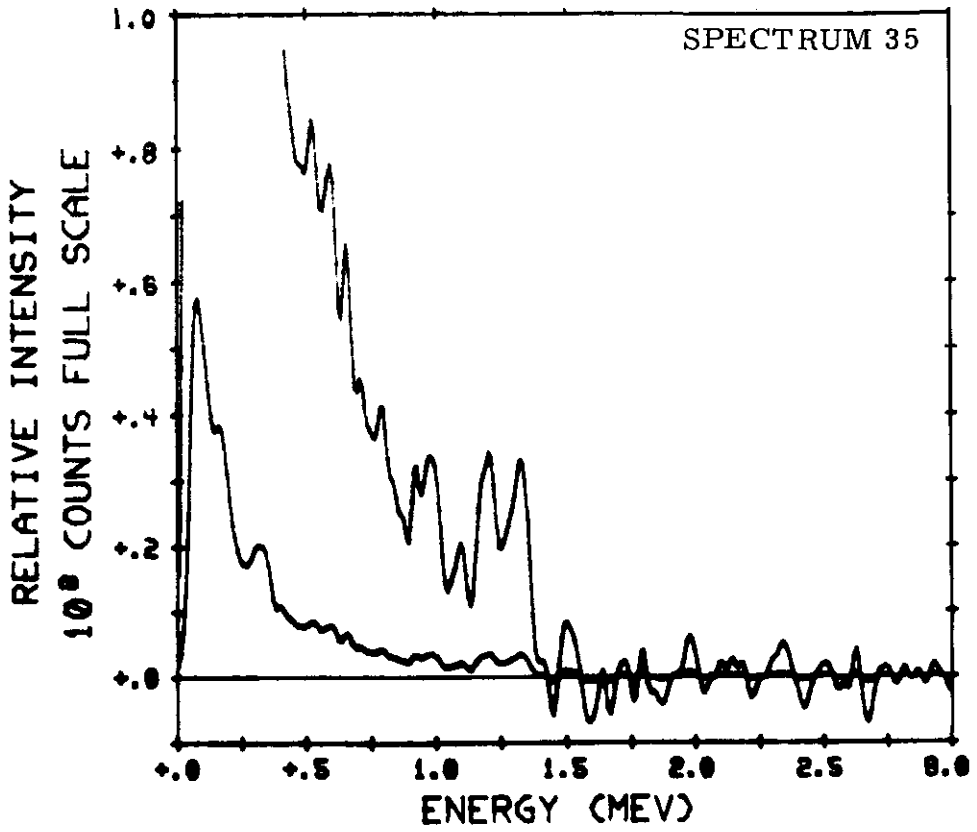
SPECTRUM 35
RELATIVE INTENSITY
10⁸ COUNTS FULL SCALE
1.0
.8
.6
.4
.2
.0
.0
.5
1.0
1.5
2.0
2.5
3.0
ENERGY (MEV)

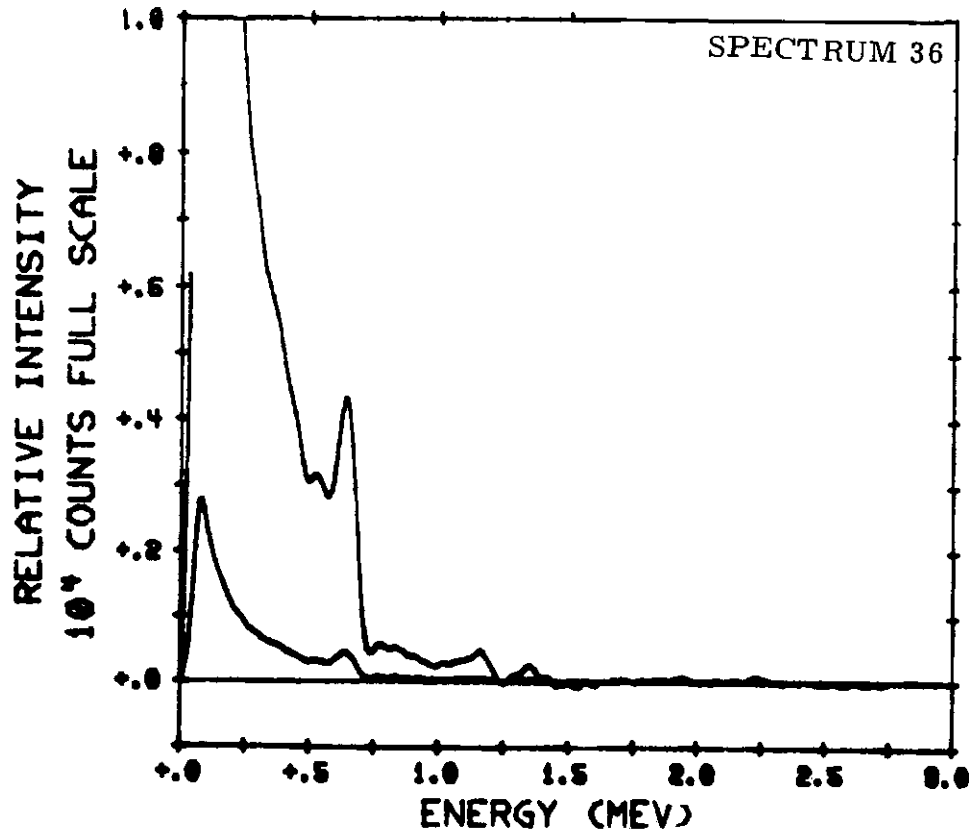
SPECTRUM 36
RELATIVE INTENSITY
10⁸ COUNTS FULL SCALE
1.0
.8
.6
.4
.2
.0
.0
.5
1.0
1.5
2.0
2.5
3.0
ENERGY (MEV)

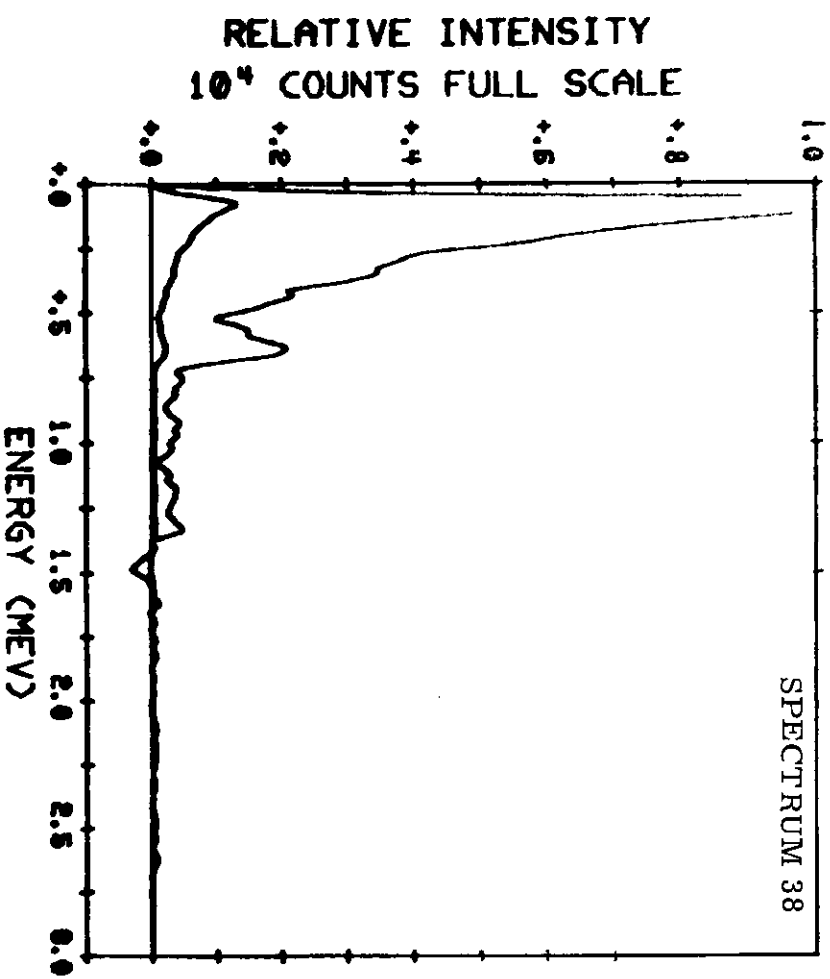
RELATIVE INTENSITY
10⁴ COUNTS FULL SCALE
0.0
.2
.4
.6
.8
1.0
0.0
.5
1.0
1.5
2.0
2.5
3.0
ENERGY (MEV)
SPECTRUM 38

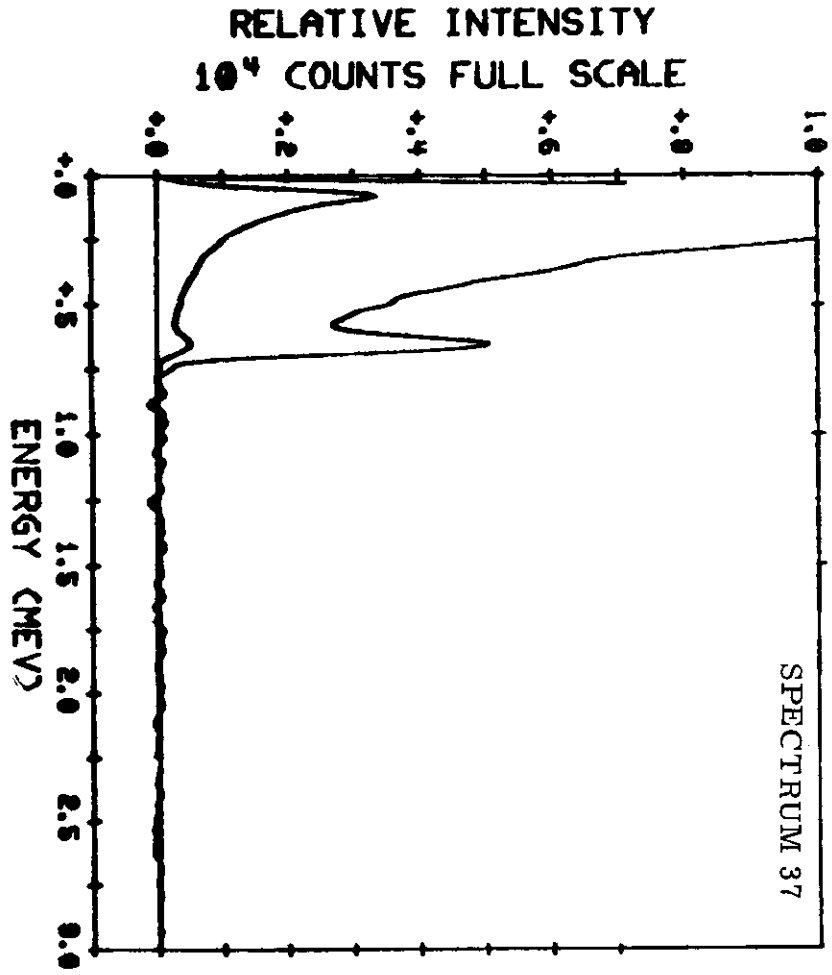
RELATIVE INTENSITY
10⁴ COUNTS FULL SCALE
0.0
.2
.4
.6
.8
1.0
0.0
.5
1.0
1.5
2.0
2.5
3.0
ENERGY (MEV)
SPECTRUM 37

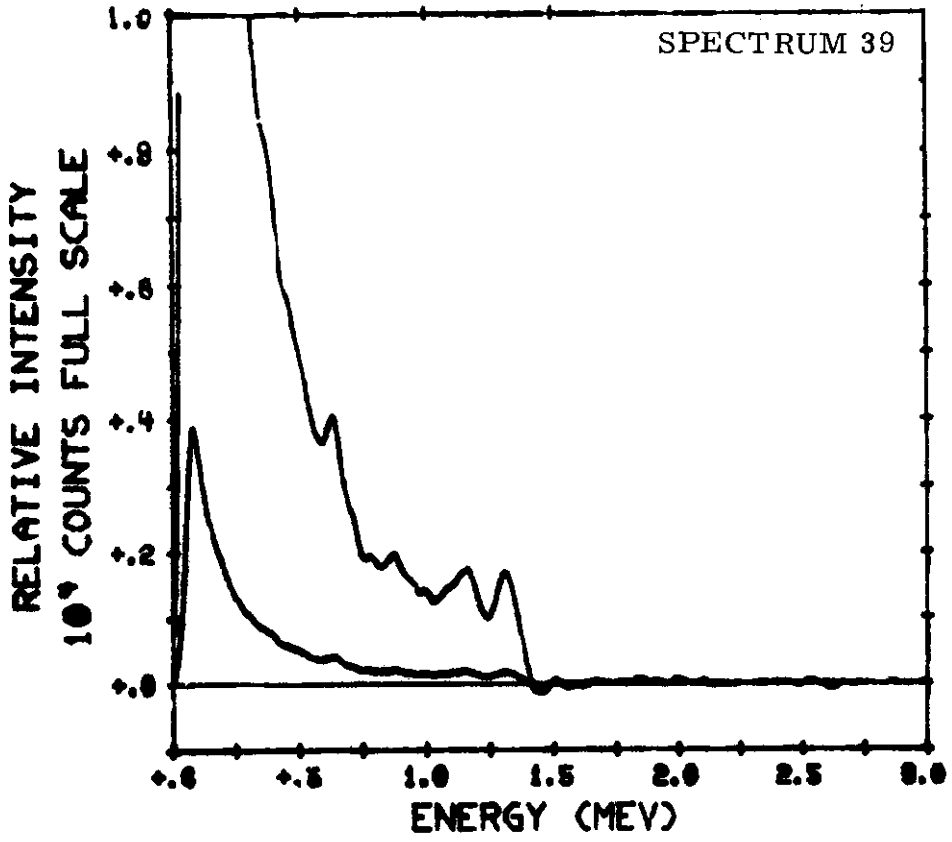
SPECTRUM 39
RELATIVE INTENSITY
10⁴ COUNTS FULL SCALE
1.0
.8
.6
.4
.2
.0
.0
.5
1.0
1.5
2.0
2.5
3.0
ENERGY (MEV)

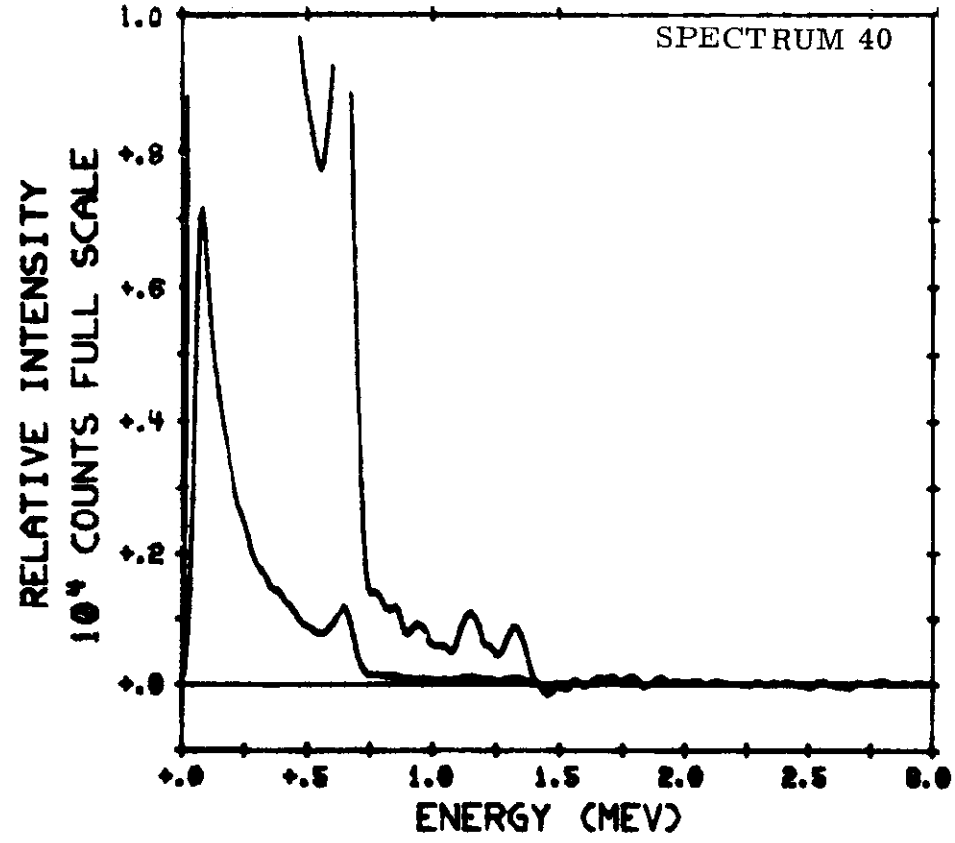
SPECTRUM 40
RELATIVE INTENSITY
10⁴ COUNTS FULL SCALE
1.0
.8
.6
.4
.2
.0
.0
.5
1.0
1.5
2.0
2.5
3.0
ENERGY (MEV)

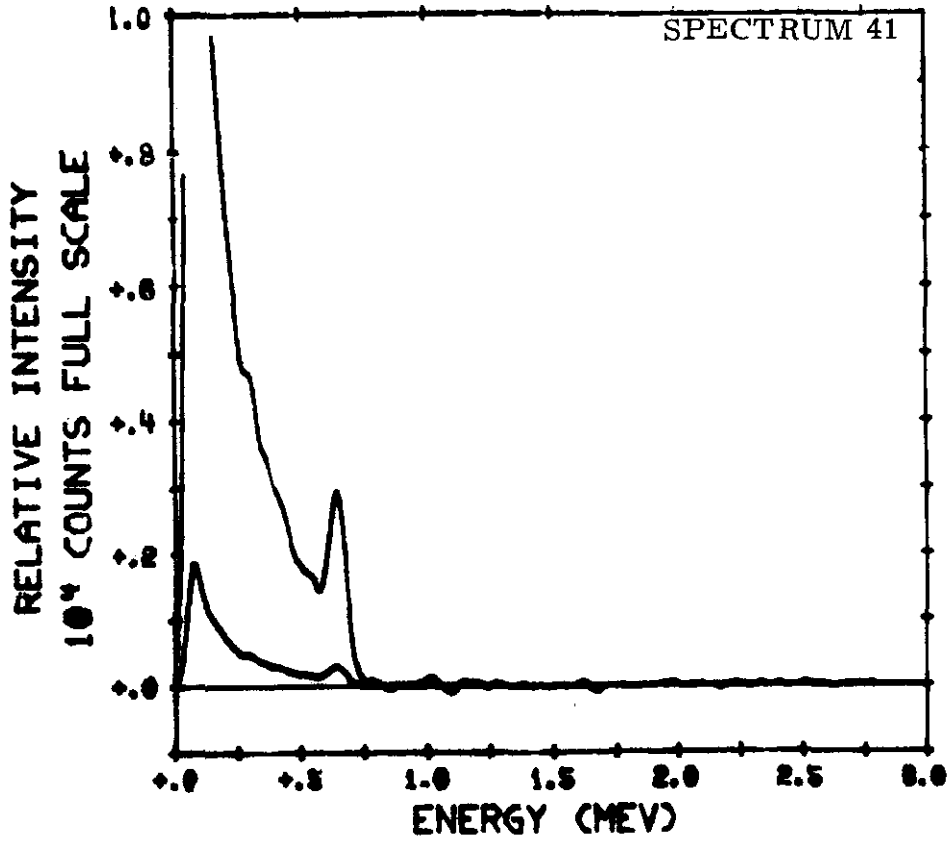
SPECTRUM 41
RELATIVE INTENSITY
10⁴ COUNTS FULL SCALE
1.0
.8
.6
.4
.2
.0
.0
.5
1.0
1.5
2.0
2.5
3.0
ENERGY (MEV)

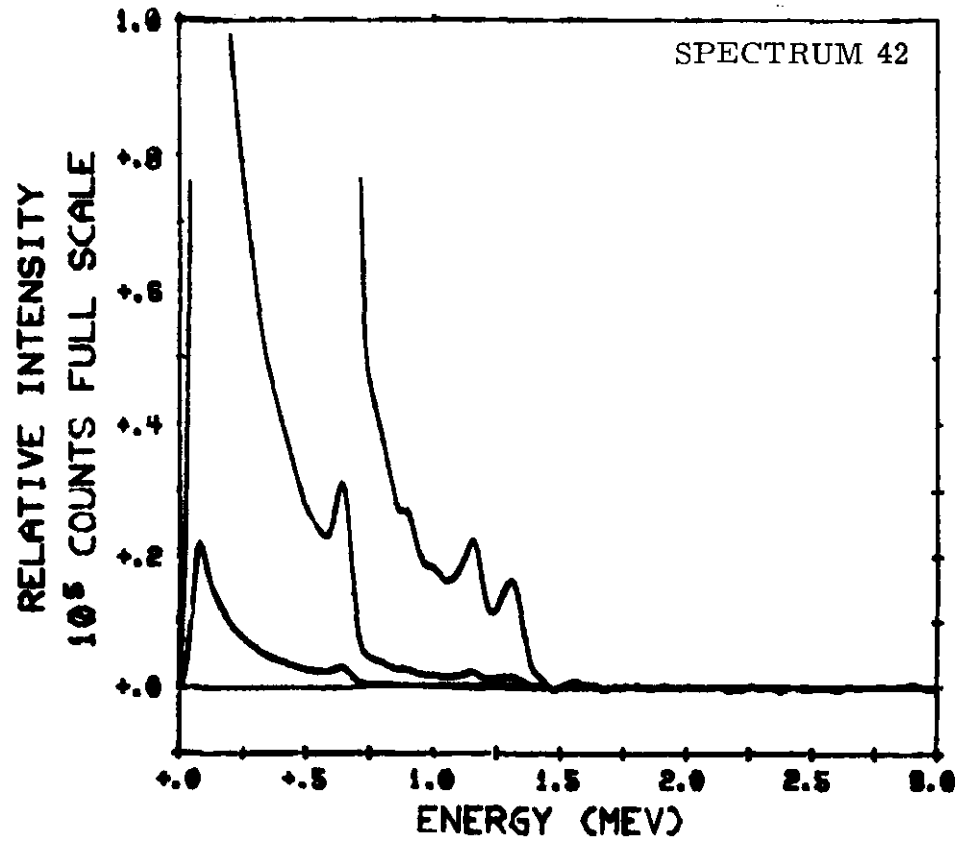
SPECTRUM 42
RELATIVE INTENSITY
10⁵ COUNTS FULL SCALE
1.0
.8
.6
.4
.2
.0
.0
.5
1.0
1.5
2.0
2.5
3.0
ENERGY (MEV)

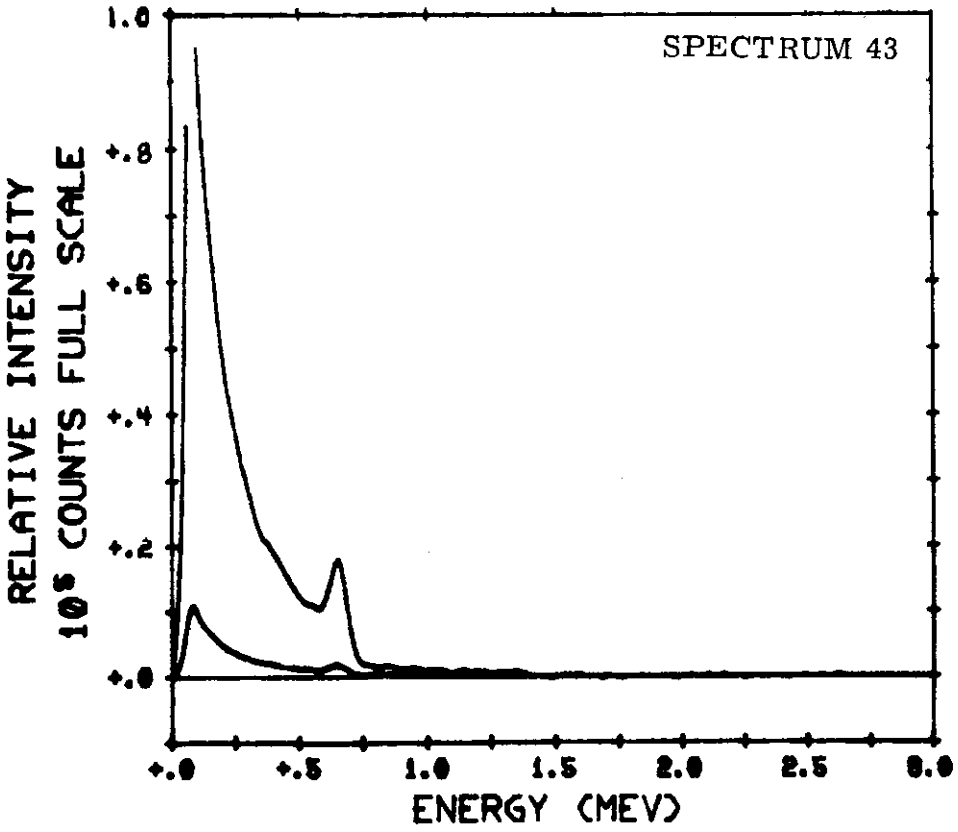
SPECTRUM 43
RELATIVE INTENSITY
10⁵ COUNTS FULL SCALE
1.0
.8
.6
.4
.2
.0
.0
.5
1.0
1.5
2.0
2.5
3.0
ENERGY (MEV)

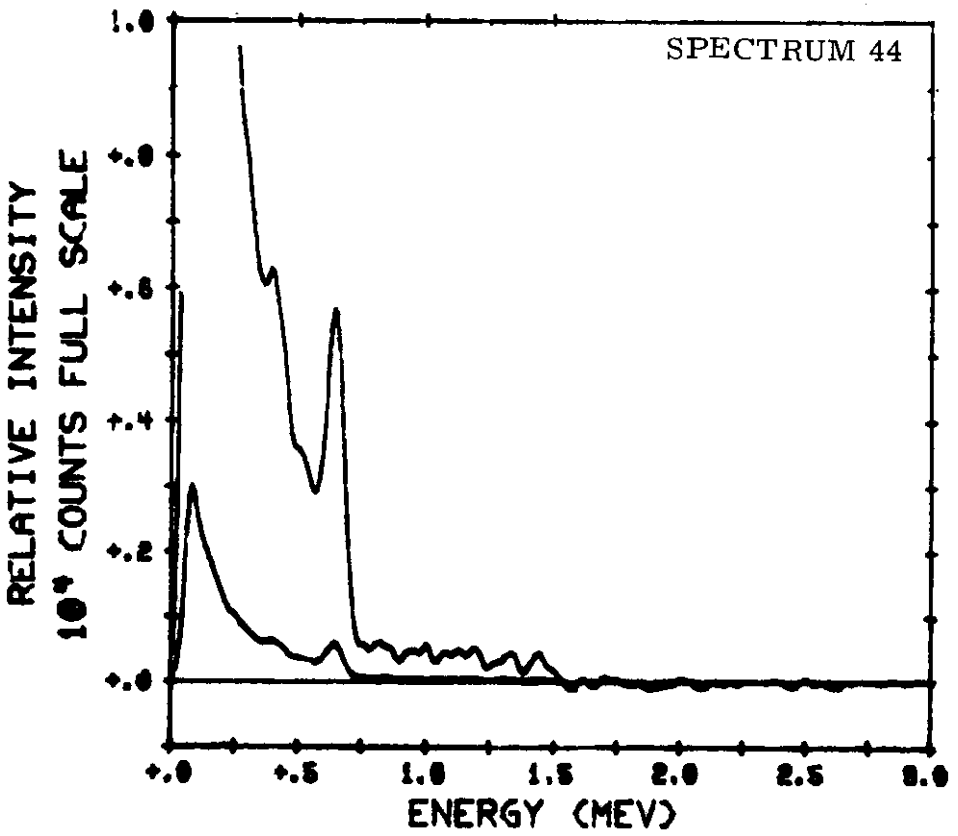
SPECTRUM 44
RELATIVE INTENSITY
10⁴ COUNTS FULL SCALE
1.0
.8
.6
.4
.2
.0
.0
.5
1.0
1.5
2.0
2.5
3.0
ENERGY (MEV)

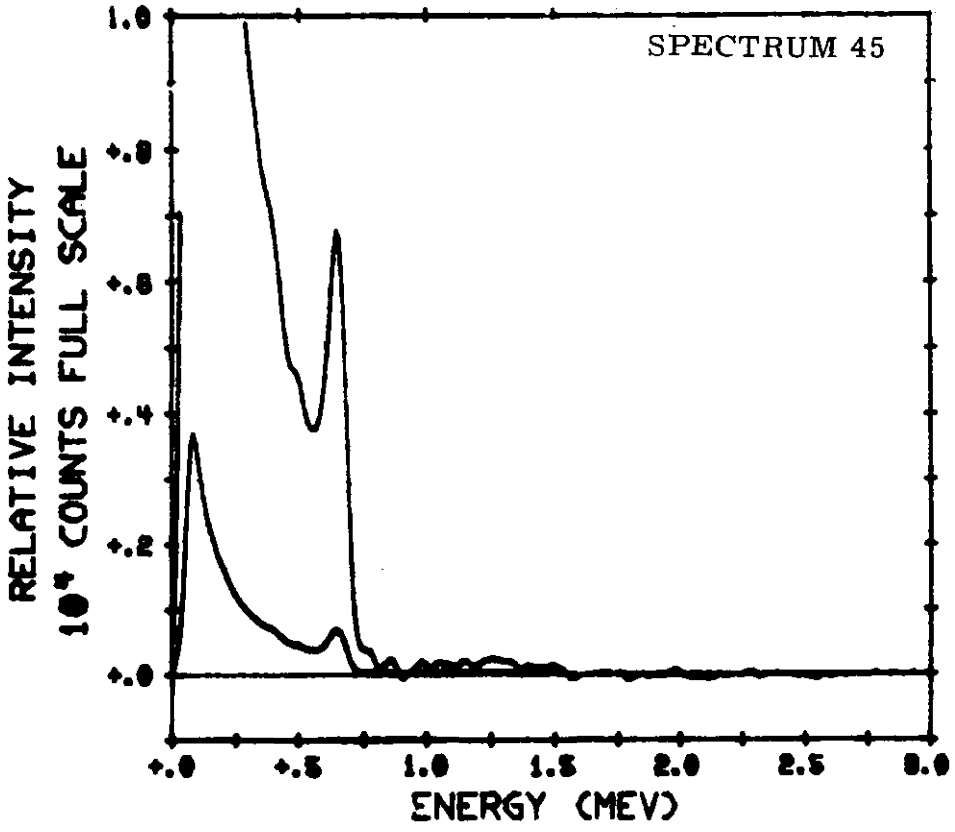
SPECTRUM 45
RELATIVE INTENSITY
10⁴ COUNTS FULL SCALE
1.0
.8
.6
.4
.2
.0
.0
.5
1.0
1.5
2.0
2.5
3.0
ENERGY (MEV)

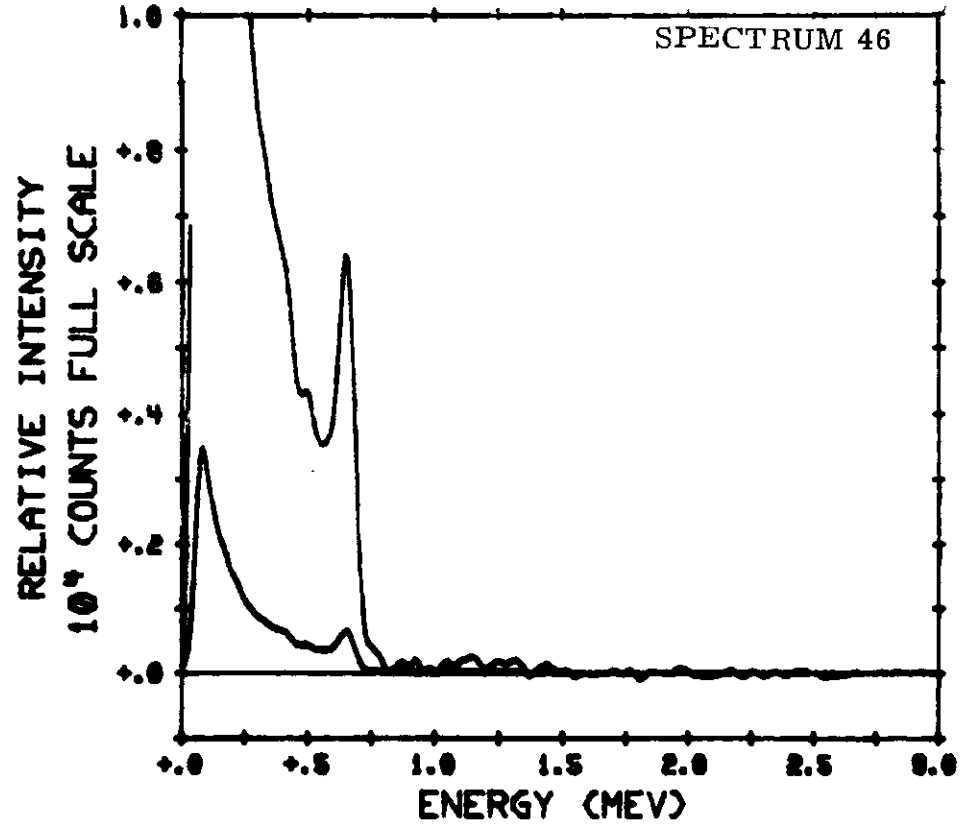
SPECTRUM 46
RELATIVE INTENSITY
10⁴ COUNTS FULL SCALE
1.0
.8
.6
.4
.2
.0
.0
.5
1.0
1.5
2.0
2.5
3.0
ENERGY (MEV)

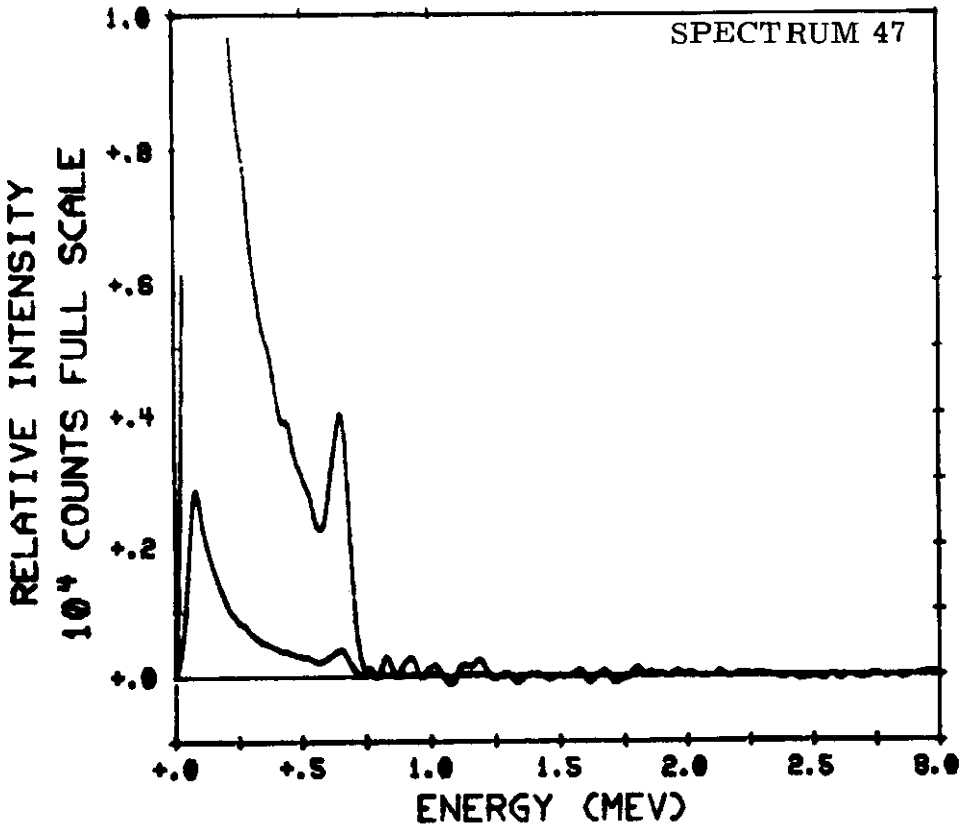
SPECTRUM 47
RELATIVE INTENSITY
10⁴ COUNTS FULL SCALE
1.0
.8
.6
.4
.2
.0
.0
.5
1.0
1.5
2.0
2.5
3.0
ENERGY (MEV)

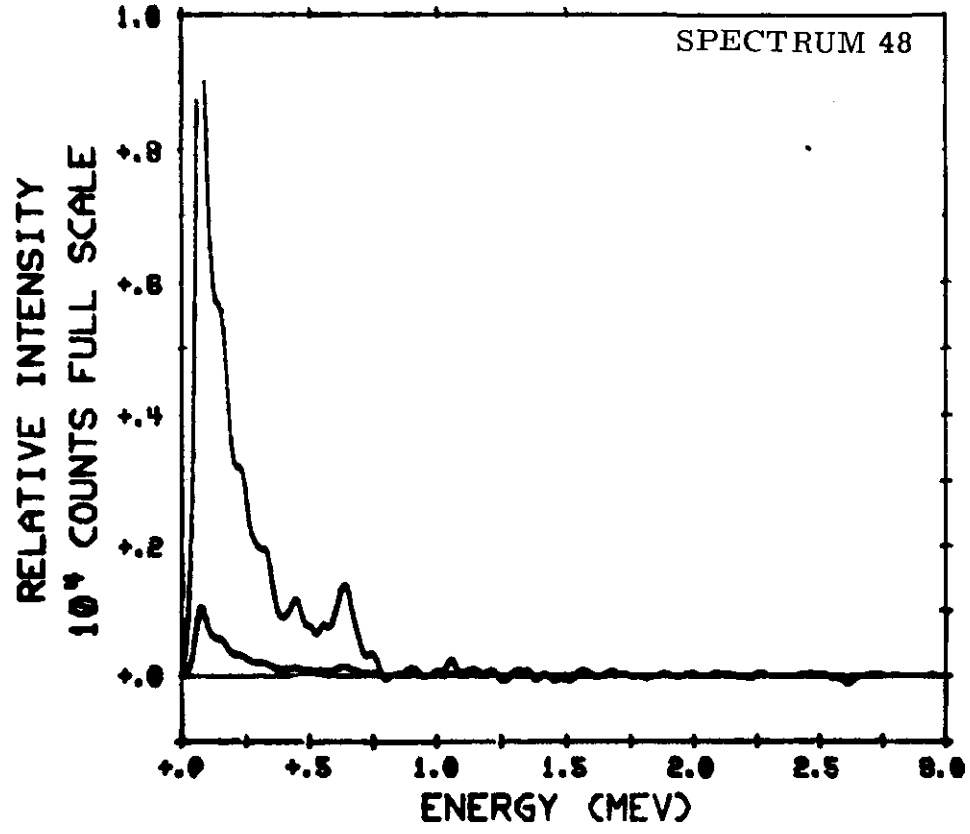
SPECTRUM 48
RELATIVE INTENSITY
10⁴ COUNTS FULL SCALE
1.0
.8
.6
.4
.2
.0
.0
.5
1.0
1.5
2.0
2.5
3.0
ENERGY (MEV)

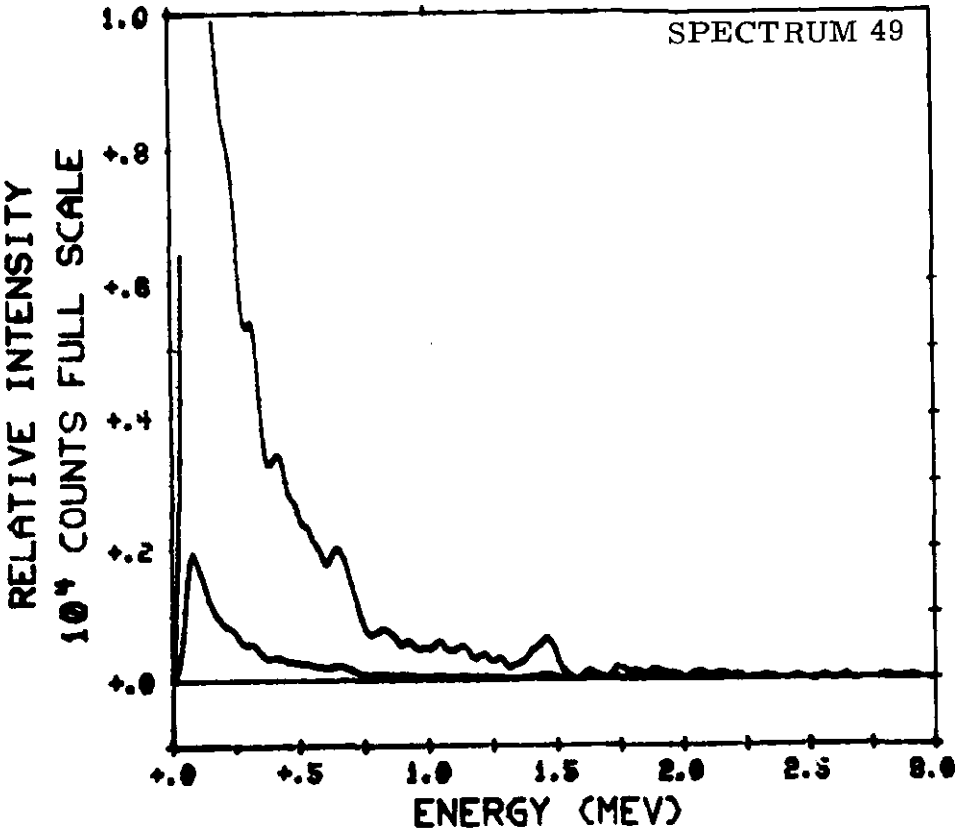
SPECTRUM 49
RELATIVE INTENSITY
10⁴ COUNTS FULL SCALE
1.0
.8
.6
.4
.2
.0
.0
.5
1.0
1.5
2.0
2.5
3.0
ENERGY (MEV)

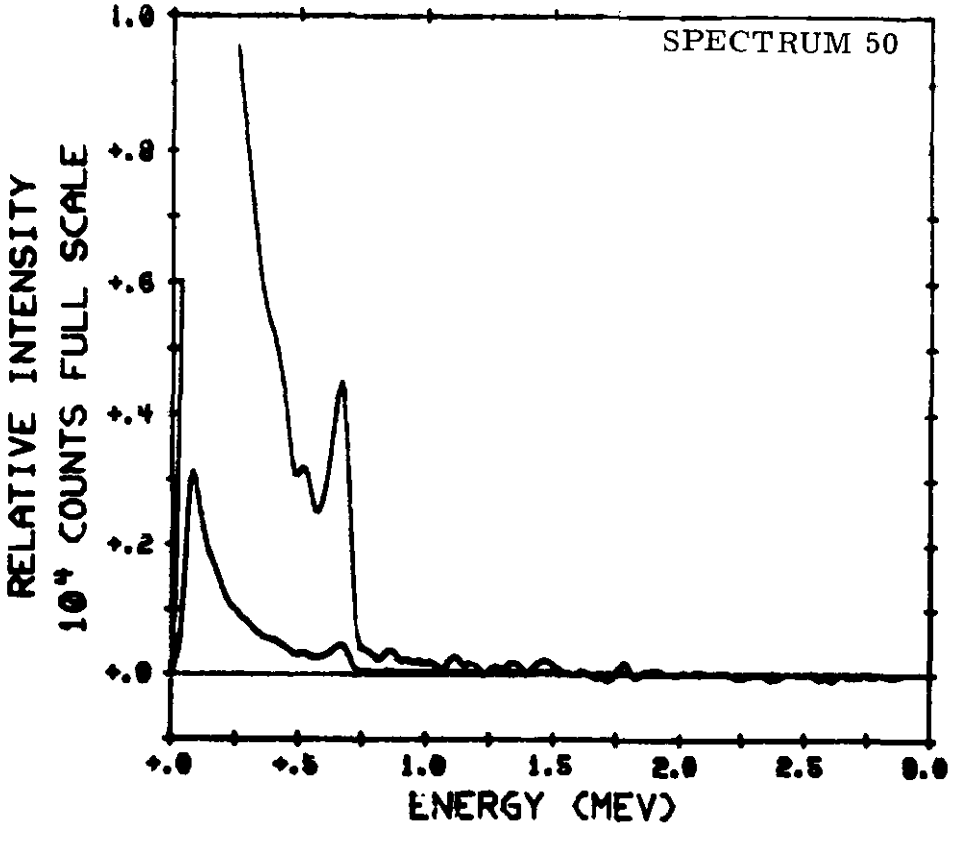
SPECTRUM 50
RELATIVE INTENSITY
10⁴ COUNTS FULL SCALE
1.0
.8
.6
.4
.2
.0
.0
.5
1.0
1.5
2.0
2.5
3.0
ENERGY (MEV)

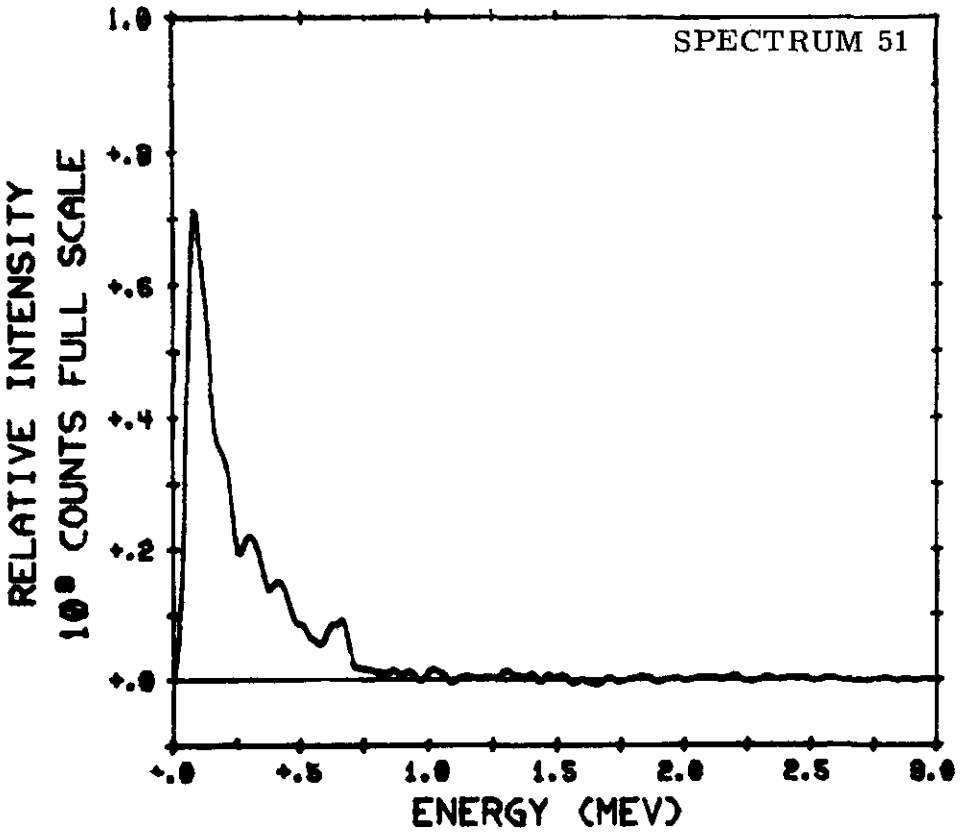
SPECTRUM 51
RELATIVE INTENSITY
10⁰ COUNTS FULL SCALE
1.0
.8
.6
.4
.2
.0
.0
.5
1.0
1.5
2.0
2.5
3.0
ENERGY (MEV)

REFERENCES

1. T. P. Stuart (report to be published).
2. "The Savannah River Plant Site," T. M. Langley and W. L. Marter, DP-1323, 1974.
3. "Radioactivity from SRP Operations in a Downstream Savannah River Swamp," W. L. Marter, DP-1370, 1974.
4. "The Aerial Radiological Measuring System Program," J. F. Doyle, EGG-1183-1558, 1972.

DISTRIBUTION

ERDA/DOS

L. J. Deal (15)

ERDA/SRP

G. Smithwick (25)

ERDA/NV

J. A. Koch
R. R. Loux
R. B. Purcell

ERDA/TIC

Librarian (2)

EG&G/LVAO

ARMS Library (50)
B. P. Warner

EG&G/SBO

Library (2)
H. Borella (2)
R. Lynn